REMOTE SENSING AS A TOOL FOR RESOURCES ASSESSMENT TOWARDS THE DETERMINATION OF THE LEGAL COMPLIANCE OF SURFACE AND GROUNDWATER USE

Report to the

Water Research Commission

by

Lesley Gibson[1], Zahn Münch[2], Jeanine Engelbrecht[3], Nicole Petersen[4] & Julian Conrad[2]

[1] ARC – Agricultural Research Council, Institute for Soil Climate and Water
Private Bag X 5017, Stellenbosch, 7599

[2] GEOSS – Geohydrological and Spatial Solutions International (Pty) Ltd
P.O. Box 12412, Die Boord, 7613

[3] Council for Geoscience, Western Cape Unit
P.O. Box 572, Bellville, 7535

[4] University of Cape Town, Environmental & Geographical Science
University of Cape Town, Private Bag X3, Rondebosch, 7701

WRC REPORT NO. 1690/1/09
ISBN 978-1-77005-913-9

DECEMBER 2009

ACKNOWLEDGEMENTS

The Reference Group involved with the project comprised the following persons:

Dr Shafick Adams	Water Research Commission (Chairperson)
Roger Parsons	Parsons and Associates Specialist Groundwater Consultants
Alta Minnaar	Department of Water Affairs and Forestry (DWAF)
Dorette Piekaar	DWAF
Eduarda Teixeira	formerly DWAF
Dechlan Pillay	CSIR
Prof Michael Inggs	University of Cape Town
Prof Abraham Thomas	formerly University of the Western Cape

The financing of the project by the Water Research Commission and the contributions of the Reference Group are gratefully acknowledged.

All land owners in the Bo-Piketberg who allowed us access to their farms are thanked, especially Eric & Michelle Starke, Geoff Southin, Rob Whitfield, Neil Paterson, Hendrik Pistorius, Margaret Matzener, Vanessa & Cliff Beautement, John Ince, Kobus & Deidré Eigelaar, Charles Edmunds, Patrick & Karen Carpenter, Geoff Lawrence, Gert Greeff, Kirby & Maggie Kent, Gert Coetzee, Jaco Kotze, Peter Herman, Dawie Stiemie, Jan Visser, Jannie Stander, Chris & Mary Watson, and Rob & Mary Duncan.

We also wish to thank our colleagues and their organizations for their scientific and technical support and their assistance:

- Pieter Haasbroek, Dawie van Zyl, Johan Malherbe and Ritha Wentzel from ARC-ISCW
- Dale Barrow and Regan Rose from GEOSS
- John Weaver for assistance with validation of lineament mapping
- Marizette de Meyer (formerly GEOSS) for lineament mapping
- Fritz Schoeman of GTI for MODIS downloads
- Cobus Stals of GTI for Definiens training
- Prof Bob Su from the ITC, Netherlands, for assistance with SEBS, and being co-supervisor on Lesley Gibson's PhD
- Dr Victor Kongo from UKZN and Lichun Wang from the ITC, Netherlands, for assistance with SEBS
- Dr Caren Jarmain from the CSIR for her help with evapotranspiration concepts
- Eddie van Wyk (DWAF) for support with regard to making the automated rainfall stations available to the project

- Frans Manamela (DWAF) for his great work in the building of the rainfall stations and installing the housings on site
- Mike Smart (DWAF) for approving the use of borehole water level data loggers and general support to the project
- Piet Havenga (DWAF) for providing the actual water level data loggers and general assistance with setting them up
- Hester Lyons, Wilna Kloppers and Bertrand van Zyl (DWAF) for initially suggesting the study area
- Ludie Nel (formerly DWAF) for initial support and data
- Dr Kevin Winter (UCT) for supervision of Nicole Petersen's Masters thesis
- Prof Okke Batelaan for use of the WetSpass model
- Wikus Nel, farm manager at Mouton's Valley
- The European Space Agency (ESA) for providing the radar data used for soil moisture quantification
- South African Weather Service and EnviroMon Weather Service for weather data
- CSIR Satellite Application Centre for SPOT images
- University of Stellenbosch for use of computers
- Dr Thomas Fyfield (ARC-ISCW) for editing the final report
- Dr Luc Chevallier (CGS) and Terry Newby (ARC-ISCW) for their support of this project, especially in its initial phases.

ACRONYMS AND ABBREVIATIONS

ALOS	Advanced Land Observing Satellite
ARC	Agricultural Research Council
ARC-ISCW	Agricultural Research Council – Institute for Soil, Climate and Water
ASAR	Advanced Synthetic Aperture Radar
ASTER	Advanced Spaceborne Thermal Emission and Reflection Radiometer
CAGE	Citrusdal Artesian Groundwater Exploration
CFB	Cape Fold Belt
CGS	Council for Geoscience
CM	Central Meridian
CMB	Chloride Mass Balance
CMWL	Cape Meteoric Water Line
CRD	Cumulative Rainfall Departure
CSIR	Council for Scientific and Industrial Research
DEM	Digital Elevation Model
DWAF	Department of Water Affairs and Forestry
EC	Electrical Conductivity
ESA	European Space Agency
ET	Evapotranspiration
FGDC	Federal Geographic Data Committee
GEOSS	Geohydrological and Spatial Solutions International (Pty) Ltd
GIS	Geographical Information System
GMWL	Global meteoric water line
GPS	Global Positioning System
GWR	Geographically Weighted Regression
HH	Horizontal transmit, horizontal receive
HV	Horizontal transmit, vertical receive
IDW	Inverse Distance Weighting
LMWL	Local meteoric water lines
MAP	Mean Annual Precipitation
MODIS	Moderate Resolution Imaging Spectroradiometer
MST	MODIS Swath Tool

NDSI	Normalized Difference Storage Index
NDVI	Normalized Difference Vegetation Index
NGDB	National Groundwater Data Base
NWA	National Water Act
P	Precipitation
PALSAR	Phased Array type L-band Synthetic Aperture Radar
Re	Recharge
RMSE	Root Mean Square Error
RMS	Root Mean Square
RO	Runoff
SAC	Satellite Applications Centre
SAR	Synthetic Aperture Radar
SEBAL	Surface Energy Balance Algorithm for Land
SEBS	Surface Energy Balance System
SMAC	Simplified Method for Atmospheric Correction
SPOT	Système Pour l'Observation de la Terre
SPW	Polarimetry Workstation Software
SVF	Saturated Volume Fluctuation
TIN	Triangulated Irregular Network
TMG	Table Mountain Group
VH	Vertical transmit, horizontal receive
VSM	Volumetric soil moisture
VV	Vertical transmit, vertical receive
WARMS	Water Authorization and Registration Management System
WetSpass	Water and Energy Transfer between Soil, Plants and Atmosphere under quasi Steady State
WGS 84	World Geodetic System 1984
WMA	Water Management Area
WMS	Water Management System
WRC	Water Research Commission
XML	Extensible Markup Language

TABLE OF CONTENTS

Acknowledgements ..... *i*

Acronyms and Abbreviations ..... *iii*

Table of Contents ..... *v*

List of Tables ..... *vii*

List of Figures ..... *viii*

Contents of Enclosed CD ..... *xi*

Executive Summary ..... *xiii*

1 Introduction 1

1.1 South African water legislation 2
1.2 Study area 3

2 Remote Sensing for Water use determination 12

2.1 Determining water balance components 12
2.2 Precipitation 13
2.2.1 Spatial variation of rainfall *13*
2.2.2 Rainfall in the study area *15*
2.2.3 Rainfall interpolation techniques *16*
2.2.4 Selected methodology *21*
2.2.5 Results *22*
2.2.6 Validation *24*
2.2.7 Uncertainties associated with rainfall estimation *27*
2.2.8 Conclusion *27*
2.3 Evapotranspiration 28
2.3.1 The energy balance approach *29*
2.3.2 Satellite data selection, acquisition and preparation *31*
2.3.3 Image preprocessing in SEBS *35*
2.3.4 Meteorological data selection and preparation *37*
2.3.5 SEBS evapotranspiration estimation *42*
2.3.6 Validation *48*
2.3.7 Conclusion *57*
2.4 Soil moisture 59
2.4.1 Introduction to soil moisture quantification *59*
2.4.2 Satellite image data obtained *60*
2.4.3 Field-based soil moisture measurements *61*
2.4.4 Data preprocessing *61*
2.4.5 Soil moisture quantification using SAR data *62*
2.4.6 Concluding remarks *69*

2.5 Surface runoff 70
2.5.1 Introduction 70
2.5.2 Suggested methodology 71
2.5.3 Results 73
2.5.4 Discussion 77
2.6 Groundwater 78
2.6.1 Introduction 78
2.6.2 Methodology 78
2.6.3 Conceptual model 80
2.6.4 Chloride Mass Balance 83
2.6.5 Stable Isotopes: oxygen-18 (O^{18}) and deuterium (H^2) 85
2.6.6 Physical methods 87
2.6.7 WetSpass model 89
2.6.8 Discussion 91
2.7 Dam volume calculations 92
2.7.1 Introduction 92
2.7.2 Definiens Software 94
2.7.3 Methodology 95
2.7.4 Discussion 103
2.7.5 Conclusion 106

3 Water Balance Result – G10K catchment 108
3.1 Annual water balance equation for the study area 108
3.2 Differencing of evapotranspiration results as an indicator of irrigation and/or recharge 113
3.3 Application of results to selected WARMS data to assess validity of methodology. 119
3.3.1 The Bo-Piketberg 120
3.3.2 Irrigated agriculture adjacent to the Berg River 121
3.3.3 Dryland agriculture where non-perennial pans are found 123

4 Discussion 125
4.1 Uncertainties and limitations 128
4.2 WARMS 130

5 Conclusion 131

6 Recommendations 134

7 References 137

LIST OF TABLES

Table 1.2.1: Lithostratigraphy of the study area 5
Table 2.2.1: Comparison of the interpolated rainfall grids value with the measured rainfall at weather stations not used in the interpolation process (1 Oct 2007-30 Sep 2008) – in millimetres 25
Table 2.2.2: Variation in measurements (mm) from weather station within or just outside the G10K catchment and the ARC-ISCW rainfall grids on a monthly basis 26
Table 2.3.1: Selected MODIS image acquisition dates in the study area for the study period 33
Table 2.3.2: Inputs required for SMAC 35
Table 2.3.3: Actual evapotranspiration (mm) for the study period analyzed by landuse 46
Table 2.4.1: Sensor configuration for Envisat data used for the study 60
Table 2.5.1: Hydrograph separation results 75
Table 2.5.2: Comparison of runoff from WetSpass with WR90 76
Table 2.6.1: Survey of estimates of recharge of TMG aquifer systems (after Parsons, 2002) 82
Table 2.6.2: Summary statistics of the chloride concentrations (mg/L) found in the groundwater samples of the NGDB and hydrocensus database 83
Table 2.6.3: Recharge estimation using the CMB method 84
Table 2.6.4: Recharge estimation using WetSpass 89
Table 2.7.1: Field surveyed dams with their calculated surface areas and TIN determined volumes 95
Table 2.7.2: Standard Deviation for Surface Area Values 104
Table 2.7.3: Differences in topography between G10K catchment and the Ghanaian study area used by Liebe (2002) 106
Table 4.1: Summary of uncertainties in calculating water balance components 130

LIST OF FIGURES

Figure 1.2.1: Orientation map showing the G10K catchment 4
Figure 1.2.2: Geology of the study area (1:250 000 geology map 3218 Clanwilliam) 7
Figure 1.2.3: Climatic variation in the study area as illustrated by Köppen Climate Zones (courtesy ARC-ISCW, 2007) 8
Figure 1.2.4: Mean Annual Precipitation (after Lynch, 2004) 9
Figure 1.2.5. Drainage patterns within the G10K catchment (1:50 000 rivers, DWAF) 10
Figure 1.2.6: Landuse map (National Land Cover 2000, courtesy ARC-ISCW) 11
Figure 2.1.1: The hydrologic cycle (after Ward, 1975) 12
Figure 2.2.1: Location, name and ownership of weather stations recording rainfall within a 20 km buffer zone of the G10K catchment 15
Figure 2.2.2: The recorded rainfall for the study period and its relation to altitude 18
Figure 2.2.3: Start dates of rainfall records at stations in the region 19
Figure 2.2.4: Semivariogram of rainfall data from weather stations in the study area 20
Figure 2.2.5: Unrealistic rainfall pattern produced by using an IDW interpolation technique 21
Figure 2.2.6: Summed monthly and total rainfall for the period 1 October 2007-30 September 2008 from ARC-ISCW decadal rainfall grids 23
Figure 2.3.1: Köppen climate zones showing the delineation of a fourth "climate zone" and the weather stations selected to be representative of each zone 39
Figure 2.3.2: Hourly averaged solar radiation at image overpass time for images acquired for WRC project 40
Figure 2.3.3: Examples of weather station data used for each climate zone 41
Figure 2.3.4: Example of the SEBS form in ILWIS showing all the required input data 43
Figure 2.3.5: An example of SEBS output – 29 December 2007 44
Figure 2.3.6: Comparison of actual evapotranspiration estimated using the SEBS model and potential evapotranspiration for the study period (1 October 2007-30 September 2008) 45
Figure 2.3.7: Actual evapotranspiration compared to landuse type using the National Landcover 2000 dataset (courtesy ARC-ISCW) 47
Figure 2.3.8: Location of the validation site (shown as Piketberg) on Mouton's Valley Farm (from Jarmain & Mengistu, 2009) 49

Figure 2.3.9 Daily total evaporation (ET) and reference evaporation (ET_o) as measured at the apple orchard 50
Figure 2.3.10: SEBS estimated actual ET on days of image acquisition compared with reference ET calculated from weather station data 51
Figure 2.3.11: Relationships derived for estimating daily total evaporation (ET) rates from estimates of reference evaporation (ET_o) 52
Figure 2.3.12: SEBS estimated daily ET (Eta) from an apple orchard, vapour pressure deficit (vpd), solar radiation (R_s) (secondary Y axis) and the product of solar radiation and vapour pressure deficit (R_s*vpd) (secondary Y axis) 52
Figure 2.3.13: Relationships derived for estimating daily total evaporation (ET) rates from the product of solar radiation and vapour pressure deficit (R_s*vpd) 53
Figure 2.3.14: SEBS estimated daily ET (Eta) and reference evaporation (ETo) as measured at the apple orchard. 53
Figure 2.3.15: SEBS ET estimates compared with field measurements on 20 Nov 2008 (DOY 325). a. Instantaneous energy balance fluxes, b. Evaporative fraction and daily ET 55
Figure 2.3.16: SEBS ET estimates compared with field measurements on 17 Nov 2008 (DOY 322). a. Instantaneous energy balance fluxes, b. Evaporative fraction and daily ET. 56
Figure 2.4.1: Soil moisture (in volumetric percentage) as quantified by linear regression models 64
Figure 2.4.2: ARC-ISCW cumulative rainfall grids over a 10-day period 65
Figure 2.4.3: Irrigated fields (high soil moisture content) in contrast to surrounding areas with low soil moisture content 66
Figure 2.4.4: Soil moisture quantification using multiple polarization models (A) compared to rainfall (B) 68
Figure 2.5.1: Location of streamflow gauges in G10K with streamflow at G1H031 72
Figure 2.5.2: Hydrograph analysis for G1H031 for hydrologic year 2007/8: 74
Figure 2.5.3: Comparison of waterlevels in Berg River at inflow (G1H031) and outflow (G1H023) to G10K catchment 75
Figure 2.5.4: Temporal variation of runoff modelled with WetSpass 76
Figure 2.5.5: Comparison of monthly runoff to monthly precipitation 77
Figure 2.6.1: Conceptual model of the study area 81
Figure 2.6.2: Cross-section of the geology of the TMG within the study area 82
Figure 2.6.3: Annual recharge (%) for the G10K catchment using the CMB method 85

Figure 2.6.4: Plot of rainfall δD versus δ18O data ... 86
Figure 2.6.5: Spatial distribution of groundwater samples ... 87
Figure 2.6.6: Plot of groundwater δD versus δ18O data ... 87
Figure 2.6.7: Simulation of groundwater fluctuation using the CRD method ... 88
Figure 2.6.8: Simulation of groundwater fluctuation using the SVF method ... 89
Figure 2.6.9: Annual recharge (%) for the G10K catchment using WetSpass ... 90
Figure 2.7.1: Hierarchical network of image objects ... 94
Figure 2.7.2: Process tree for Object Oriented Classification of Surface Water Bodies (Pilot Study Area) ... 97
Figure 2.7.3: Object Oriented Classified of Farm Dams for Pilot Study Area ... 98
Figure 2.7.4: Field validation points for Dam B ... 98
Figure 2.7.5: Classification of dams in the larger study area ... 99
Figure 2.7.6 : Volume results using the formula by Sawunyama et al. (2006) on surface area of dams mapped from satellite images (Definiens) and from the field survey data (ArcGIS). 102
Figure 2.7.7 : Volume results using the formula by Van de Giesen et al. (2004) on surface area of dams mapped from satellite images (Definiens) and from the field survey data (ArcGIS). 102
Figure 2.7.8: Comparison of dam volumes calculated from field data using a TIN, the two formulae obtained from the literature and the volumes registered on the WARMS database. ... 105
Figure 3.1.1: Results of applying the water balance equation to the modelled water balance components for the G10K catchment for the study period (1 Oct 2008-30 Sept 2008) ... 110
Figure 3.1.2: The normalized difference storage index for G10K catchment for the study period ... 112
Figure 3.2.1: Comparison of WetSpass modelled ET constrained by A-pan evaporation vs. Penman-Monteith Potential evapotranspiration ... 114
Figure 3.2.2: Comparison of SEBS modelled ET and WetSpass modelled ET, with ET difference for summer ... 117
Figure 3.2.3: Comparison of SEBS modelled ET and WetSpass modelled ET, with ET difference for winter ... 118
Figure 3.3.1 Calculated dam volume storage and dam volume storage from WARMS database ... 121

Figure 3.3.2: Source of water registered on WARMS database with the NDVI from an ASTER image (29 Feb 2008) used as a back drop. Irrigated agriculture is clearly visible in white 122

Figure 3.3.3: Volume water usage per farm as calculated from the results shown in Figure 3.3.2. Water use values indicated as negative (low values equal high water use) 123

Figure 3.3.4: Volume water usage per farm as calculated from the results shown in Figure 3.1.1. Water use values indicated as negative (low values equal high water use) 124

CONTENTS OF ENCLOSED CD

Project Deliverables

- Deliverable 1a: Progress Report (2006/12/15)
- Deliverable 1b: Literature Review. (2006/12/15)
- Deliverable 2: Progress Report. (2007/03/31)
- Deliverable 3a: Progress Report (2007/10/31)
- Deliverable 3b: Methodology Development. (2007/10/31)
- Deliverable 4: Progress Report. (2008/03/31)
- Deliverable 5: Progress Report. (2008/10/31)

Reports

- Evapotranspiration concepts and the SEBS model explained
- WetSpass Methodology
- WRC Consultancy Report No K8/824 – C. Jarmain and M.G. Mengistu:
  - Validating energy fluxes estimated using the Surface Energy Balance System (SEBS) model for a small catchment

Project data

EXECUTIVE SUMMARY

Introduction

Since South Africa is such a water scarce country, it is important for water resource managers to have accurate information on all aspects of water resource occurrence and use. This includes knowledge of the level of compliance of water users to water use licence legislation and the quantity of unlicensed water usage and storage. In terms of the National Water Act of 1998, a person may only use or store water, according to certain limitations, if the activity is authorized and licensed. Remote sensing, based on aerial photography and satellite imagery, can be used to detect and map features on the earth's surface. Archives of these images are excellent sources of historical data which in the case of aerial photography, go back to the early- to mid-20th century, and in the case of satellite images, go back to the 1970s.

The overall objective of this project is to determine the usefulness and applicability of using remote sensing technologies as a tool for resource assessment towards the determination of the legal compliance of surface and groundwater use. This project focuses on the creation of new knowledge and being at the innovative edge of the topic.

Water balance approach

At the catchment level, the water cycle can be represented by the water balance equation which is a simple statement of the law of mass conservation and is expressed as

Inflow = outflow ± changes in storage

or

$$\Delta S = P - ET - Re - RO$$

where ΔS is the change in water storage in the catchment, P is precipitation, ET is evapotranspiration, Re is groundwater recharge and RO is surface and subsurface water runoff. At a catchment level, it can be determined whether a catchment is experiencing water stress on an annual basis by using the water balance equation. If $\Delta S > 0$ for a particular year, the catchment is not experiencing water stress, but if $\Delta S < 0$, water stress is occurring. If ΔS is calculated for a few years in succession, the overall water stress can be determined. Furthermore, since the approach of the project is spatial rather than point

based (as far as possible), each component was determined on a grid basis in order to highlight those sections of the catchment which are experiencing the most water stress.

Precipitation

The ARC-ISCW decadal rainfall grids were summed month by month and for the total study period. It was found that for the G10K catchment, there is a good correlation between the total measured rainfall for the study period and the ARC-ISCW interpolated grid values, and as expected, the correlations are more variable at a monthly time scale. The spatial rainfall pattern provided by the ARC-ISCW interpolated rainfall grids appears to be sound, however, it is apparent that there is a significant underestimation of rainfall in the G10K catchment as a result of: 1) underestimation of rainfall in ARC-ISCW interpolated grid; 2) random and systematic error in the collection of rainfall; and 3) the as yet unquantified contribution of condensation to precipitation. This corroborates previous reports of uncertainties in rainfall measurements.

Evapotranspiration

The Surface Energy Balance System (SEBS) model was used to estimate daily actual evapotranspiration for 30 days in the study period from 1000 m MODIS data. The daily evapotranspiration was upscaled to monthly and annual evapotranspiration using relative and potential evapotranspiration. Using this method, there appears to have been an overestimation of actual evapotranspiration for the study period if the results are compared with the rainfall results. Since the evapotranspiration results have only been validated for an irrigated apple orchard and not other land use types, it is difficult to draw conclusions as to where possible errors may be occurring but the possibilities include: 1) the need for additional parameterization specific to the study area for the accurate estimation of roughness lengths; 2) errors in atmospheric correction due to difficulties in obtaining input data for the SMAC model; 3) the lack of interpolated weather station data; or 4) possible errors in implementing the model due to the absence of direct supervision. Furthermore, the issue of image resolution and landscape heterogeneity may also be impacting on the accuracy of results. The 1000 m pixel resolution of MODIS data makes it unsuitable for quaternary catchments and the heterogeneous landscape in the Bo-Piketberg compounds this.

Soil moisture

Soil moisture quantification was achieved by employing a variety of algorithms on Envisat ASAR and ALOS PALSAR data. The image data was provided by the European Space Agency (ESA). Field verification of the results could not be achieved since distributed field-based soil moisture measurements were unavailable for the time of image capture. However, the results obtained are very encouraging and correlate well with rainfall patterns recorded during the period of image capture. The results of the soil moisture quantification could not be converted to a mean annual measure of soil moisture content since high resolution radar data over a long time series were unavailable at the time of the study. However, it is believed that soil moisture data at high resolution will become routinely available in the near future.

Runoff

Runoff was modelled using the GIS-based WetSpass model. The WetSpass model simulates runoff in two stages: firstly potential surface runoff is calculated based on vegetation type, soil texture, slope and groundwater saturated areas. In stage two, the potential surface runoff is adjusted for recharge areas taking the seasonal precipitation intensity in relation to the soil infiltration capacity into account. In groundwater discharge areas all potential runoff is assumed to contribute to surface runoff, while in infiltration areas only high intensity storms will generate surface runoff. The WetSpass model was adapted in ArcView to produce monthly runoff figures using monthly precipitation data. Hydrograph baseflow separation analysis was done using DWAF streamflow data, but this represents the runoff at entry to the G10K catchment, since streamflow is not measured at the outflow from the catchment.

Recharge

A conceptual model of the geology and hydrogeology of the area was constructed. This assisted in the understanding of recharge and discharge areas. Using remote sensing based analysis, geological structure was investigated using lineament mapping. Three main recharge zones were identified. Chemical and isotope tracer methods as well as physical methods were used to estimate and characterize recharge on a local and regional scale.

The WetSpass model was also implemented in which recharge is calculated as the residual of a water balance in which precipitation is the principal input. Runoff and evapotranspiration are calculated as a function of landuse, soil, slope and potential evapotranspiration. Similarly recharge was also calculated using the evapotranspiration layer from remote sensing rather than modelling. The resultant recharge layer can be used as input to a MODFLOW model for further verification.

Dam volume calculations

For the storage component of this study, remote sensing was used to calculate the volume of water held in storage in farm dams. A relatively simple classification process was developed using object-oriented Definiens™ software on high resolution SPOT data so as to identify farm dams and obtain an estimate for surface area, a key input for volume calculation.

In order to obtain a value for water stored in farm dams, a capacity equation, $C = 0.023 * A^{1.33}$, was used to convert surface area to volume. The equation makes use of surface area and a constant as inputs so that implicit assumptions and errors may exist. However, the value generated using the equation still provides a useful estimate for the amount of water stored.

This study found that in the context of illegal water use, using remote sensing as a tool to quantify water storage may be appropriate in identifying water bodies and generating a fair estimate of volumes stored. It was found that the model works well for the general identification of surface water bodies. However, it is necessary to modify the rule set in Definiens as the areas of study differ and minor discrepancies in surface area results can cause a significant difference in the calculated volume. From there, dams that have the potential to be in violation of the legislation can be dealt with on a case-by-case basis, using conventional methods.

Water balance results

The results from the water balance equation were evaluated using output from the various components generated in the project, each with its own limitations. The results of combining the individual components of the water balance equation were not expected to reflect a real change in storage value, but the exercise was completed to analyze whether any patterns and variations within the catchment could be discerned and explained.

Due to the many uncertainties associated with the input data into the water balance equation, a unitless index was created to assess the spatial variation across the catchment rather than to look at absolute values. For this purpose, the concept of the normalized difference storage index (NDSI) was coined, which resulted in a value of between -1 and 1 with a negative value meaning a decrease in storage (more outflow than inflow) and a positive value meaning an increase in storage (more inflow than outflow). The higher the positive value, the larger the increase in water stored, and the higher the negative, the larger the decrease in water storage. The value of using the NDSI was illustrated as a useful tool to highlight areas of relative water stress within a catchment.

Actual evapotranspiration was calculated using two different models in this project and gave very different results based on the fact that the one model was constrained by precipitation. Therefore, if the assumption is made that both models have been implemented correctly with accurate input data, then it was envisaged that the difference between the SEBS modelled evapotranspiration and the WetSpass modelled evapotranspiration could be explained by irrigation from stored water sources (dams), precipitation incorrectly partitioned to runoff, or additional water entering the catchment as recharge via fractured systems.

To illustrate the application of the results to the WARMS database, three different areas in the catchment were considered. Results from the water balance output compared to WARMS need additional interpretation. The 1000 m pixel resolution of the MODIS data used in evapotranspiration estimation has a moderating effect on local variations of the results.

Discussion/Conclusion

The uncertainties, limitations and challenges encountered during this research project can be categorized into four sections: 1) the accuracy, availability and accessibility of input data, 2) heterogeneity of the study area, 3) skills shortage at supervisory level in South Africa, and 4) computer resource intensive models and software. The anomalies in the WARMS database also made it difficult to compare water use and storage results to the registered values.

In conclusion, it can be said that the application of the water balance equation to the G10K catchment did not determine the level of legal compliance of water users to legislation. However, new methodologies, untested in South Africa, were applied to the study area with many challenges encountered. There is much hope that, as remote sensing technology develops and remotely sensed data becomes available at a higher spatial and temporal resolution, the full potential of these models will be able to be fully tested and if proven accurate, could possibly be used operationally in the future. In addition, if the uncertainties and limitations encountered in the course of the research project are considered and acted upon, it is may be possible that at least parts of the methodology may be relevant at a later stage for water use determination.

Assessment regarding the completion of project objectives

Aim 1:

To highlight available remote sensing/other technologies which can be used for quantifying the legal compliance of water users to licensing legislation.

Aim 1 was achieved in the form of a literature review which was submitted as part of Deliverable 1 in December 2006.

Aim 2:

To develop a framework of the appropriate technologies to be used under various budget, timeframe, scale and resource scenarios

Aim 2 was included in the proposal to determine what information is required by water managers in order to fulfil their job function, and if and how remote sensing derived data could be included as an information source. A questionnaire was designed and distributed amongst water managers with varying levels of responsibility in terms of area and mandate, but no response was received. A meeting was envisaged, but did not come to fruition.

Aim 3:

Enhancement of existing models or creation of new models and application to a pilot study area. It is envisaged that this may include all or some of the following:

1. The use of remote sensing and GIS to develop methodologies to: identify small dams in a catchment, to determine the volume of water stored in selected dams, to

determine whether selected dams are authorized, and to determine the quantity of unauthorized water usage from selected small dams.

2. To use remote sensing and GIS to develop methodologies to: identify agricultural land use within selected cadastral farm boundaries in a catchment, to calculate crop water use based on evapotranspiration, to determine the probability of groundwater as water resource, to quantify groundwater use based on identifiable agriculture and to compare this use against licensed water use.
3. To apply the new methodology to a larger catchment in order to test its universal applicability.

Aim 3 reflected the major objective of the project and since some of the sub-objectives were achieved, it is regarded that the project has been successfully completed. Even though the application of the water balance equation to the G10K catchment did not determine the level of legal compliance of water users to legislation, Definiens software was used with success for dam determination, methodologies were developed using remote sensing and GIS and quantification of water use on the basis of evapotranspiration was investigated. Since the proposal was written, the Department of Agriculture undertook to map all field boundaries which removed the need to identify agricultural land within selected cadastral farm boundaries using remote sensing from the selected methodology. New methodologies (SEBS, Soil moisture, WetSpass), untested in South Africa, were applied to the study area with varying success. Many challenges were encountered and addressed.

1 INTRODUCTION

The Water Research Commission (WRC) awarded a research project (K5/1690) to Geohydrological and Spatial Solutions International (Pty) Ltd (GEOSS), the Agricultural Research Council (ARC) and the Council for Geoscience (CGS), entitled *"Remote Sensing as a tool for resource management and determination of the legal compliance of surface and groundwater use (QLC)*". The project is directed toward researching the usefulness and applicability of using Remote Sensing technologies as a tool for resource assessment and determination of the legal compliance of surface and groundwater use.

The original aims of the project as indicated in the Agreement are:

1. To highlight available remote sensing/other technologies which can be used for quantifying the legal compliance of water users to licensing legislation.
2. To develop a framework of the appropriate technologies to be used under various budget, timeframe, scale and resource scenarios
3. Enhancement of existing models or creation of new models and application to a pilot study area. It is envisaged that this may include all or some of the following:.
    a. The use of remote sensing and GIS to develop methodologies to: identify small dams in a catchment, to determine the volume of water stored in selected dams, to determine whether selected dams are authorized, and to determine the quantity of unauthorized water usage from selected small dams.
    b. To use remote sensing and GIS to develop methodologies to: identify agricultural land use within selected cadastral farm boundaries in a catchment, to calculate crop water use based on evapotranspiration, to determine the probability of groundwater as water resource, to quantify groundwater use based on identifiable agriculture and to compare this use against licensed water use.
    c. To apply the new methodology to a larger catchment in order to test its universal applicability.

During the execution of the project the focus of the project changed to resource assessment, rather than legal compliance, due to the resolution of the satellite imagery available. The project team revised the title of the project to *"Remote Sensing as a tool for resource assessment towards the determination of the legal compliance of surface and groundwater use"*. This change has been approved by the Reference Group. The focus of the project then became the third aim, in which the application of new technologies and methodologies would be used for resource assessment.

1.1 South African water legislation

According to section 27 of the Bill of Rights in the Constitution of South Africa (No. 108 of 1996), everyone has the right to have access to sufficient water and the state must take reasonable legislative and other measures, within its available resources, to achieve the progressive realization of these rights. The most prominent water legislation in South Africa is the National Water Act (Act 36 of 1998) which replaced the Water Act of 1956. The National Water Act (NWA) resulted in a change in paradigm in terms of the ownership of water. Rather than water rights being tied to land ownership, the minister is the custodian of the nation's water. The NWA set out general principles for regulating water use (Chapter 4, sections 21-55). In general, a water use must be licensed unless it is listed in schedule 1, is an existing lawful use, is permissible under a general authorization, or if a responsible authority waives the need for a licence. Existing lawful water use (registered as an annual volume of water) at the date of promulgation (1998) of the NWA is currently allowed to continue until a licence is required under compulsory licensing or an entitlement is made under section 22(5) or section 32 of the NWA (Kriek, 2005).

In issuing a licence, a responsible authority must take into account all relevant factors which include *inter alia*: existing lawful use, the need to redress past discrimination, socio-economic benefits, the class and resource quality of the water resource, and the likely effect of the water use on the water resource and on other water users. (National Water Act, section 27).

"Registered water use" was one of the concepts underpinning the NWA. It means that the location and amount of water used by an individual, farmer, or industry must be registered. In terms of legislation, water users were to register their water use during the qualifying period which is defined as the two years prior to the NWA coming into effect. In most cases this period was from 1 October 1996 to 30 September 1998, however, exceptions to this time period do exist. The water use registration information required for the qualifying period is the:

- Volume of water abstracted per annum
- Source of water abstracted
- Volume of water impounded
- Areas of commercial forest

It should also be noted that water use need not to have taken place for the entire qualifying period in order for it to be registered as an existing lawful use. (Quibell, 2005)

The registration process began in 2000 and is ongoing. The information is placed in the Water Authorization and Resource Management System (WARMS) spatial decision support system. The aim of this system is to determine the true demand for water in a catchment and thereby allow for more accurate storage and equitable allocation decisions as well as being a basis for managing water resources and billing users. Large quantities of, especially irrigation water, are currently not being monitored (Kriek, 2005) and since the registration process relied on the accurate registration of water by the user, it is not known to what extent water use is lawful or if the volume of water registered as being used is in fact a reflection of reality. According to DWAF & DFID (2005) it is currently estimated that as much as 60% of water use in certain catchments could be illegal under the National Water Act and Kriek (2005) considers it fact that there are many individuals who have registered their water use and are now under the impression that they are legally entitled to the registered use. Kriek (2005) believes that under these circumstances it is essential that the verification process should be completed as soon as possible and once this has been done, a sound practice for the continued control of water abstractions should be in place.

1.2 Study area

Based on a number of selection criteria, the study area was selected in consultation with the Regional Office of the Department of Water Affairs and Forestry (DWAF). The study area is in the Piketberg region, approximately 120 km north of Cape Town. It is an area that includes the Berg River and the Piketberg Mountains in the north. This includes the area called Bo-Piketberg. The western edge of the study area is approximately 30 km from the sea. The town of Piketberg is just to the east of the study area.

The area has a varied topography with the highest point being in the mountainous region above Piketberg (~1300 m) and down to the plains of the Berg River within the space of a few kilometres. The area is drained by the perennial Berg River which enters the Atlantic Ocean at Velddrif on the West Coast (Figure 1.2.1).

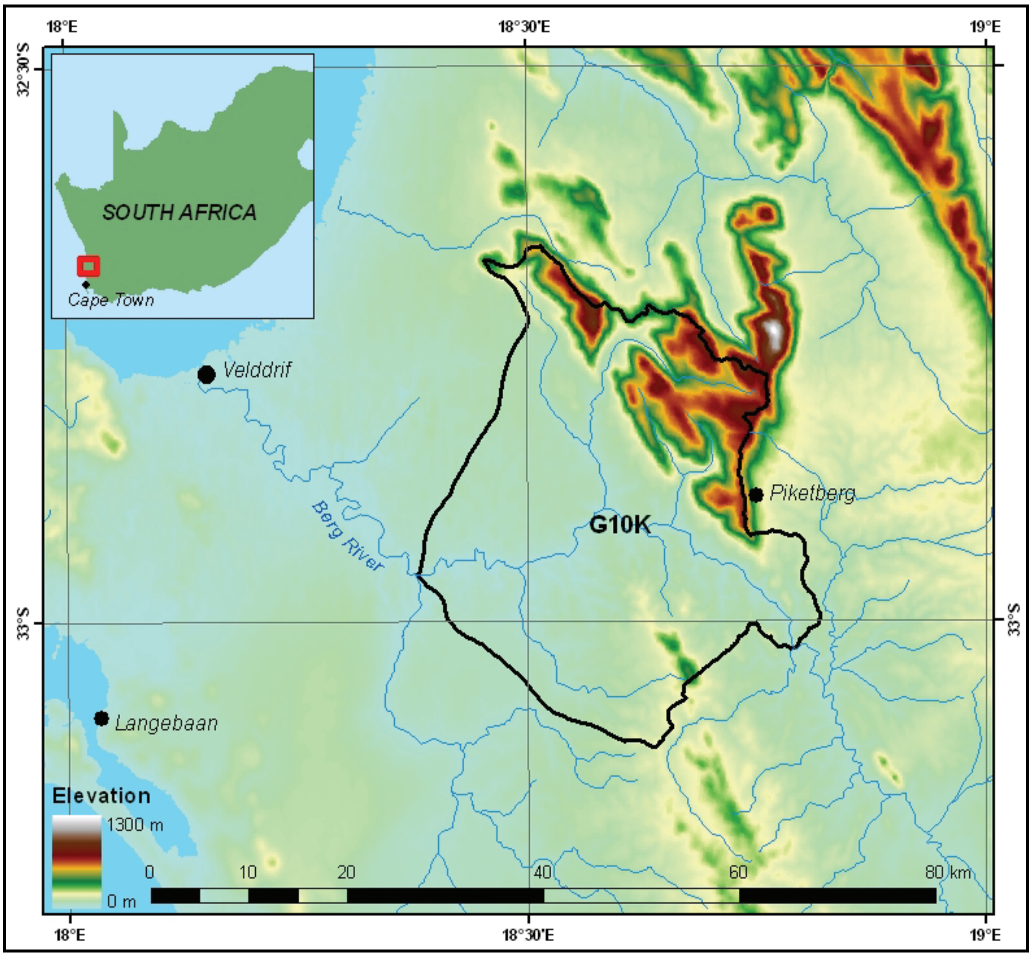

Figure 1.2.1: Orientation map showing the G10K catchment

The geology of the study area is dominated in the south by the Precambrian rocks represented by the Malmesbury Group. The full succession of the Malmesbury Group is exposed in the study area. The Malmesbury Group is represented by the Bergrivier, Klipplaat, Bridgetown, Moorreesburg, Piketberg and Porterville formations (Table 1.2.1).

TABLE 1.2.1: LITHOSTRATIGRAPHY OF THE STUDY AREA

SYMBOL	FORMATION	SUBGROUP	GROUP_SUIT	LITHOLOGY	% OF STUDY AREA
Qa				Alluvium	1.55
Qt				Scree & gritty sand	0.97
Qg				Sandy loam soil	18.66
Qs	Springfontein		Sandveld	Sandy soil	15.38
Sn	-	Nardouw	Table Mountain	Thick to thin bedded quartzose to feldspathic sandstone and siltstone	3.50
Ow	Pakhuis & Cedarberg	Winterhoek		Diamictite, shale, siltstone and sandstone	0.79
Ope	Peninsula			Thick bedded quartzose sandstone with minor shale and small-pebble conglomerate	17.16
Og	Graafwater			Thin bedded, red and brown sandstone, subordinate mudrock, small-pebble conglomerate and grit	1.37
Op	Piekenierskloof			Thick bedded quartzose sandstone and conglomerate	2.52
Cp	Populierbos		Klipheuwel	Mudrock, minor sandstone	0.29
Npo	Porterville		Malmesbury	Phyllite shale, schist and greywacke with dark grey limestone; sporadic quartzitic sandstone and conglomerate beds	1.63
Np	Piketberg			Feldspathic grit, greywacke, quartz schist, conglomerate and limestone beds with thin lenses of phyllite.	1.40
Nm	Moorreessburg			Greywacke, phyllite and quartz schist with thin lenses of limestone and grit	30.87
Et	Bridgetown			Greenstone with dolomite and chert lenses	0.21
Nk	Klipplaat			Quartz schist with phyllite beds and minor limestone and chlorite – schist lenses	1.65
Nb	Bergrivier			Schist, fine grained greywacke with bedds and lenses of quartz schist and limestone	1.67

The Bergrivier Formation consists of schist, fine grained greywacke with beds and lenses of quartz schist and limestone. The Klipplaat Formation consists of quartz schist with phyllite beds and minor limestone and chlorite – schist lenses. The Bridgetown Formation consists of greenstone with dolomite and chert lenses. The Moorreesburg Formation consists of greywacke, phyllites, quartz schist and lenses of limestone. The Piketberg Formation comprises feldspathic grit and greywacke, whilst the Porterville Formation consists of phyllite shale, schist and greywacke with dark limestone, sporadic quartzitic sandstone beds and conglomerate beds.

Two major fault systems, both having similar orientations, i.e. northwest – southeast striking, occur within the Precambrian rocks. They are:

1) Large northwest – southeast trending fault at the base of the Piketberg Mountain between Aurora and Piketberg. This fault caused major displacement resulting in the Moorreesburg Formation being juxtapositioned against the Table Mountain Group.
2) Large northwest – southeast trending fault that extends from Moorreesburg to Riebeeck Kasteel to Wellington.

In addition to the above, smaller east – west striking faults occur south of Piketberg. Structurally the Malmesbury Group of rocks south of Piketberg forms an anticline with the fold axial plane striking roughly north – south. In the northwest of the G10K catchment, the Malmesbury Group is limited to only a few isolated outcrops dipping steeply (60-75°) to the northeast. The latter area is covered by the Quaternary sand deposits of the Sandveld Group. Note that the Sandveld Group is well documented in Deliverable 2 (WRC, 2007a). The geology of the study area is depicted in Figure 1.2.2.

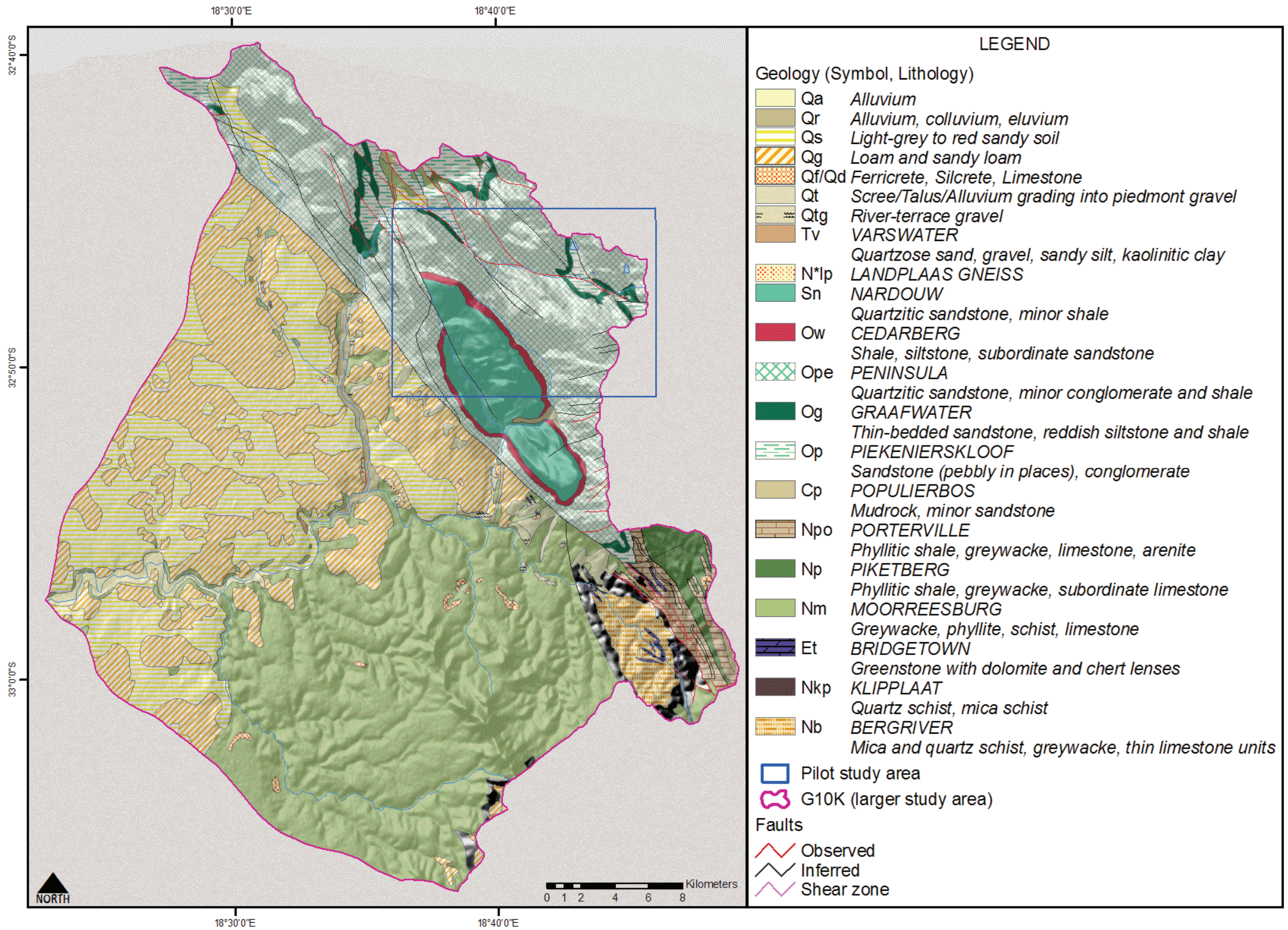

Figure 1.2.2: Geology of the study area (1:250 000 geology map 3218 Clanwilliam)

There is a varied climate in the area with most of the study area experiencing a Mediterranean climate with maritime influence and therefore cooler in the west and hotter to the east with continental influence (Figure 1.2.3).

Due to the influence of elevation on climate, the climate of the Bo-Piketberg should not be described in the same way as the surrounding low-lying areas. This is discussed later in the text in section 2.2 Precipitation.

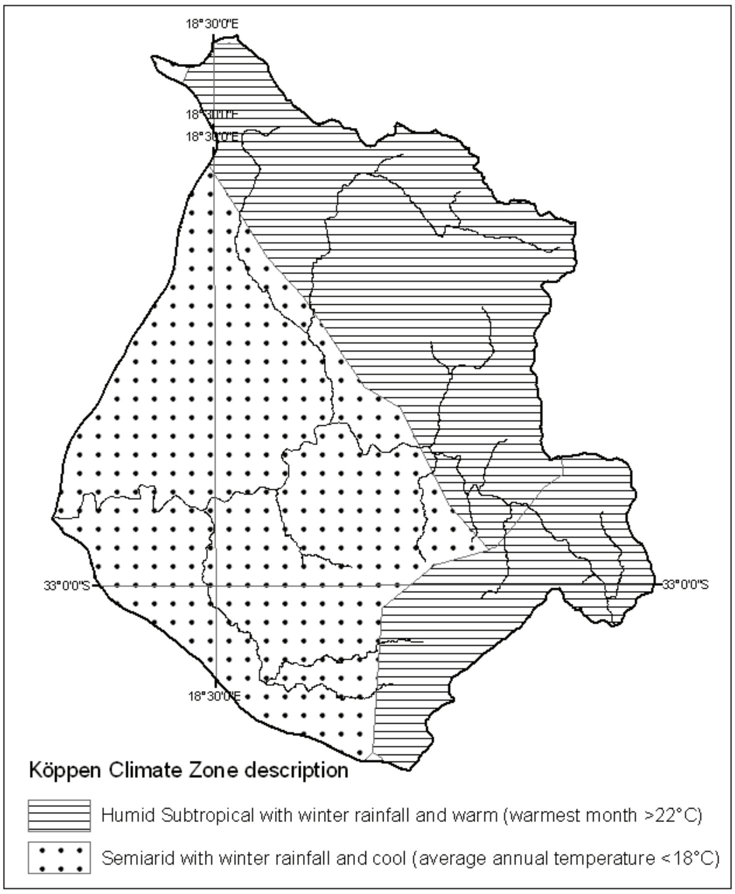

Figure 1.2.3: Climatic variation in the study area as illustrated by Köppen Climate Zones[1] (courtesy ARC-ISCW, 2007)

[1] The Köppen Climate Classification System is the most widely used system for classifying the world's climates. Developed early in the 20th century by a German climatologist, Dr. Vladimir Köppen, the classification system identifies climate zone boundaries based on vegetation distribution as well as temperature, precipitation and seasonal variation (ARC-ISCW, 2007). The Köppen system recognizes five major climatic types (Pidwirny, 2006) and each category is further divided into sub-categories based on temperature and precipitation. It is a useful representation of the earth's climate.

Figure 1.2.4 shows the Mean Annual Precipitation (MAP) for the G10K catchment as estimated by Lynch (2004). According to Lynch (2004) MAP in the study area varies from ~300 mm to ~800 mm per annum.

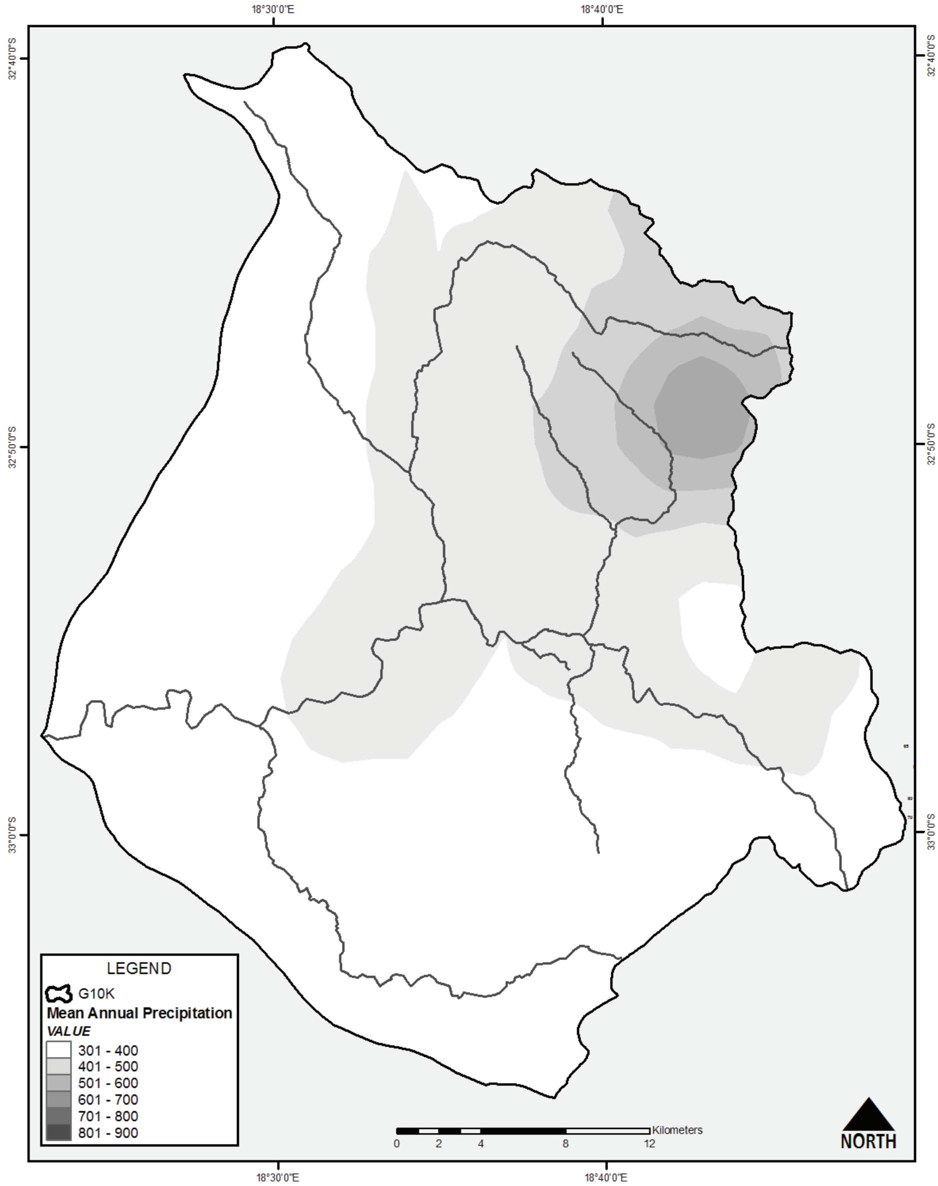

Figure 1.2.4: Mean Annual Precipitation (after Lynch, 2004)

The two major tributaries of the Berg River in the G10K are the Boesmans and Plattekloof Rivers, both having their source in the elevated Bo-Piketberg (Figure 1.2.5).

With the exception of these tributaries and the Kuilders River which feeds the Boesmans River, the catchment is characterized by:

1) non-perennial streams with a high drainage density to the south of the Berg River (corresponding to the Moorreesburg Formation);
2) high drainage density in the Bo-Piketberg corresponding to Table Mountain Group geology;
3) the absence of surface streams to the west of the Boesmans River and to the north of the Berg River corresponding to Quaternary deposits (Figure 1.2.2); and
4) non-perennial pans in the south of the catchment (Figure 1.2.6, mapped as water bodies).

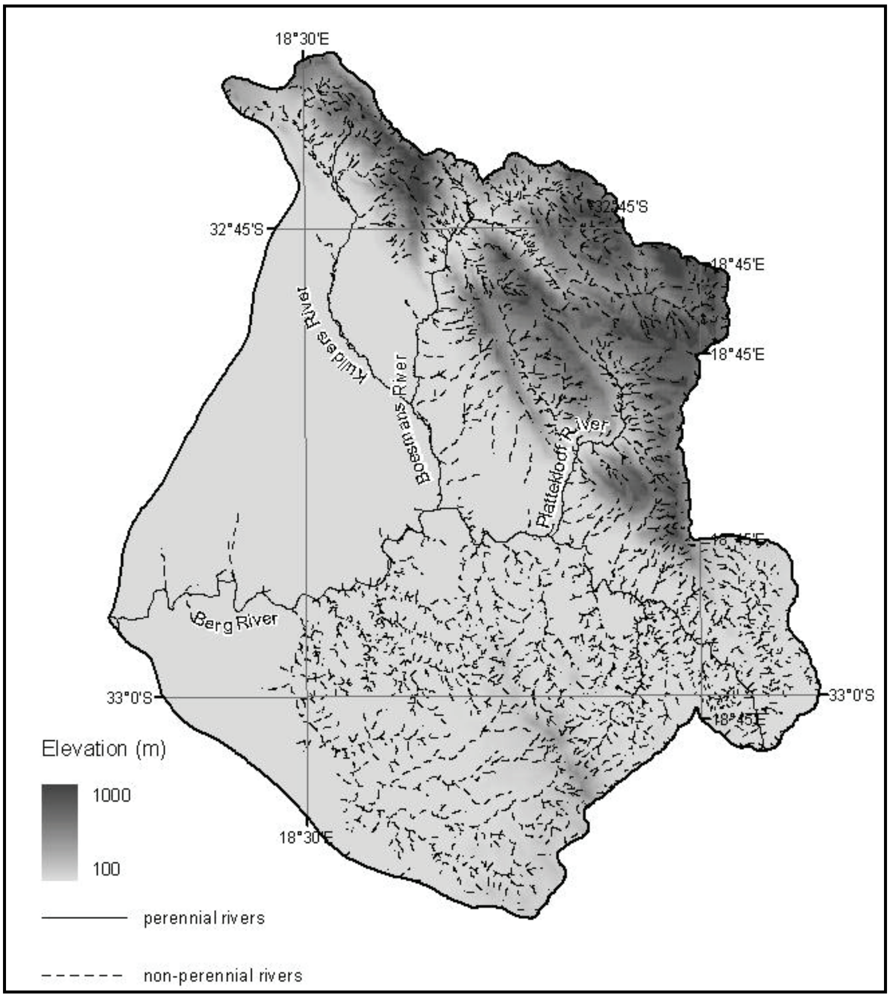

Figure 1.2.5. Drainage patterns within the G10K catchment (1:50 000 rivers, DWAF)

The landuse in the area is varied (Figure 1.2.6). On the low lying areas, in the eastern regions of the catchment and to the south of the Berg River (corresponding, for the most part, with the Morreessburg Formation), dryland agriculture (wheat) is practised. To the west of the Boesmans River, pockets of natural vegetation described as shrublands and low fynbos are found. Temporary commercial agriculture (potatoes) with central pivot irrigation occurs to the west of the Boesmans River and on either side of the Berg River as it exits the catchment. Vineyards are found in the vicinity of the confluence of the Plattekloof River with the Berg River although this is a recent development as it is not mapped on the National Landcover 2000 database (Figure 1.2.6). On the elevated areas of the Bo-Piketberg, natural vegetation in the form of Low and High Fynbos is found with reported alien vegetation infestations. Pockets of cultivated irrigated land are found with fruit tree orchards (deciduous and citrus) being farmed.

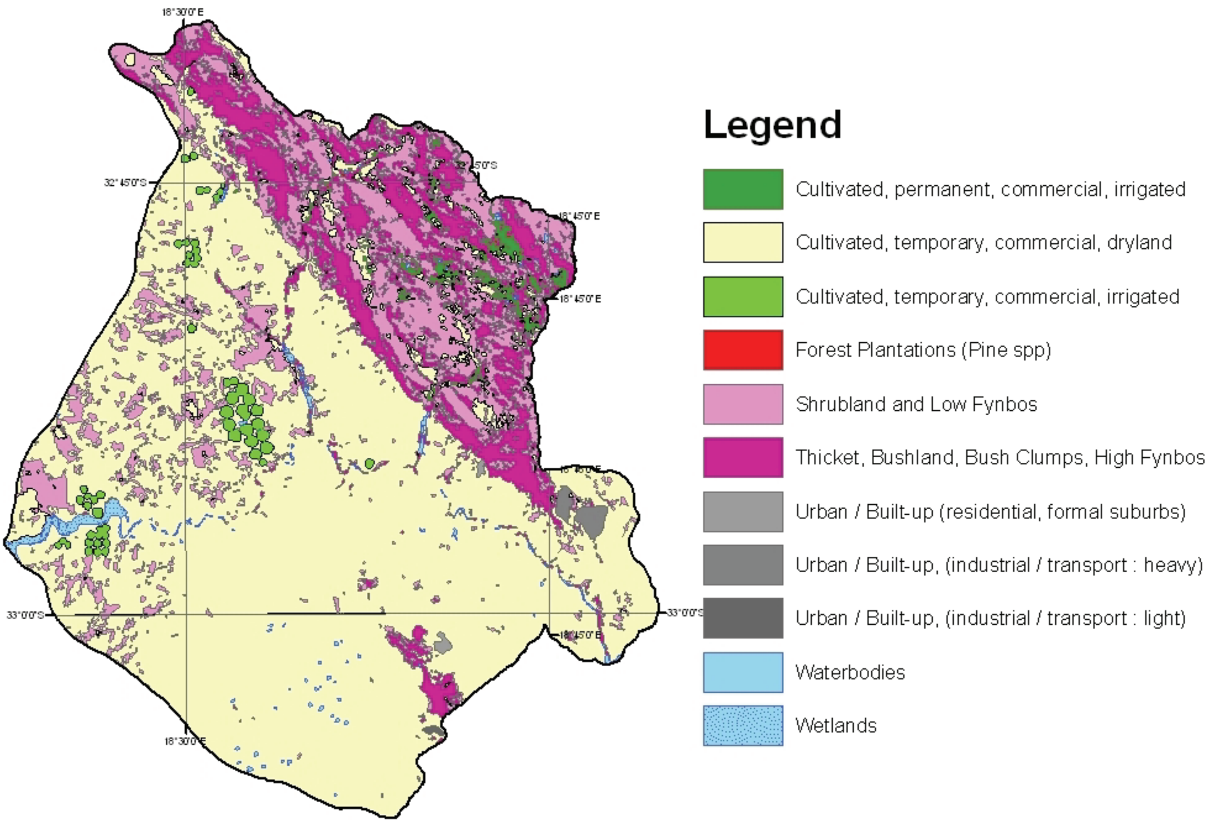

Figure 1.2.6: Landuse map (National Land Cover 2000, courtesy ARC-ISCW)

2 REMOTE SENSING FOR WATER USE DETERMINATION

A complete literature review on the use of remote sensing for water use determination was completed as Deliverable 1 (WRC, 2006) and is included on the enclosed CD.

2.1 Determining water balance components

The hydrologic cycle (Figure 2.1.1) is an open system in which solar radiation serves as a source of constant energy, which can be measured by remote sensing. Water from the surface of oceans evaporates, water vapour moves through the air and under suitable atmospheric conditions, condenses to form droplets. Precipitation falling on the land surface enters into the hydrologic cycle where some is stored, some drains across the land and some seeps deep into the ground, feeding the soil water zone or vadose zone. Excess vadose water is pulled down by gravity and reaches the zone of saturation or water table. Transpiration by plants and evaporation from land surfaces is called evapotranspiration. Total flow in a stream is runoff (Fetter, 2001).

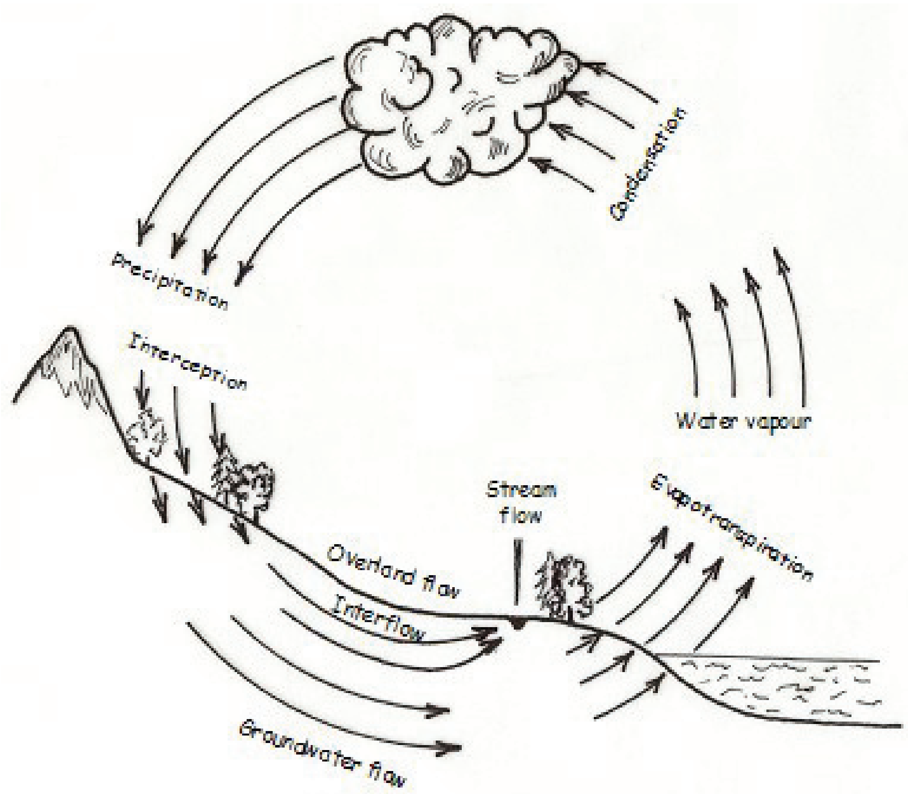

Figure 2.1.1: The hydrologic cycle (after Ward, 1975)

The hydrologic equation is a simple statement of the law of mass conservation and is expressed as

Inflow = outflow ± changes in storage

or

Precipitation = Evapotranspiration and Runoff ± changes in Water Storage

Many of the components of the water balance can be measured using remote sensing. The water balance integrates the effects of climate on patterns of vegetation distribution and productivity. Functional relationships can be established using water balance variables as predictors of vegetation response. Landuse change causes modification of ecological processes. Relationships exist between precipitation, actual evapotranspiration and vegetation productivity (Mora & Iverson, 1998) with evapotranspiration being the dominant term of the water balance, especially in irrigated landscapes.

2.2 Precipitation

The possibility of measuring rainfall using remote sensing technologies was discussed on pp. 46-47 of the literature review (WRC, 2006). It was noted that precipitation figures derived directly from satellite imagery are instantaneous and do not necessarily provide reliable estimates of daily accumulated precipitation. Although great advances have been made in precipitation monitoring using remote sensing, it may be true to state that when considering actual daily, monthly or annual precipitation figures, weather station data may still be the most accurate even though it does not provide the spatial or temporal distribution advantages of remote sensing. Perhaps the best approach is that of the ARC-ISCW whereby data from weather stations are used in combination with remotely sensed data and long-term averages to create rainfall grids which reflect the spatial variation of precipitation (ARC-ISCW, 2005).

2.2.1 Spatial variation of rainfall

The spatial variation in the annual amount of rainfall depends chiefly on geography, i.e. latitude, distance from the ocean, elevation and shape of the terrain (Linacre, 1992). Given that the study area is, in climatic terms, small, the latitude and distance from the sea will not be considered as their effect on the spatial variation within the study area will be negligible. The effect of elevation is due to the orographic uplift on windward slopes which enhances the likelihood of clouds dense enough for raindrops to form (Linacre, 1992). It should be noted that the precipitation falling on a mountainous area consists of an amount that would occur in the absence of mountains as a result of convection and cyclonic convergence, and an orographic component due to the intensification of these processes over the mountains, as well as to the forced uplift of air by the terrain (Barry, 1992).

The increase in rainfall with elevation is reported to be greater at lower latitudes and greater in summer. However, the gradient of rainfall with elevation also depends on elevation itself and orientation. The gradient increases with height, especially in winter at the mid-latitudes (such as the study area) as cloud formation is not due to thermal convection (Linacre, 1992). The orientation, which refers to whether the slope is on the windward or leeward side of a mountain, also plays a role.

The pattern of rainfall depends partly on the shape of the terrain. A western Colorado study (Spreen, 1947, reported in Barry, 1992) showed by graphical analysis that mean winter precipitation amounts are highly correlated with the combined influence of station elevation, the maximum relative relief within an 8 km radius, exposure (fractional circumference of a circle, 32 km in radius, not containing a barrier more than 300 m higher than the station) and orientation (the direction to the sector of greatest exposure). By comparison, precipitation against elevation alone showed much less correlation. Furthermore, Pedgley (1970, reported in Barry, 1992) noted that in general, the precipitation maxima over mid-latitude mountain ranges are closely related to the 'smoothed' topography. Rainfall gauges in small valleys within a mountain complex may therefore record totals more characteristic of the surrounding ranges (Barry, 1992).

The correlation between rainfall measured at two places depends on their distance apart, the nature of the terrain and the rainfall, including whether daily, monthly or annual rainfall is considered. The correlation is highest for places which are close together, in a flat landscape, away from the coast where light rain affects a large area and when annual rainfall is considered (Linacre, 1992).

2.2.2 Rainfall in the study area

Rainfall records, for the study period, in and around the G10K catchment were sourced from the ARC-ISCW, Hortec, South African Weather Service (SAWS) and private farms or individuals. As only three of these weather stations fall within the G10K catchment, a 20 km buffer zone around the G10K catchment was used to improve the number of sample points to be used in the interpolation. A total of 19 weather stations are located within this buffer zone. It can be seen in Figure 2.2.1 that these weather stations are well distributed and if there is inadequate distribution, it is to the west of the G10K catchment in a topographically uniform area.

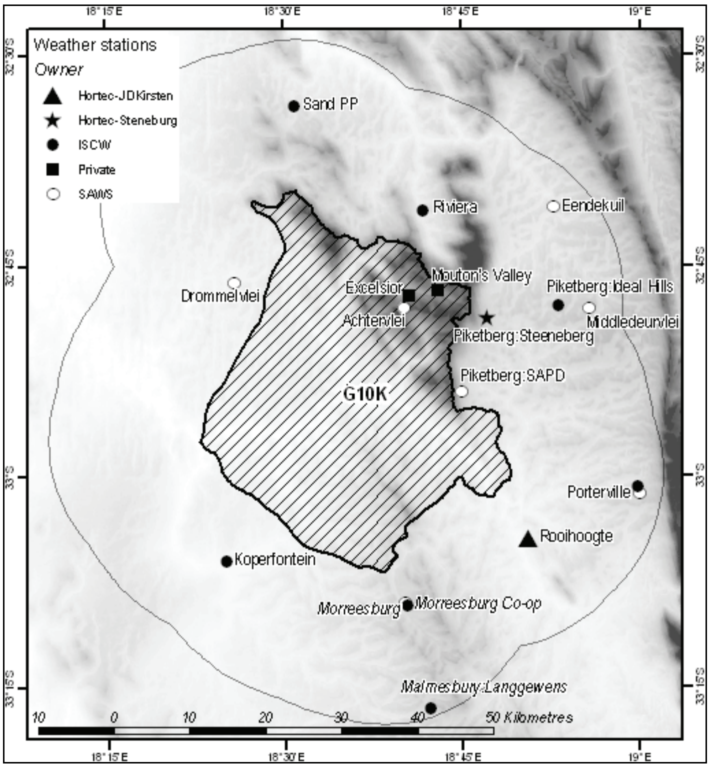

Figure 2.2.1: Location, name and ownership of weather stations recording rainfall within a 20 km buffer zone of the G10K catchment

It can be seen in Figure 2.2.2 that the rainfall for the study period was highly variable with values ranging from less than 400 mm at the Sand PP and Rooihoogte station, to more than 1100 mm at Mouton's Valley and Achtervlei in Bo-Piketberg. This large fluctuation occurred within the space of 30 km. If the data is explored to uncover any correlations between rainfall and altitude (Figure 2.2.2), it can be seen that although the most elevated sites did receive the most rainfall and the lowest lying sites received the least amount of rainfall, the lower altitudes received highly variable amounts of rain.

It would be more accurate to draw conclusions about the effect of topography on rainfall in the study area, rather than the more simplistic rainfall/elevation relationship. The study area receives most of its rain during the winter months as a result of cold front systems which approach from the Atlantic seaboard to the west (Haasbroek, 2008). In Figure 2.2.2 it can be seen that the rainfall is generally low on the flat plains to the west of Bo-Piketberg but on the Bo-Piketberg itself and the elevated areas around Moorreesburg, there is an increase in rainfall. As the areas of elevated topography are small relative to the size of the rain bearing weather systems, there are low lying areas such as recorded at Riveira and Piketberg:Steeneberg which benefit from the close proximity of elevated topography. Pedgley (1970, in Barry, 1992) noted that in general, the precipitation maxima over mid-latitude mountain ranges are closely related to the 'smoothed' topography. Rainfall gauges in small valleys within a mountain complex may therefore record totals more characteristic of the surrounding ranges (Barry, 1992). It appears that the observation by Pedgley (1970, in Barry, 1992) regarding the maximum precipitation following a smoothed topography holds true for a number of weather stations in the study area.

2.2.3 Rainfall interpolation techniques

When dealing with environmental data such as rainfall, it is not possible to measure these variables at all relevant points in space. Interpolation is a method to extract values for variables at unsampled points from measurements made at known locations within the same area. Data is converted from point observations to continuous surfaces so as to observe and compare spatial patterns. The theory of interpolation is based on the assumption that, on average, values at points close together in space are more likely to be similar than points further apart (Burrough & McDonnell, 1998, cited by Műnch, 2004). When interpolating rainfall data, three factors should be considered when assessing the accuracy of the interpolation: 1) the spatial distribution of the weather stations, 2) the number of weather stations in the study area and 3) the variation in the recorded data. On this note it should be stated that of all the weather elements, rainfall records the largest amount of variation and is therefore the most difficult to interpolate.

Often data may be available for more than one attribute per sampled location. If the attributes are spatially correlated, it may be possible to use the information about one variable to help derive the other. Co-kriging, a multi-variant extension of kriging, can be used. Műnch (2004) used co-kriging of the DEM (which was only weakly correlated to rainfall) as additional input in the interpolation procedure.

Műnch (2004) presented a comprehensive discussion on the various interpolation techniques and applied and compared the results of the various techniques to rainfall data and other data. The reader is referred to Műnch (2004) for more detail. Importantly, the study area used by Műnch was the Sandveld which is situated adjacent to the study area of this project on the northern boundary. The assumption was therefore that the interpolation technique which proved most accurate in the Műnch (2004) study can be used with confidence in the study area for this project.

Műnch (2004) reported that kriging with a quadratic drift gave the best result, whether it be point kriging or block kriging. However, point kriging with quadratic drift had the smallest amount of over- and under-prediction of rainfall values. It was also noted that none of the methods can predict the high rainfall values accurately, leading one to believe that there would be an underestimation of rainfall using any of these methods. The limitations of these rainfall interpolation techniques are noted.

Műnch (2004) also reported that interpolation techniques were less accurate in areas of high rainfall and, as can be seen in Figure 2.2.2, the Bo-Piketberg, for 2007/8, had high rainfall compared with the surrounding low-lying plains. The result of the interpolation should therefore be used with caution, particularly as it appears that 2007/8 was a high rainfall year.

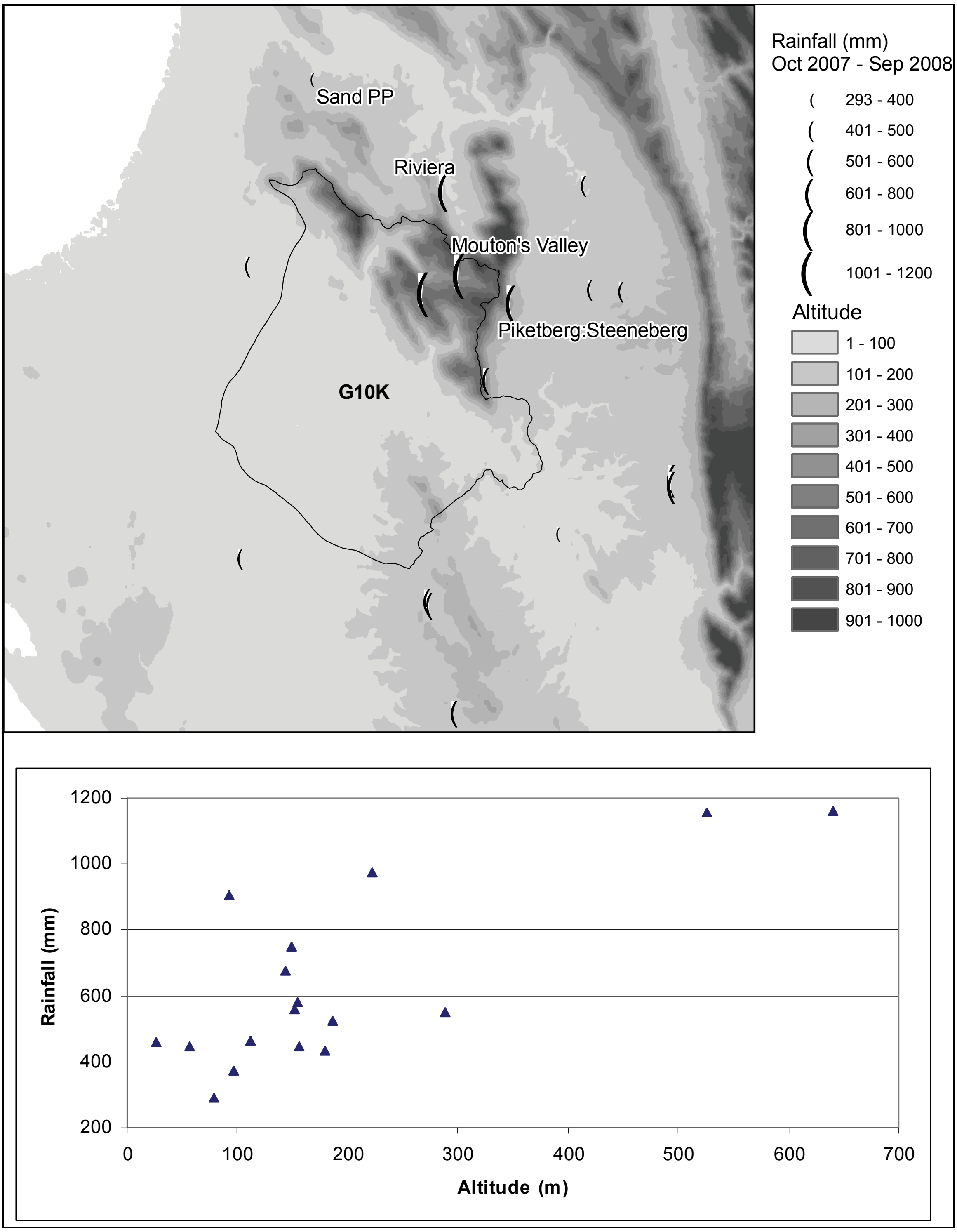

Figure 2.2.2: The recorded rainfall for the study period and its relation to altitude

It would have been useful to analyze the spatial distribution of the long-term average rainfall to determine which interpolation method would be best suited for the study area. It can be seen in Figure 2.2.3 that although rainfall has been recorded since 1879 in Piketberg, many of the recording stations have been erected recently so calculating long-term averages would be problematic.

Comparing Figure 2.2.2 and the MAP shown in Figure 1.2.4 it can be seen that the rainfall for the study period was higher than average.

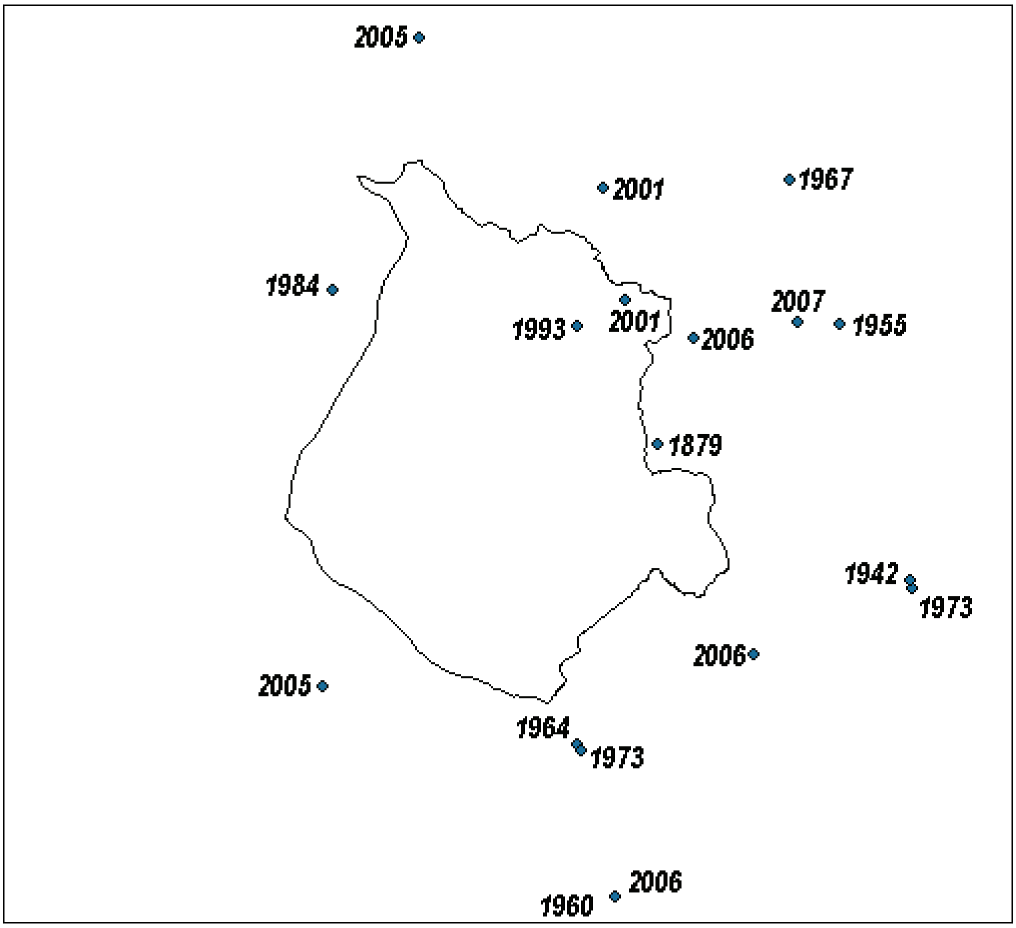

Figure 2.2.3: Start dates of rainfall records at stations in the region

Since Műnch (2004) found kriging to be the most accurate interpolation technique in the Sandveld study area, the possibility of using kriging was explored. However, due to the large variation in the data and the distance over which these variations occur, kriging could not be used. A semivariogram was plotted as the first step in the kriging process and, as can be seen in Figure 2.2.4, no trends could be detected. For this reason, kriging was not explored further.

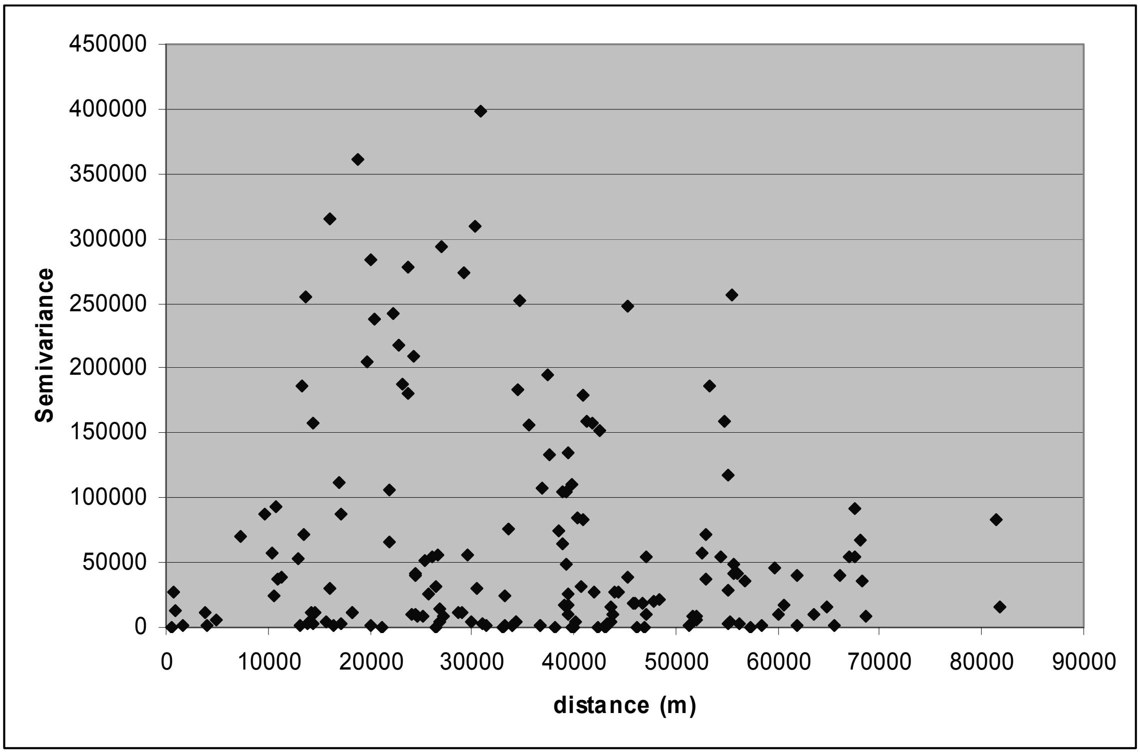

Figure 2.2.4: Semivariogram of rainfall data from weather stations in the study area

The Inverse Distance Weighting (IDW) interpolation explicitly implements the assumption that things that are close to one another are more alike than those that are further apart. To predict a value for any unmeasured location, IDW will use the measured values surrounding the prediction location. Those measured values closest to the prediction location will have more influence on the predicted value than those further away. Thus, IDW assumes that each measured point has a local influence that diminishes with distance. It weights the points closer to the prediction location greater than those further away, hence the name Inverse Distance Weighting (ESRI, 2006). Original input data is also not adjusted and it was for these reasons that the IDW method was chosen.

The IDW method was used to interpolate both monthly and annual rainfall and the results of the annual and monthly 2007 interpolated rainfall are given in Deliverable 5. The influence of topography on the amount of rainfall, especially in the winter months, can clearly be seen; however, the shape of the high rainfall areas does not realistically follow the topography even though its influence can be seen Figure 2.2.5.

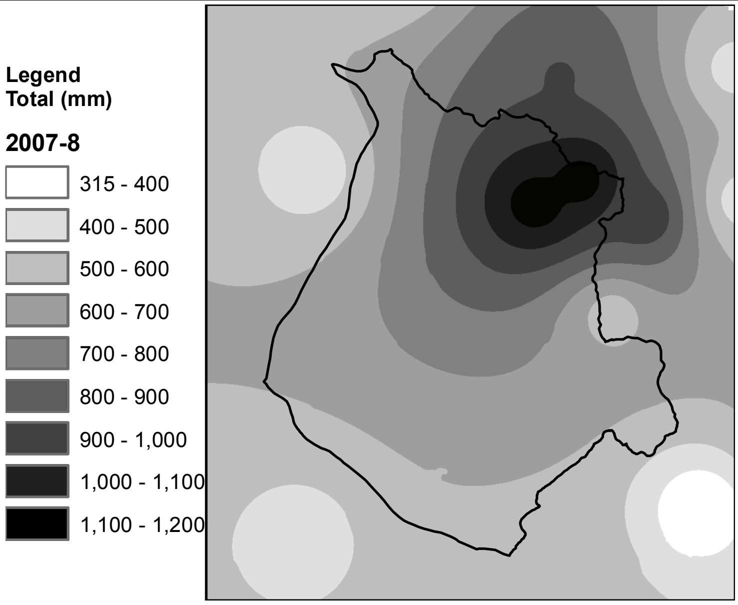

Figure 2.2.5: Unrealistic rainfall pattern produced by using an IDW interpolation technique

2.2.4 Selected methodology

The ARC-ISCW creates rainfall grids using a combination of automatic weather station rainfall data and downloaded satellite rainfall data. Each grid can be used for the identification of the actual decadal rainfall total in mm across South Africa and can be summed to obtain the total rainfall over specified time periods (ARC-ISCW, 2005).

The methodology for plateau and coastal regions given in the grids' metadata is as follows:

- Rainfall data from about 550 automatic stations is extracted.
- Satellite rainfall estimates are downloaded from African Data Dissemination Service.
- The interpolation method assigns a rainfall value to a specific point based on the measured rainfall at the five closest rainfall stations and the satellite rainfall estimate.
- Rainfall data from stations are combined with the satellite rainfall estimate data for 11 500 points spread evenly over South Africa.
- New combined estimate values are interpolated through the IDW method. (ARC-ISCW, 2005).

There is, however, a resolution limitation pertaining to the use of this dataset. The resolution of the rainfall grids is 1 km and the resolution of the original satellite rainfall estimate is 8 km. In addition, weather stations are irregularly spaced over South Africa which should allow for regional modelling rather than analyzing data at a microclimate scale (ARC-ISCW, 2005).

2.2.5 Results

The ARC-ISCW decadal datasets were obtained for the study period and summed in order to obtain monthly rainfall grids and an annual rainfall grid for the period 1 October 2007 to 30 September 2008. These grids are shown in Figure 2.2.6.

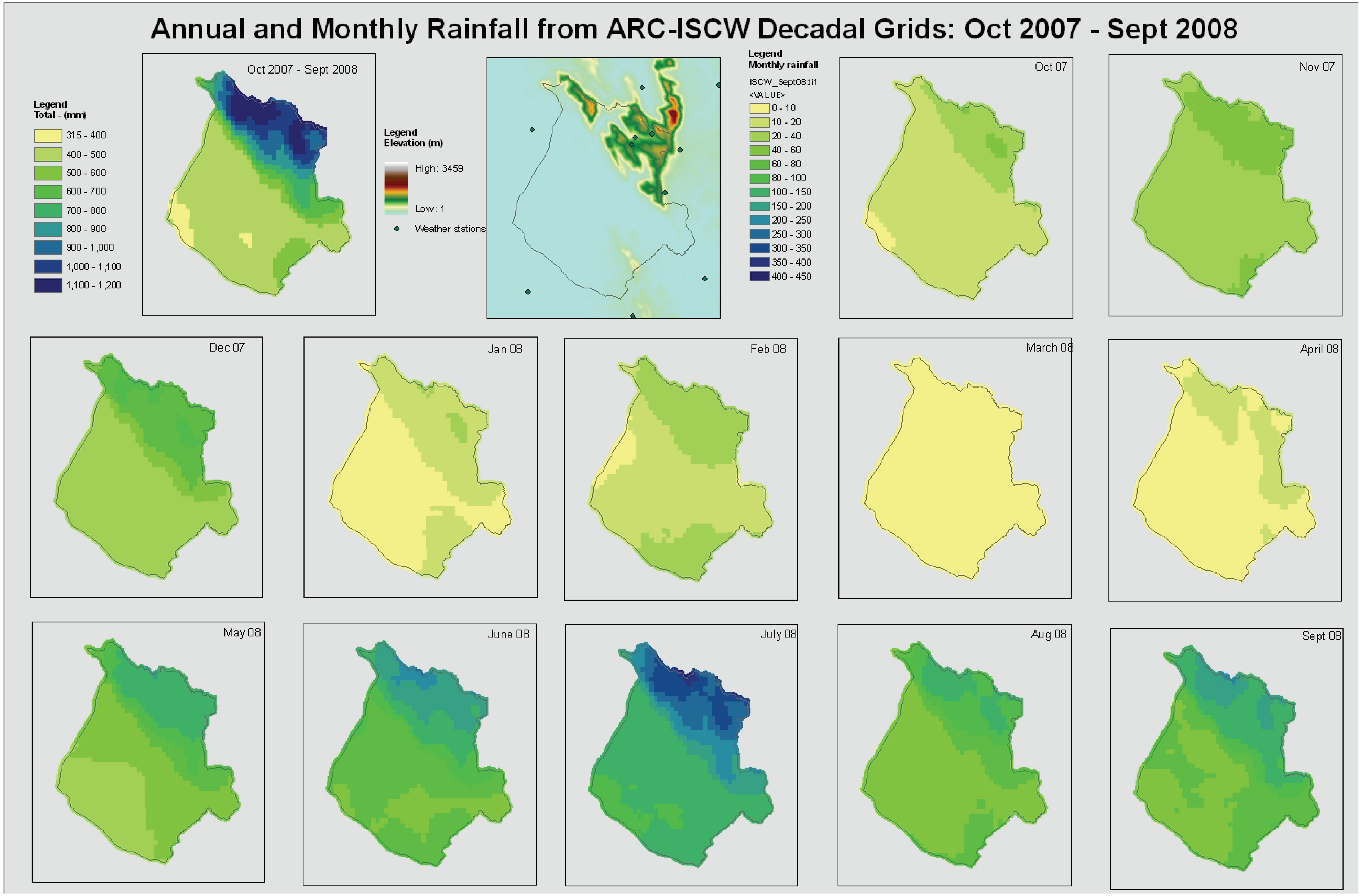

Figure 2.2.6: Summed monthly and total rainfall for the period 1 October 2007- 30 September 2008 from ARC-ISCW decadal rainfall grids

If the results shown in Figure 2.2.6 are examined, it can be seen that the ARC-ISCW rainfall grids show a realistic spatial and temporal rainfall pattern. In general, the highest amount of rain falls on the Bo-Piketberg mountainous area with significantly less rain falling on the low lying areas in the rest of the catchment. As expected, the winter months show the highest amounts of rainfall, with July being particularly wet in the mountainous areas (up to 450 mm) and in some places, almost 50% of rain for the period fell in July. June and September also recorded high rainfall with highs of 267 and 230 mm respectively. The range in values across the catchment (up to 340 mm in July) especially in the wet months highlights the significant role the mountain plays in the rainfall patterns of the G10K catchment. As expected, rainfall in the summer months is much lower than in the winter months, with a peak in December, but the same spatial distribution throughout the year is noted. The total volume of water which fell as rain for the G10K catchment in the study period can be calculated as:

Total volume rainfall (m^3) = Mean rainfall for study area (m) x catchment area (m^2)
= 0.6 x 1 260 372 503
= 771 650 461 m^3

This equates to 0.771 km^3 for the twelve month period from 1 October 2007 to 30 September 2008.

2.2.6 Validation

The usual approach to validate interpolations is to exclude some of the data from the interpolation process and to use this data to validate the results. Since the interpolation was not done by the project team, a list of automatic weather station locations which were used as input in the creation of the ARC-ISCW decadal rainfall grids was obtained and plotted. In the 20 km buffer zone around the G10K catchment (see Figure 2.2.1), a total of eight stations for which rainfall data had been obtained, were not used in the ARC-ISCW interpolation process.

Validation at a monthly level is also necessary since the water balance will be calculated at monthly as well as at annual level. It is expected that the correlation between the measured dataset and the interpolated dataset will be weaker at monthly scale than at annual scale as was noted earlier in the text.

The rainfall grids were validated firstly according to the summed results for the entire study period (one hydrological year, 1 October 2007-30 September 2008) and then rainfall grids for each month were validated. The rainfall record from each of these weather stations is noted in Table 2.2.1 and the corresponding value from the ARC-ISCW grid is listed alongside with a correlation coefficient of 0.96 being calculated.

TABLE 2.2.1: COMPARISON OF THE INTERPOLATED RAINFALL GRIDS VALUE WITH THE MEASURED RAINFALL AT WEATHER STATIONS NOT USED IN THE INTERPOLATION PROCESS (1 OCT 2007- 30 SEP 2008) – IN MILLIMETRES

WEATHER STATION NAME	WEATHER STATION MEASURED RAINFALL	ARC-ISCW GRID INTERPOLATED VALUE	DIFFERENCE (MEASURED VALUE MINUS INTERPOLATED VALUE)
Drommelvlei	447	435	12
Sand PP	507	372	135
Mouton's Valley	1155	1069	86
Achtervlei	1163	1056	107
Piketberg:Steeneberg	973	1109	-136
Piketberg:ideal Pools	447	421	26
Middeldeurvlei	433	508	-75
Porterville	675	611	64
Correlation coefficient	0.96		
Covariance	87410		

It can be seen that when using the ARC-ISCW interpolated grids, there is an underestimation of annual rainfall in the Bo-Piketberg region (~100 mm), Porterville (64 mm) and at Sand PP (135 mm). This is quite significant as it amounts to about 10% of total annual rainfall in the case of the mountainous Bo-Piketberg and Porterville and over 30% at the more arid Sand PP station. There is a good correlation at Drommelvlei and Piketberg: Ideal Hills with the two results being within roughly 5% of each other. The interpolation technique overestimates rainfall at only two of the stations with a 15% overestimation at Middeldeurvlei and a 12% overestimation at the Piketberg: Steeneberg station probably due to the close proximity of the mountain. It should be highlighted that annual rainfall at the stations within the G10K catchment (Achtervlei and Moutons Valley) was underestimated by about 10%. This may be significant when calculating the water balance and contributes to uncertainty in the modelled data.

TABLE 2.2.2: VARIATION IN MEASUREMENTS (MM) FROM WEATHER STATION WITHIN OR JUST OUTSIDE THE G10K CATCHMENT AND THE ARC-ISCW RAINFALL GRIDS ON A MONTHLY BASIS

	OCT	NOV	DEC	JAN	FEB	MAR	APR	MAY	JUNE	JULY	AUG	SEPT
Drommelvlei												
A	11	18	30	0	3	3	0	47	87	137	43	68
B	43	22	27	5	9	2	8	45	84	108	51	65
Correlation coefficient (by station)						0.96			Covariance (by station)			1256
Mouton's Valley												
A	42	83	40	20	20	10	13	159	192	272	121	182
B	32	44	73	18	34	7	10	128	177	301	97	146
Correlation coefficient (by station)						0.97			Covariance (by station)			6755
Achtervlei												
A	74	59	43	21	5	10	11	131	213	310	106	180
B	37	49	79	19	33	8	10	125	171	292	103	144
Correlation coefficient (by station)						0.97			Covariance (by station)			7186
Piketberg: Steeneberg												
A	26	36	41	7	13	11	11	103	131	292	143	158
B	88	49	76	19	35	9	11	125	164	311	97	149
Correlation coefficient (by station)						0.95			Covariance (by station)			6566
Correlation coefficient by month												
	-0.39	0.61	0.99	0.76	0.65	0.99	0.89	0.89	0.85	0.97	0.9	0.97

A = Weather station measured rainfall

B = ARC-ISCW grid interpolated value

It can be seen from Table 2.2.2 that there is generally a good correlation between monthly measured data and interpolated values for each individual station with the correlation coefficient ranging from 0.95 at Piketberg: Steeneberg to 0.97 at Achtervlei and Mouton's Valley. The correlation coefficients of monthly values across the four stations were more varied ranging from -0.37 in October to 0.99 in December and March. It can be seen that there is generally a stronger correlation in higher rainfall months as in these months the rain is probably as a result of frontal systems leading to a more even distribution of rain.

It should be reiterated that the ARC-ISCW grids were not intended to be used for quaternary scale catchments but until such time as higher resolution data is available it may be the best approach.

2.2.7 Uncertainties associated with rainfall estimation

Haasbroek (2009) reports that the quality of raingauge data may be affected by mechanical or electrical failure, human or animal interference, or debris settling inside the collector funnel hindering rainwater from reaching the measuring device. Systematic errors may include the proper calibration of the gauge measuring mechanism (e.g. tipping bucket) and problems with the tipping bucket mechanism itself, the correctness of gauge installation (whether or not the gauge is level) the sharpness of the outer rim of the gauge (whether a drop will be cut in two or fall completely inside or outside the gauge), depth of the collector funnel (leading to splash out), and the effect of wind (Haasbroek, 2009).

In the Atlas of Climatology and Agrohydrology, Schulze (2007) explains some of the uncertainties associated with rainfall estimation. It is stated that the measurement of rainfall is a simple procedure provided that accuracy is not essential, as an exact measurement of rainfall is impossible to obtain owing to the random and systematic errors which occur in measuring rainfall (Schulze, 1985, in Schulze 2007). Point estimations (from raingauges) are reported to frequently underestimate rainfall by 20% and the conversion of point to areal rainfall can add a further 10-20% error which may increase to 60% in mountainous areas.

Fog contributions to precipitation are not recorded by standard raingauges and it has been reported that in many mountainous areas so-called fog catch may in fact exceed total rainfall recorded (Schulze, 1979, and Schmidt & Schulze, 1989; both in Schulze, 2007). It is possible that coastal fog may also play an important contributing and unmeasured role to precipitation.

It can almost certainly be accepted that the rainfall for the G10K catchment was underestimated for the study period due to the above uncertainties in rainfall measurements and the challenge is to try to quantify this uncertainty.

2.2.8 Conclusion

It was found that for the G10K catchment and its 20 km buffer zone, there is a good correlation between the total measured rainfall for the study period and the ARC-ISCW interpolated grid values. As expected, the correlations are more variable at monthly time scale.

On the whole, for the G10K catchment, the ARC-ISCW interpolated rainfall grids underestimate rainfall for the study period by up to 10%.

The effects of wind and other inaccuracies may cause an underestimation of annual rainfall of up to 20%.

It is probable that condensation from fog onto plant surfaces contributes to total precipitation but further research would be needed before this can be quantified.

In conclusion, it can be said that the spatial rainfall pattern provided by the ARC-ISCW interpolated rainfall grids appears to be sound and this was validated using weather station data which was not included in the interpolation process. Although many uncertainties have been introduced, on the whole it can be said that there is a significant underestimation of rainfall in the G10K catchment as a result of: 1) underestimation of rainfall in the ARC-ISCW interpolated grid; 2) random and systematic errors in the collection of rainfall; and 3) the as yet unquantified contribution of condensation to precipitation. Other sources of inaccuracies are also possible and the reader is advised to consult Schulze (2007) for elucidation.

2.3 Evapotranspiration

The various approaches to estimating evapotranspiration were explained on pp. 35-47 of the literature review (WRC, 2006) with the emphasis being on the energy balance approach. To avoid confusion in terminology, it is recommended that readers who are not familiar with the subject should consult Appendix I for definitions and descriptions of the various evapotranspiration terms which will be used in the text. Amongst literature published subsequent to the writing of the literature review a report was published which should be mentioned. WaterWatch (2008) executed a very successful study (initiated by the Western Cape Department of Agriculture) on the water use efficiency of winelands of the Western Cape. The Surface Energy Balance Algorithm for Land (SEBAL) was applied in conjunction with Landsat satellite imagery to estimate water consumption and water use efficiency of vineyards. The results of the study are reported to have improved the understanding of the spatial and temporal variation of water use efficiency in grape cultivation.

Evapotranspiration is the combined process whereby water is lost from the soil surface by evaporation and from the plant by transpiration. The two processes occur simultaneously and it is difficult to distinguish between the two processes. However, it can be said that with the exclusion of water availability, evaporation is mainly determined by the fraction of solar radiation reaching the soil surface and this is largely determined by plant canopy (Allen *et al.*, 1998). Water loss during transpiration through the stomata on the leaf is dependent on the genetics and stage in growth of the plant as well as external factors such as radiation, air temperature and humidity, and wind. It can therefore be said that under the same physical conditions, different species of plants will have different rates of evapotranspiration.

It is important to state at the outset that the evapotranspiration calculated using these remote sensing energy balance models is actual evapotranspiration, in other words, the amount of water that actually evapotranspired (in mm or converted to a volume) from the study area will be calculated.

2.3.1 The energy balance approach

Evapotranspiration can be estimated as a residual in the surface energy balance. The net incoming solar radiation at any location is converted into heat energy, heating the air above the soil surface and the soil itself, and into latent heat of evapotranspiration from the soil surface. If the net incoming radiation and the energy consumed in heating the air and the soil can be measured, then the latent heat of evaporation from the soil can be estimated and the rate of evaporation of water deduced (Blight, 2002). These exchanges of energy or heat are called fluxes.

Energy flux density available at the earth's surface is either sensible heat which results in temperature change with no change of phase of water, or latent energy which results in a phase change of water usually from liquid to vapour with no temperature change (Savage *et al.*, 2004). The estimation of these fluxes at the land surface has long been recognized as the most important process in the determination of the exchanges of energy and mass among hydrosphere, atmosphere and biosphere (Su, 2002).

The sources of energy in the soil-plant-atmosphere system include:

- Solar energy during the day and terrestrial radiant energy at night;
- Heat energy carried into the area by wind (advected energy);
- Heat energy stored by vegetation and in land masses;
- Heat energy stored in water bodies.

The most important of these energy sources is usually solar energy but advected energy may on occasion be considerable. However, due to its complex nature, advected energy is not routinely accounted for when using methods to estimate surface sensible heat and latent energy flux densities (Savage *et al.*, 2004).

The advantage of using the energy balance approach with remote sensing data is that it is not scale dependent, not delimited by catchment boundaries and not restricted to one crop type. The energy balance approach is based on a complete energy balance for each pixel where evapotranspiration is predicted from the residual amount of energy remaining from the energy balance equation. The model to be used in this research is known as the Surface Energy Balance System algorithm and will now be discussed further.

The Surface Energy Balance System (SEBS) is a scale independent model proposed by Su (2002) for the estimation of atmospheric turbulent fluxes and evaporative fraction using satellite earth observation data in combination with meteorological information. Reflectance and radiance measured by the satellite are used to calculate land surface parameters – albedo, emissivity, surface temperature, Normalized Difference Vegetation Index (NDVI), fractional vegetation cover and leaf area index. If a detailed land use map is available then associated surface parameters (canopy height, displacement height and surface roughness) can be obtained from here; alternatively, these parameters can be modelled from the remotely sensed data. Meteorological inputs are radiation[2], temperature[2 & 3], air pressure[2] at surface and at reference height, humidity[2], wind speed[2] at reference

[2] Instantaneous i.e. hourly average at time of satellite overpass

height and sunshine duration[3] all obtained from weather stations. Other inputs include solar zenith angle, digital elevation model and Julian day.

The SEBS algorithm has been used to estimate evapotranspiration in the Netherlands (Hailegiorgis, 2006), China (Jin *et al.*, 2005; Xin, 2007; Su *et al.*, 2003; Su & Roerink, 2004), and Spain (Jia *et al.*, 2003). The mean error of SEBS estimates is expected to be around 20% relative to the mean sensible heat flux *H*, when the input geometrical and physical variables are reliable (Su, 2002).

The SEBS model is available as part of the free open source software package ILWIS (available at *www.52north.org*), making it a good choice to use for research purposes as researchers may use the already programmed model without having to programme the formulae in themselves or to have to pay consultants to provide an evapotranspiration estimate using models protected by intellectual property constraints.

2.3.2 Satellite data selection, acquisition and preparation

Satellite data availability has been a reported problem during the course of this project (WRC, 2008a, p. 7; WRC, 2007b, pp. 12-13) and the issue of spatial scale and temporal scale was discussed in the literature review (WRC, 2006, p. 75). The uncertainty of data availability due to the fact that the study period was chosen to run concurrently with the project, led to indecision as to which data would be the best to use for the study as it was not known *a priori* exactly what data would be acquired (WRC, 2007b, pp. 13-15; WRC, 2008a, p. 7). Once the study period had passed, it was possible to analyze the data availability and make a final decision as to which imagery has the best spatial, spectral and temporal resolution.

The data availability is documented in Deliverable 5 (WRC, 2008b, pp. 15-20) where it is reported that despite the desirable spatial and spectral resolution of ASTER, only two usable images were acquired for the entire study period. Additionally, ASTER shortwave infrared data acquired since April 2008 are not useable, and show saturation of values and severe striping (JPL, 2009). The shortwave infrared bands are used in the calculation of

[3] Daily average

broadband albedo and an alternative method of converting narrow to broadband albedo, using only the visible and near infrared bands, will need to be investigated before the ASTER images can be used to estimate evapotranspiration. Landsat 5 was not available for the study period and the well documented scan-line corrector problem of Landsat 7 along with a hiatus of 96 days in the winter and 48 days at a crucial time of year with respect to water use, resulted in Landsat being excluded as the imagery of choice for the project.

MODIS images are captured daily and therefore it is possible, in South Africa, to obtain a good coverage throughout the year. A data search revealed that usable data could be obtained at least every 10-20 days with a higher temporal resolution being possible. It was reported in the third progress report (WRC, 2007b, p. 14) that the resolution of MODIS (1000 m when using MODIS level 1, i.e. MOD02 or MYD02) makes it unsuitable for a small study area such as quaternary catchments. However, in the absence of an alternative suitable image source and the fact that the image resolution may be downscaled to 250 m (Kustas *et al.*, 2003) if MODIS data products are used, MODIS was selected, at the very least, to illustrate the methodology and show the variation in evapotranspiration across the G10K catchment. MODIS images were selected, ordered and downloaded for the dates shown in Table 2.3.1.

TABLE 2.3.1: SELECTED MODIS IMAGE ACQUISITION DATES IN THE STUDY AREA FOR THE STUDY PERIOD

DATE	JULIAN DAY	INTERVAL (DAYS)
04 October 2007	277	
16 October 2007	289	12
01 November 2007	305	16
11 November 2007	315	10
27 November 2007	331	16
07 December 2007	341	10
19 December 2007	353	12
29 December 2007	363	10
08 January 2008	8	10
18 January 2008	18	10
28 January 2008	28	10
07 February 2008	38	10
18 February 2008	49	11
28 February 2008	59	10
13 March 2008	73	14
24 March 2008	84	11
03 April 2008	94	10
13 April 2008	104	10
23 April 2008	114	10
07 May 2008	128	14
17 May 2008	138	10
01 June 2008	153	15
08 June 2008	160	7
24 June 2008	176	16
12 July 2008	194	18
26 July 2008	208	14
08 August 2008	221	13
18 August 2008	231	10
02 September 2008	246	15
13 September 2008	257	11
28 September 2008	272	15

MODIS level 1 (MOD02) data can be selected and ordered online at *http://ladsweb.nascom.nasa.gov/data/search.html*. The bands required are reflectance bands 1-5 & 7 and emissive bands 31 & 32 as well as geolocation files. The MODIS Swath Tool (MST) is required to process the HDF files, convert the images to a map projection, geographically subset the image, extract the relevant bands and save the image in geoTIFF format. The MST can be downloaded from *lpdaac.usgs.gov/landdaac/tools/mrtswath/index.asp*. The MST is used to project the images to the map projection used in the project (Gauss conform, central meridian 19°, WGS84 datum). The MST is also used to subset the image so that the image processing time is reduced and evapotranspiration estimates are carried out over the same geographical space (TL: -32.5°S, 18°E; BR: -33.25°S, 19°E). Finally the

MST converts the selected bands – cropped by geographical area and transformed to the required map projection – to geoTIFF format. In a similar process the "Height" (used as digital elevation model), "SensorZenith", "SensorAzimuth", "SolarZenith" and "SolarAzimuth" bands (all used for atmospheric correction) need to be extracted from the geolocation file using the MST.

The data is then imported into ILWIS. The data recorded in the original HDF is in digital number format. The data must be converted to reflectance (bands 1-5 & 7) for the reflective bands or radiance (bands 31 & 32) for the thermal bands in order to be of use in quantitative remote sensing studies. For each band the reflectance/radiance scales and offsets must be obtained from the original HDF file. The freeware HDF Explorer can be used to do this and can be downloaded from *www.space-research.org/explorer_download.html*. Using these scales and offset values, the data is converted to radiance/reflectance values.

The accurate retrieval of surface reflectance and temperature is very important in deriving land surface biophysical parameters and in determination of fluxes. In mapping the surface physical properties, the surface information is highly affected by atmospheric components (scattering by aerosols and absorption by gases, such as oxygen, water vapour and ozone) and their magnitude (Hailegiorgis, 2006). The simplified method for atmospheric correction (SMAC) proposed by Rahman & Dedieu (1994) has been programmed into ILWIS to correct for the effects of the atmosphere on MODIS visible, near infrared and shortwave infrared data. SMAC is radiative transfer model and therefore requires a description of the components in the atmospheric profile in order to correct for these effects. The required inputs into SMAC are shown in Table 2.3.2 along with the unit of measurement, the valid range and where the data can be obtained. Coefficient files for the sensor are also a requirement and this is provided for in ILWIS.

Table 2.3.2: Inputs required for SMAC

REQUIRED INPUT	UNIT	VALID RANGE	DATA SOURCE
Optical thickness	µm	0.05-0.8	MODIS Atmospheric products (MOD04) *http://ladsweb.nascom.nasa.gov/data/search.html*
Water vapour content	$g.cm^{-2}$	0.0-6	MODIS Atmospheric products (MOD05) *http://ladsweb.nascom.nasa.gov/data/search.html*
Ozone content	g.atm.cm	0.0- 0.7	Total Ozone Mapping Spectrometer (TOMS) *http://toms.gsfc.nasa.gov/*
Surface pressure map	hPa	Calculated from air temperature and elevation data formula given in Allen *et al.*(1998)	
Solar zenith angle	degree	0-50	Geolocation file described in text
Sensor zenith angle	degree	0-50	Geolocation file described in text
Solar azimuth angle	degree		Geolocation file described in text
Sensor azimuth angle	degree		Geolocation file described in text

Each of the reflective bands (bands 1-5 & 7) is atmospherically corrected using SMAC. It must be noted that a restriction of this model is the fact that solar zenith angles must be less than 50° in order to use this model correctly. In the study area, between the autumn and spring equinox, the solar zenith angle is greater than 50° at the time of image acquisition and for this reason the SMAC method for atmospheric correction could not be used on images acquired during this period. For the winter period, MODIS data products (obtainable from ARC-ISCW's Coarse Resolution Image Database) were used in place of MODIS level 1 data, negating the need for atmospheric correction. This may in fact be a better route to take, as obtaining the atmospheric input data is time consuming and there is some doubt as to whether or not it is accurate. There are many pixels of missing data in the MODIS Atmospheric products so mean values across the study area were used to correct for the entire study area. Values used for each image are included in spreadsheet format on the accompanying CD (ET_input_data.xls). Both approaches can be tested using the field validation results (Jarmain & Mengistu, 2009).

2.3.3 Image preprocessing in SEBS

The brightness (blackbody) temperature of bands 31 & 32 are one of the inputs needed in the calculation of land surface temperature. The conversion of the radiance values of bands 31 & 32 to brightness temperature is done by applying Plank's equation.

Land surface albedo is determined using the narrow to broadband albedo MODIS specific calculation formulated by Liang (2001):

$$albedo = 0.160\alpha_1 + 0.291\alpha_2 + 0.243\alpha_3 + 0.116\alpha_4 + 0.112\alpha_5 + 0.081\alpha_7 - 0.0015$$

where α_1, α_2, α_3, α_4, α_5 and α_7 are surface reflectance derived from MODIS bands 1-5 & 7 respectively.

Land surface emissivity and emissivity difference is calculated by considering the NDVI value for individual pixels. The NDVI value is used to distinguish between bare soil pixels, mixed pixels and vegetated pixels and emissivity is calculated accordingly (Sobrino, 2000, cited in Wang, 2008). Albedo of less than 0.035 is used to identify water pixels and a constant emissivity of 0.995 is assigned.

1. Bare soil pixels: taken as being where NDVI < 0.2, then

$$Emissivity = 0.9825 - 0.051 * \alpha_1$$
$$Emissivity\ difference = -0.0001 - 0.041 * \alpha_{red}$$

2. Vegetation pixels: taken as being where NDVI > 0.5

$$Emissivity = 0.990_1$$
$$Emissivity\ difference = 0$$

3. Mixed pixels: taken as being where 0.2 =< NDVI <= 0.5

$$Emissivity = 0.997 - 0.018 * fc$$
$$Emissivity\ difference = 0.006 * (1 - fc)$$

where *fc* is vegetation cover is calculated by

$$fc = \left[\frac{NDVI - NDVI_{min}}{NDVI_{max} - NDVI_{min}} \right] * (NDVI_{max} - NDVI_{min})$$

where NDVI max = 0.5 and NDVI min = 0.2 (Wang, 2008).

The land surface temperature is calculated with brightness temperatures, surface emissivity, emissivity difference, and water vapour content using a split window method as described by Sobrino & Raissouni (2000) in Wang (2008).

$$LST = btm2 + (1.97 + 0.2 * W) * (btm2 - btm1) - (0.26 - 0.08 * W) * \sqrt{btm2 - btm1} + (0.2 - 0.67 * W) + (64.5 - 7.35 * W) * (1 - \varepsilon) - (110 - 20.4 * W) * d\varepsilon$$

where *LST* is land surface temperature

btm1 is brightness temperature for MODIS band 31

btm2 is brightness temperature for MODIS band 32

W is water vapour content

ε is surface emissivity

*d*ε is surface emissivity difference

2.3.4 Meteorological data selection and preparation

The near-surface meteorological conditions (as measured by weather stations) have a direct influence on the evaporation process and inaccuracies in measurements can lead to distorted reference evapotranspiration measurements and actual evapotranspiration estimates. For this reason, accurate meteorological measurements are needed at the weather stations themselves; and when using a model such as SEBS, an accurate interpolation of meteorological data across the study area will increase the likelihood of accurate evapotranspiration estimates. This is because of the spatial variations of surface characteristics which have a large influence on the near-surface weather conditions (Voogt, 2006).

As already stated in the description of the G10K catchment, the area is quite diverse in terms of climate and the landscape could be described as heterogeneous. For this reason, using observations from a single weather station as input into the SEBS model for evapotranspiration estimation is unlikely to yield accurate results across the entire catchment. Ideally, accurately interpolated meteorological data for each pixel would be the most appropriate since the energy balance is calculated on a pixel by pixel basis. The Meteolook model (Voogt, 2006) is a distribution method for meteorological variables which takes into account the processes that influence meteorological variables such as elevation, surface roughness, albedo, incoming radiation, land wetness and distance to the sea (Voogt, 2006). The Meteolook model is used to interpolate meteorological data as input into the SEBAL model and is protected by intellectual property and to develop such a model was beyond the scope and budget of the project so an alternative method was needed.

One weather station per Köppen climate zone was selected on the assumption that this one weather station would be representing weather conditions for that entire climate zone. However, it should be noted that the Köppen system boundaries do not represent instantaneous shifts in climate but are merely transition zones where climate, and especially weather, can fluctuate. This approach therefore introduces some uncertainties as the measured meteorological data may vary significantly from pixel to pixel dependent on, amongst others, landcover and exposure, and as a result, the partitioning of the energy balance and resulting evapotranspiration estimate will be influenced. Despite this, it may be more accurate than using a single value across the entire study area given the heterogeneity of the landscape in terms of land use, topography and climate. The area processed for the evapotranspiration modelling is larger than the G10K catchment according to the co-ordinates used to clip the MODIS data (TL: -32.5°S, 18°E; BR: -33.25°S, 19°E). It can be seen in Figure 2.3.1 that there are three Köppen climate zones with extensive representation in the study area, Csa, Csb and Bssk. However, since the topographic effect can have a significant impact on recorded weather parameters, it was decided to introduce a fourth "climate zone" to delineate the mountainous area to the north and west of Piketberg. It should be noted that even though an additional zone was chosen to represent the Bo-Piketberg, the nature of mountainous terrain sets up such a variety of weather stations that any station is likely to be representative of only a limited range of sites (Barry, 1992). Additional motivation for the fourth climate zone is that field validation is taking place in this area, so as accurate results as possible are desired for this particular section of the study area in particular. The delineation of the fourth climatic zone was done by visual inspection of weather station data in and around the area looking specifically at temperature and relative humidity values. This is shown in Figure 2.3.1 along with the name and location of the weather stations selected as being representative of each climatic zone. They are: Mouton's Valley (Private), Piketberg: Ideal Hills, Malmesbury: Langgewens and Koperfontein (all ARC-ISCW).

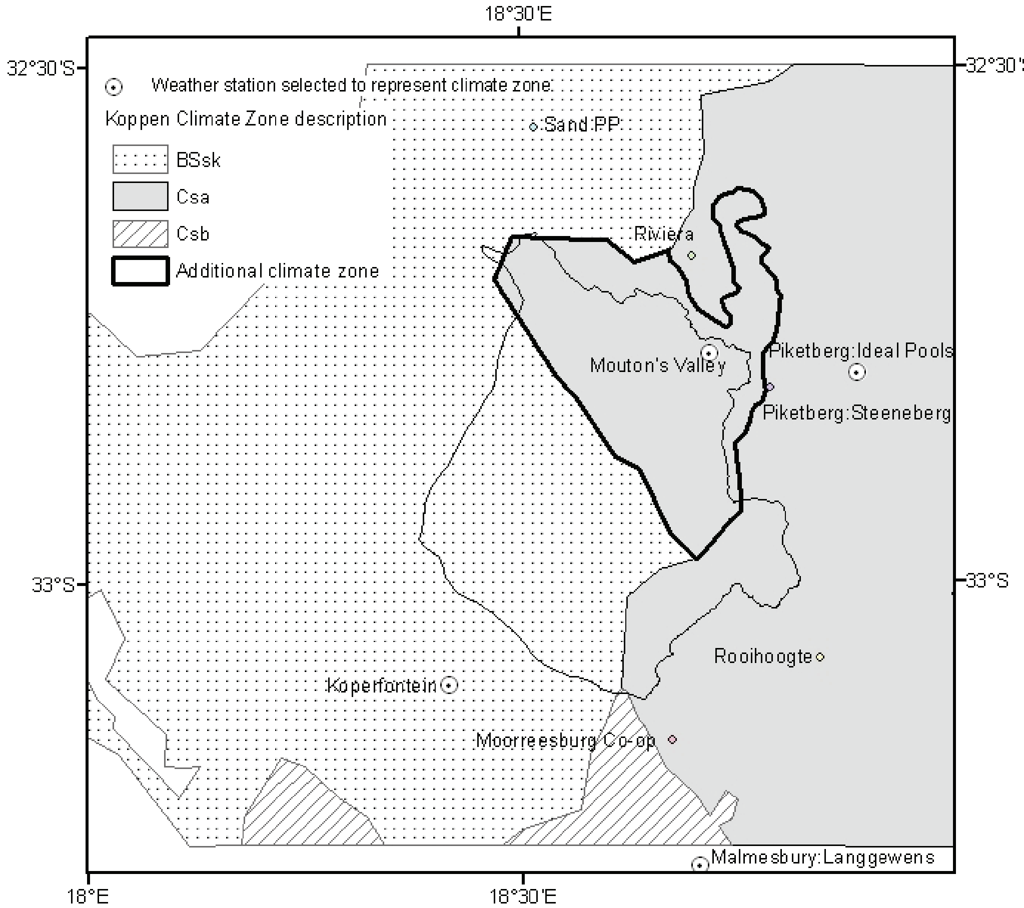

Figure 2.3.1: Köppen climate zones showing the delineation of a fourth "climate zone" and the weather stations selected to be representative of each zone

BSsk: Semi-arid with winter rainfall and cool (average annual temperature <18°C)

Csa: Humid Subtropical with winter rainfall and warm (warmest month >22°C)

Csb: Humid Subtropical with winter rainfall and cool (warmest month <22°C)

The selected MODIS images were not all captured at the same time on every day of image capture and vary from 10:10 to 11:20 local time. Hourly meteorological data was selected for each of the weather stations for the hour corresponding to the image acquisition time. With the exception of radiation, weather data (dry bulb temperature, relative humidity and wind speed) was used from all four stations. Specific humidity was calculated using a conversion formula (courtesy ARC-ISCW) with dry bulb temperature and relative humidity as inputs.

Solar radiation values were carefully studied for the weather stations over a period of time. This can be seen in Figure 2.3.2 where the hourly averaged solar radiation for each weather station is plotted at the time of selected MODIS image capture. It appeared that not all stations give consistently reliable readings as no explanation can be given for the switch in high/low values for Koperfontein and Ideal Hills. However, Mouton's Valley and Malmesbury: Langgewens appeared to be reliable when tracked across the time period. The solar radiation values for the study were taken as an average between Mouton's Valley and Malmesbury: Langgewens and these values along with other meteorological data used, are given in ET_input_data.xls on the accompanying CD.

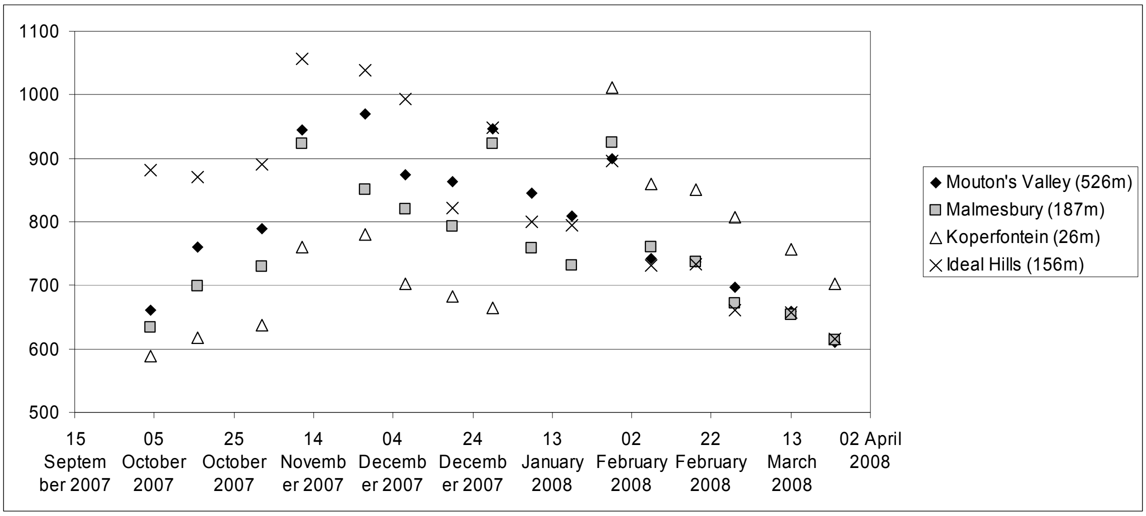

Figure 2.3.2: Hourly averaged solar radiation at image overpass time for images acquired for WRC project

The meteorological data for each parameter and for each day of image acquisition were input into grids (Figure 2.3.3) corresponding to MODIS images so that they could be input into the SEBS model as maps rather than as a single value for each parameter across the study area.

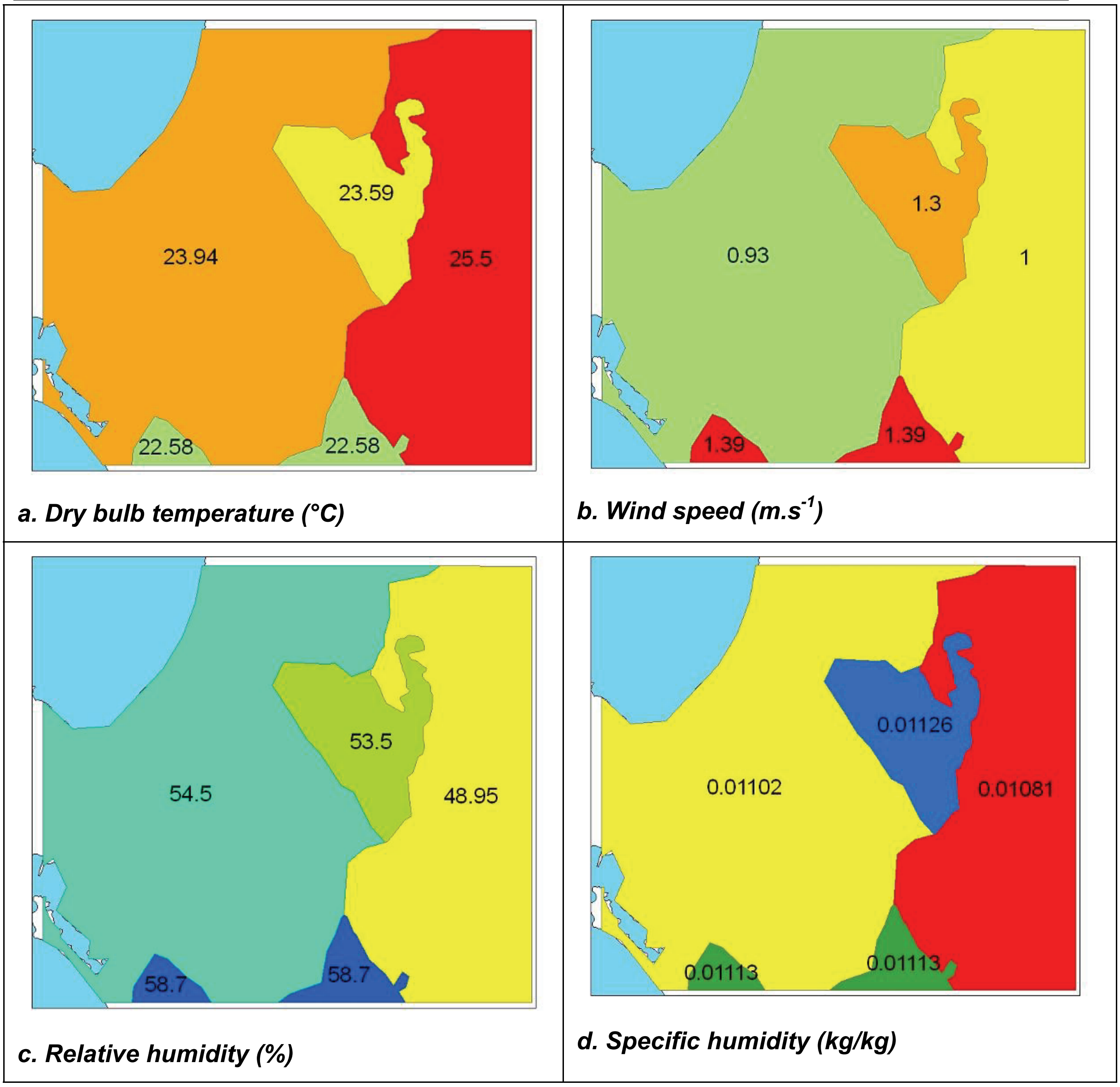

Figure 2.3.3: Examples of weather station data used for each climate zone

In addition to the above mentioned hourly meteorological parameters, a number of daily parameters are required to upscale the instantaneous evaporative fraction into daily actual evapotranspiration. These are: daily average temperature and sunshine hours per day. Sunshine hours per day are only measured at the Mouton's Valley weather station and not at the ARC-ISCW stations so one value across the entire study area was used. This may cause some small errors as due to the steep topography of the Bo-Piketberg, sunshine duration will be less than in other parts of the study area. Daily average temperature was calculated as a grid in the same way as the hourly weather parameters.

Daily potential evapotranspiration is required for every day of the year in order to upscale the daily actual evaporation to monthly or annual values.

$$ET_{relative} = \frac{ET_{actual}}{ET_{potential}}$$

where $ET_{relative}$ is relative evapotranspiration calculated in SEBS (Su, 2009a), so by rearranging the formula,

$$ET_{actual} = ET_{relative} * ET_{potential}$$

If the relative evapotranspiration is assumed to be constant between image acquisition dates (on the assumption that the soil moisture status remains the same (Su, 2009a)), and daily potential evapotranspiration is known, daily actual evapotranspiration can be estimated for every day of the year. It can be seen by this assumption that daily image acquisition is the way to ensure the most accurate upscaling of daily evapotranspiration to monthly and annual estimates. However, in reality, cloud cover and operational constraints (size of data for downloads and processing) limit the use of daily images so a trade-off is needed and a decision must be made as to the appropriate image acquisition frequency for each study.

2.3.5 SEBS evapotranspiration estimation

Once all the data preparation and preprocessing has been completed, the data can be input into the SEBS model (Figure 2.3.4) for each date of MODIS acquisition. For this study this entailed repeating the process thirty times. It can be seen that it is possible to include landuse maps with associated surface roughness, canopy height and displacement height but where these data are not available (such as in this project) these parameters can be modelled by SEBS from the input image data. Interested readers are referred to Hailegiorgis (2006) for ILWIS scripts containing these formulae.

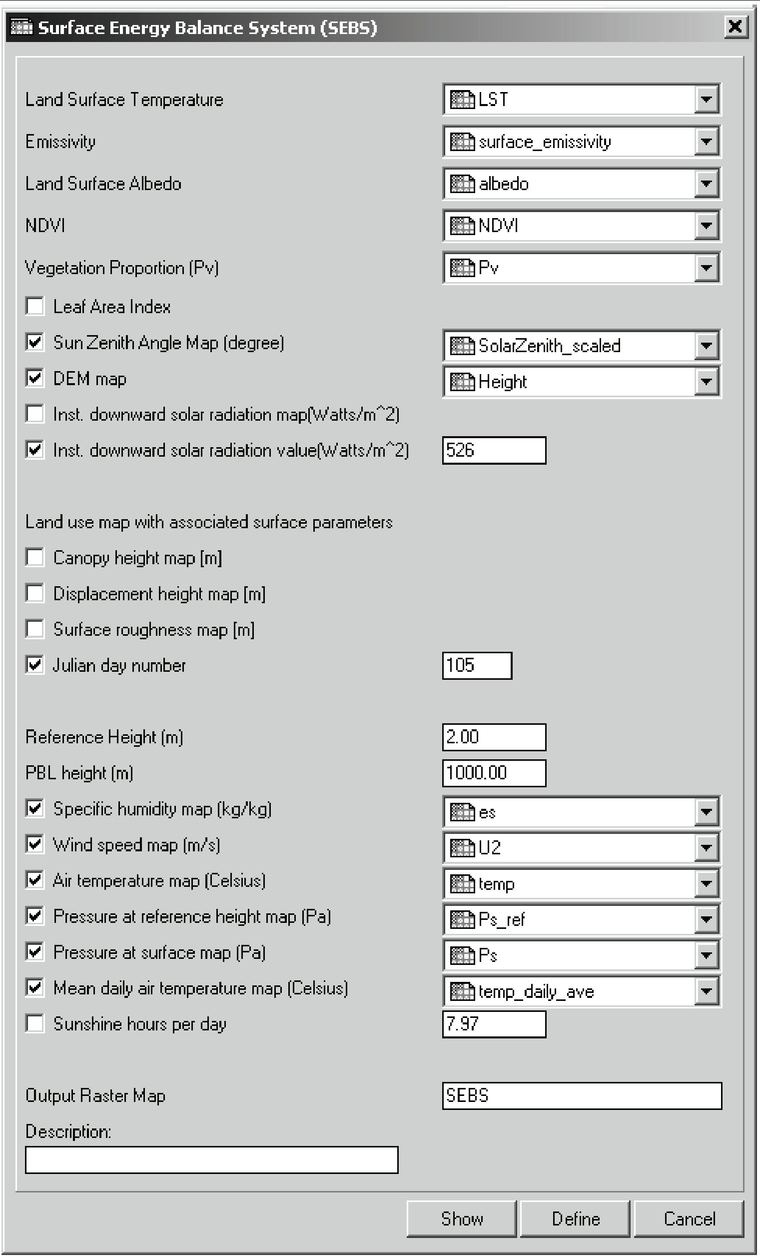

Figure 2.3.4: Example of the SEBS form in ILWIS showing all the required input data

The SEBS outputs for one day are shown in Figure 2.3.5 by way of example.

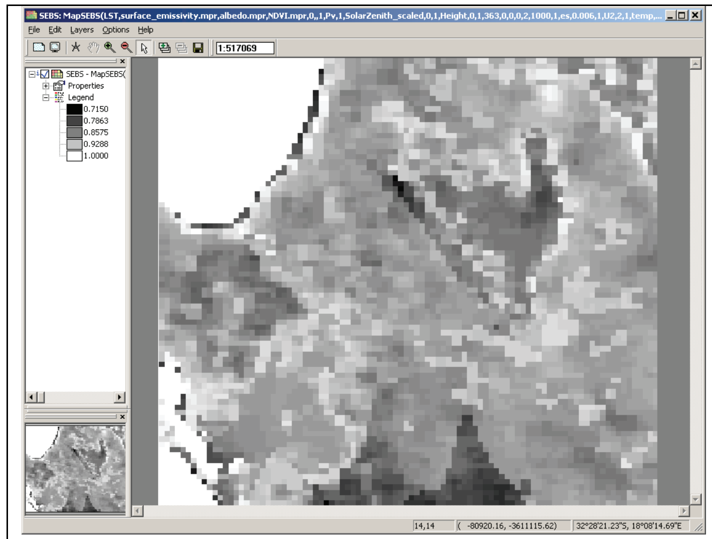

Evaporative fraction: data range shown: 0.7150-1

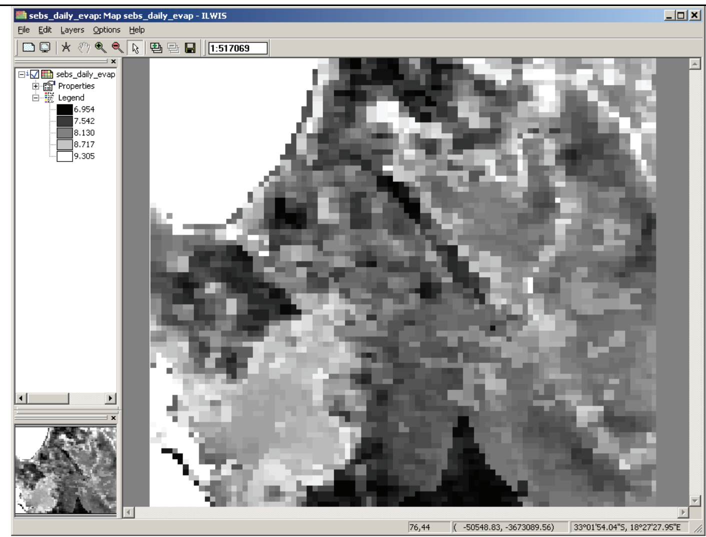

Daily actual evapotranspiration: data range shown: 6.954-9.305 mm

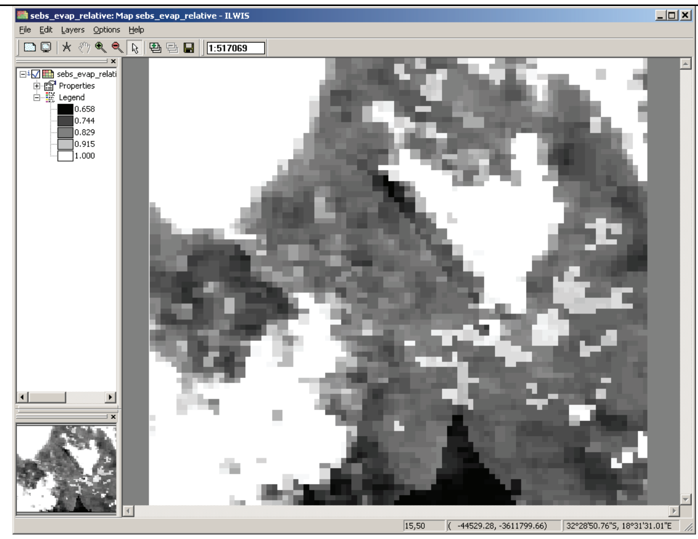

Relative evapotranspiration: data range shown: 0.658-1

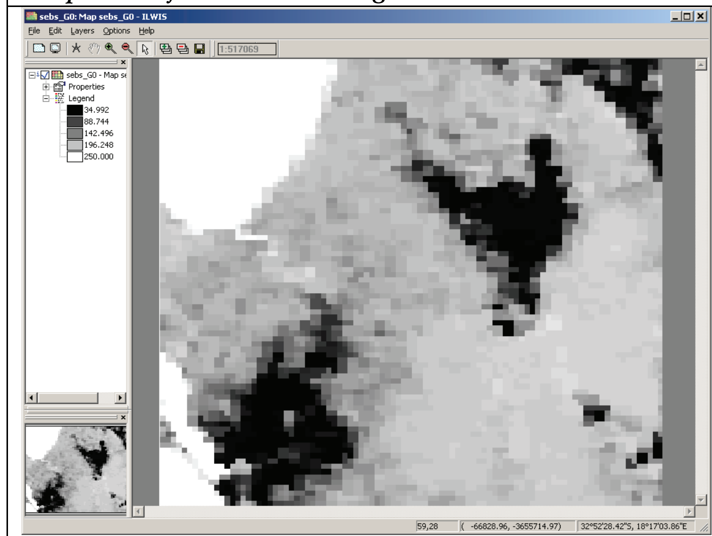

Soil heat flux: data range shown: 35-250

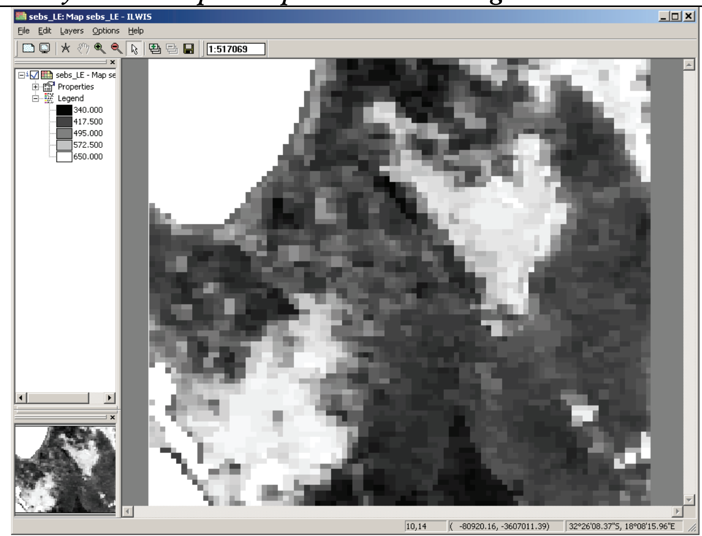

Latent heat flux: data range shown: 340-650

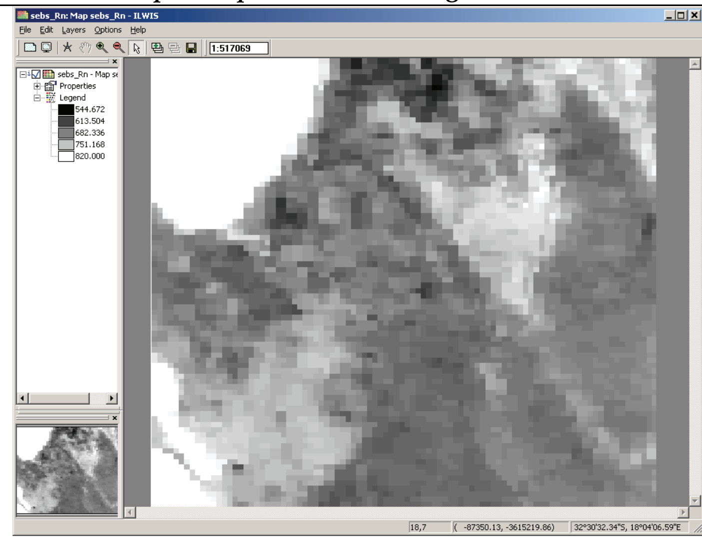

Net radiation: data range shown: 544-820

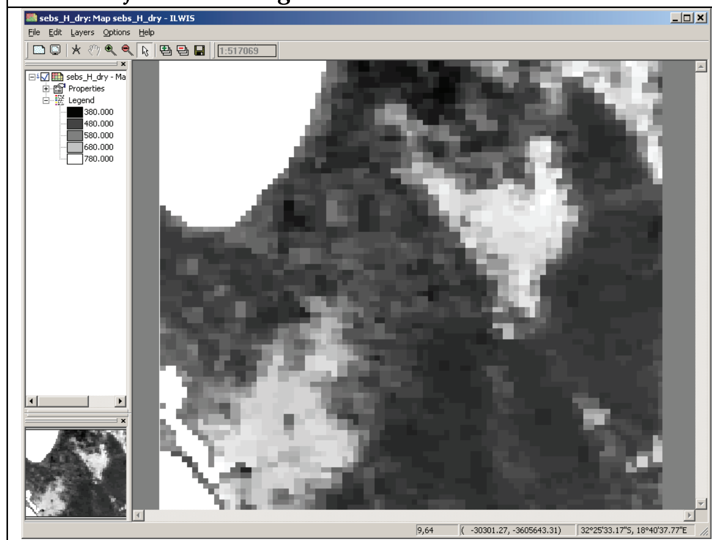

Sensible heat flux at the dry limit: data range shown: 380-780

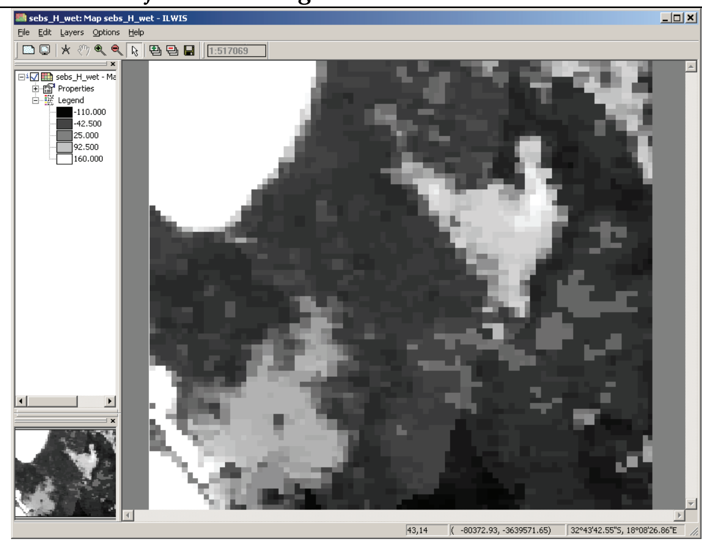

Sensible heat flux at the wet limit: data range shown: -110-160

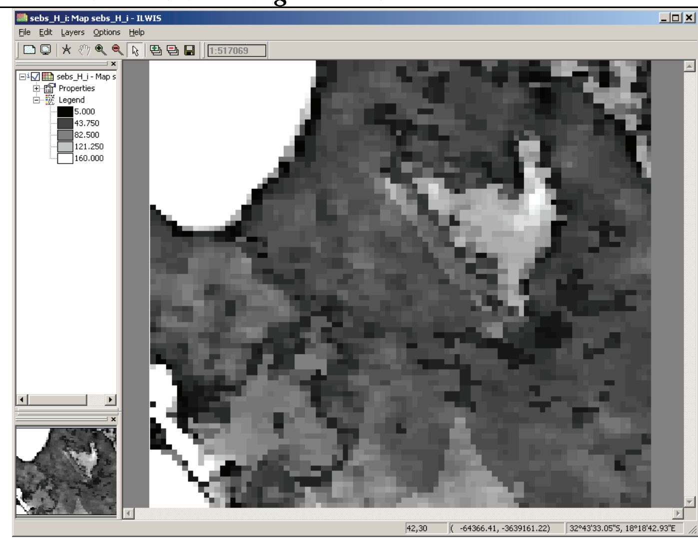

Sensible heat flux: data range shown: 5-160

Figure 2.3.5: An example of SEBS output – 29 December 2007

Potential evapotranspiration for dates between image acquisitions is summed and this is multiplied by the relative evapotranspiration of the last MODIS image processed to arrive at an accumulative evapotranspiration total for the period.. In this way, accumulative actual evapotranspiration between images can be summed with the daily actual evapotranspiration for image acquisition dates and totaled for the entire year. By making minor adjustments to the summed potential evapotranspiration to represent monthly values, monthly actual evapotranspiration can also be calculated. The cumulative actual evapotranspiration results for the study period (1 October 2007-30 September 2008) are shown in Figure 2.3.6 together with the cumulative potential evapotranspiration results for the same period. It can be seen from Figure 2.3.6 that in some areas such as the Bo-Piketberg, actual evapotranspiration was very close to potential evapotranspiration for the same period (Note different legends used). If this is true, it implies that the evaporative demand of the atmosphere was met by the water available in the environment either by natural processes or through irrigation.

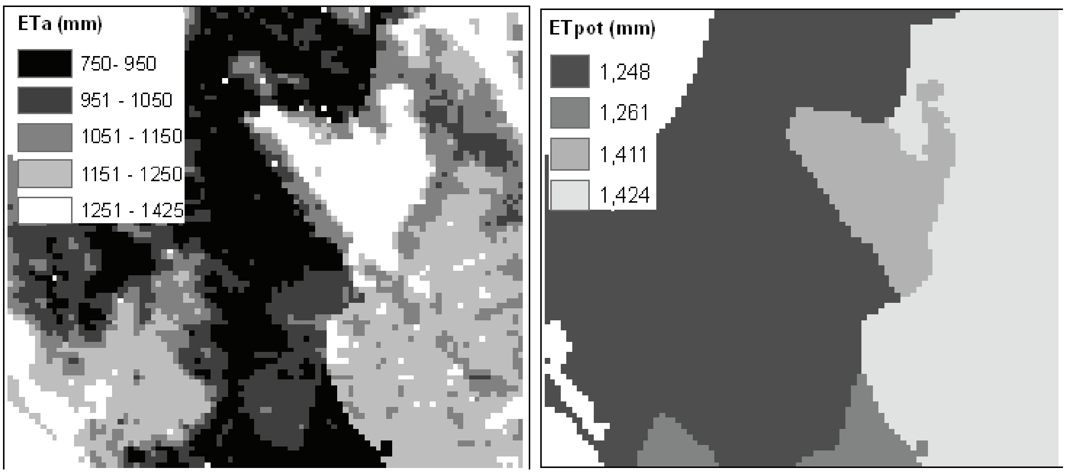

Figure 2.3.6: Comparison of actual evapotranspiration estimated using the SEBS model and potential evapotranspiration for the study period (1 October 2007- 30 September 2008)

The actual evapotranspiration results for the study period were compared to landuse type using the National Landcover 2000 dataset (courtesy ARC-ISCW) to see if any patterns could be discerned (Figure 2.3.7). It can be seen in Table 2.3.3 that there was a wide range in actual evapotranspiration by landuse as there was a significant variation of actual evapotranspiration values within landuse classes. If Table 2.3.3 and Figure 2.3.7 are examined, the following is noted:

1. the highest mean values by landuse are for the classes
   a. "cultivated, permanent, commercial, irrigated" which for this study area is orchards,
   b. "forest plantations" of which there are only a few pixels classified, and
   c. "Thicket, Bushland, Bush Clumps, High Fynbos" which for this study area is High Fynbos with reported alien infestation.

   These classes are found, in the most part, in Bo-Piketberg area where highest actual evapotranspiration for the catchment can be seen in Figure 2.3.7.
2. "Cultivated, temporary, commercial, irrigated" which for this study area refers to potato fields, shows the lowest mean value.
3. "Wetlands" and "Waterbodies" show anomalously low values
4. "Cultivated, temporary, commercial, dryland" in the most part wheat, for this study area shows amongst the lowest actual evapotranspiration values. It is noteworthy that this is the most extensive and most homogeneous of the landuse classes in the study area and as a result, the most accurate actual evapotranspirtation estimates would be expected in this landuse class.

TABLE 2.3.3: ACTUAL EVAPOTRANSPIRATION (MM) FOR THE STUDY PERIOD ANALYZED BY LANDUSE

DESCRIPTION	COUNT	MIN	MAX	RANGE	MEAN	STD	SUM	AREA (HA)
Cultivated, permanent, commercial, irrigated	1840	1042	1413	371	1388	34	2554790	1490
Forest plantations	51	907	1406	499	1373	97	69999	41
Thicket, Bushland, Bush Clumps, High Fynbos	19359	849	1413	564	1334	109	25823200	15681
Urban	835	1117	1401	284	1225	58	1022600	676
Shrubland and Low Fynbos	26367	839	1413	575	1203	207	31715500	21357
Waterbodies	323	875	1406	531	1108	162	357859	262
Cultivated, temporary, commercial, dryland	103097	821	1408	587	1042	143	107448000	83509
Wetlands	977	878	1413	535	989	113	966115	791
Cultivated, temporary, commercial, irrigated	1946	839	1400	561	912	75	1775170	1576

Note all landuse classes not shown as the purpose is to highlight landscape heterogeneity. Refer to Figure 2.3.7 for landuse classes

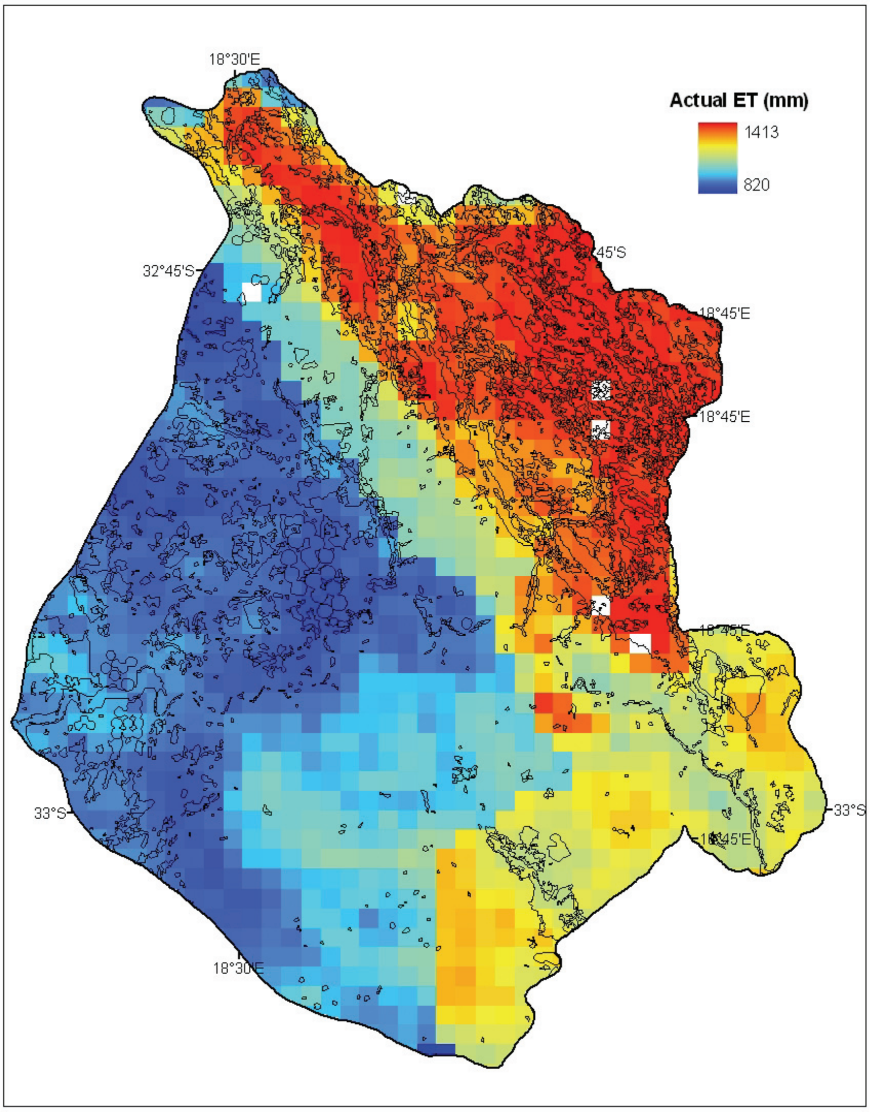

Figure 2.3.7: Actual evapotranspiration compared to landuse type using the National Landcover 2000 dataset (courtesy ARC-ISCW)

In the same way that total rainfall for the G10K catchment was calculated, so the total evapotranspiration can be determined.

Total volume evapotranspiration (m^3) = Mean evapotranspiration of study area (m) x catchment area (m^2)

= 1.109 x 1 260 372 503

= 1 397 753 105 m^3

This equates to 1.397 km^3 for the twelve month period from 1 October 2007 to 30 September 2008.

2.3.6 Validation

A complete validation exercise is only possible if the field measurements were conducted at the same time as satellite images were acquired and if that period is within the study time period. Since the field validation was carried out in November 2008 after the study period used in this research project, precise validation is difficult. For the purposes of this exercise, the general trends in actual ET as compared to relationships with climatic data established during the field measurements are examined to determine whether or not the results of the SEBS model have returned realistic estimates. In addition, two MODIS images corresponding to the field validation date were processed using the SEBS model and direct comparisons are made. Further validation will form a major part of Lesley Gibson's PhD research.

Field measurements using a simplified one sensor type eddy covariance system took place in November 2008 for an apple orchard on the Mouton's Valley Farm by the CSIR (Figure 2.3.8). This is included as a report on the accompanying CD (Jarmain & Mengistu, 2009) but relevant sections are inserted here to assist the reader. The apple orchard selected covered an area of 3.18 ha. The apple orchard was made up of three different apple cultivars – 11 rows of Braestarr (0.77 ha), 16 rows of Royal Gala (1.24 ha) and 15 rows of Redchief (1.17 ha). At the time of the energy balance and total evaporation measurements in November 2008, the average canopy height was 3.2 m. The apple trees did not cover the soil surface completely, rather by about 75 %. The inter-row areas were planted with grass

Figure 2.3.8: Location of the validation site (shown as Piketberg) on Mouton's Valley Farm (from Jarmain & Mengistu, 2009)

Jarmian & Mengistu (2009) estimated daily total evaporation (ET) from the latent energy flux density estimates for the period DOY 315 to 325 (10-20 November 2008). Total evaporation rates measured at the beginning of the period were around 4 mm/d (DOY 315) and increased to values exceeding 5 mm/d following two rainfall events (totalling to 34.2 mm on DOY 316 and 317). After the rainfall events the vapour pressure deficit and solar radiation values also further increased (to 1.8 and 28 MJ m-2 d-1 respectively) which led to a further increase in the daily ETs – up to 7.3 mm/d.

Figure 2.3.9 shows the total evaporation calculated using these relationships for a 28 day period. It is clear that the relationships used yielded agreeable daily total evaporation rates. The total evaporation estimated over this period (ET(ET_o) and ET(R_s*vpd)), showed a similar trend to the measured ET. The ETs calculated and measured over the 9 day period using the different methods, yielded exactly the same results – 46.6 mm (or a daily average of 5.2 mm/d). The 28-day estimate of ET subsequently calculated using the two approaches, differed by only 5 mm (125.9 mm vs. 130.6 mm with the ET_o and R_s*vpd relationships respectively). It was however reported that it was possible that higher actual ET was possible with an increase in solar radiation and vapour pressure deficit as at a pink lady apple orchard in Ceres, a maximum daily ET of 8.5 mm was recorded in December (Jarmain & Mengistu, 2009).

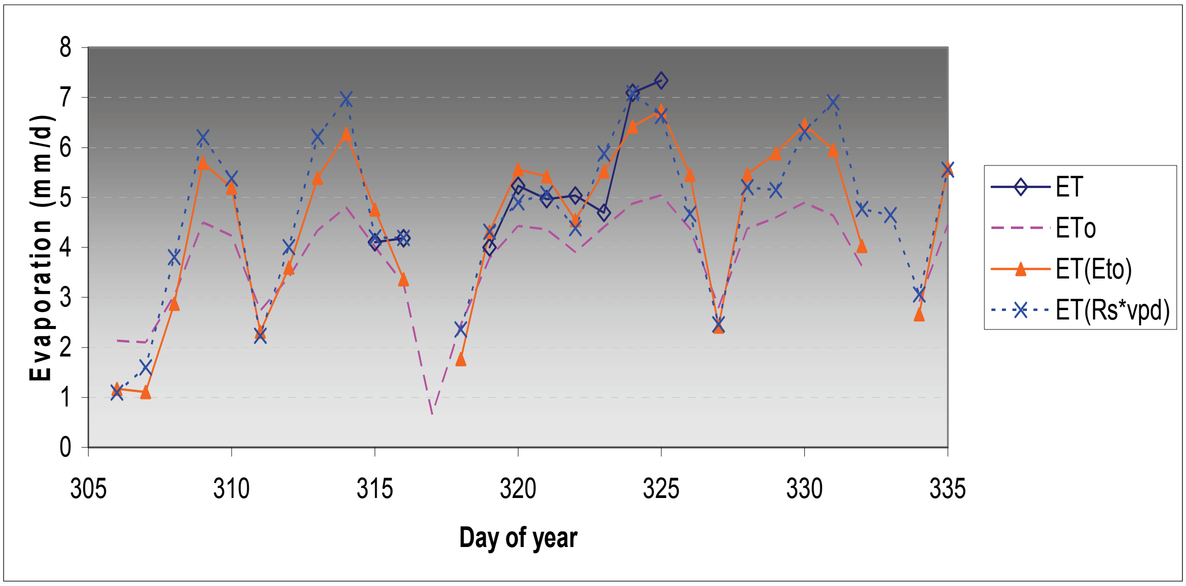

Figure 2.3.9: Daily total evaporation (ET) and reference evaporation (ET_o) as measured at the apple orchard.

*ET (ET_o) and ET(R_s*vpd) refers to the total evaporation calculated as a function of reference evaporation and the product of solar radiation and vapour pressure deficit respectively.*

In the study period (1 October 2007-30 September 2008), actual ET estimates using the SEBS model for the apple orchard on day of image acquisition ranged from 1.2 mm/day in mid winter (8 June & 12 July 2008) up to 8.1 & 8.2 mm/day in summer (29 December 2007 & 18 January 2008). In the summer period when it is expected that actual ET should exceed reference ET – as the apple orchard is irrigated – this was generally found to be the case (Figure 2.3.10). In the winter (May 2007-September 2008) where the apple trees are bare and only cover crop remains, reference ET exceeded the SEBS estimated actual ET as expected.

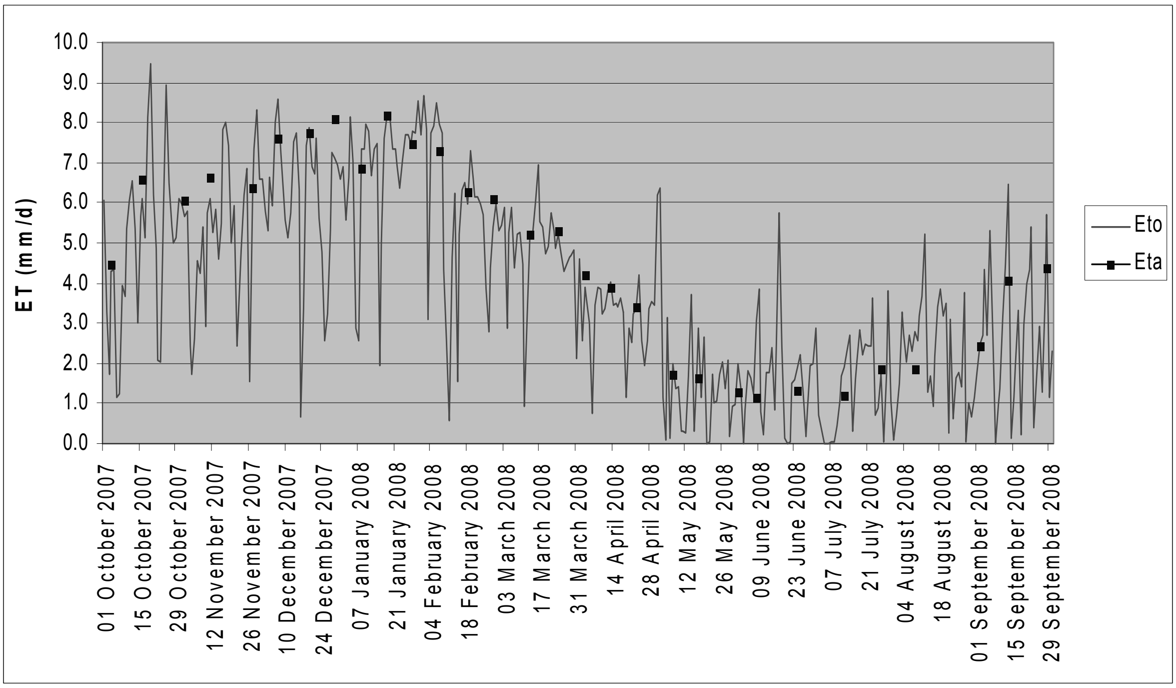

Figure 2.3.10: SEBS estimated actual ET on days of image acquisition compared with reference ET calculated from weather station data

In the same way that Jarmain & Mengistu (2009) investigated climatic relationships between total evaporation and climatic parameters, so the relationship between SEBS estimated ET and climatic parameters were investigated for 1 October 2007 to 30 September 2008. The linear relationship between SEBS daily ET and ET_o and the exponential relationship between daily ET and the product of solar radiation and vapour pressure deficit (R_s*vpd) were subsequently found to describe SEBS daily ETs from the apple orchard to within 90 and 94% respectively (Figures 2.3.11-2.3.14)

From the basis of these seasonal trends and relationships with other climatic data, the SEBS estimation of actual ET appears to be sound for an irrigated apple orchard.

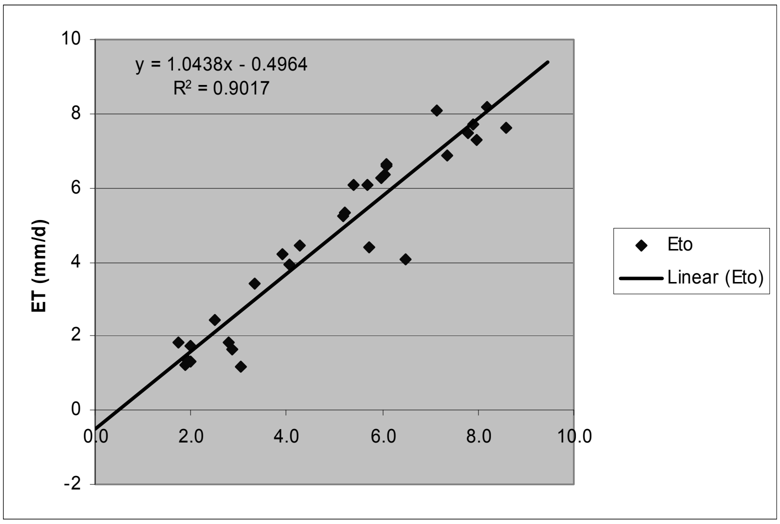

Figure 2.3.11: Relationships derived for estimating daily total evaporation (ET) rates from estimates of reference evaporation (ET_o)

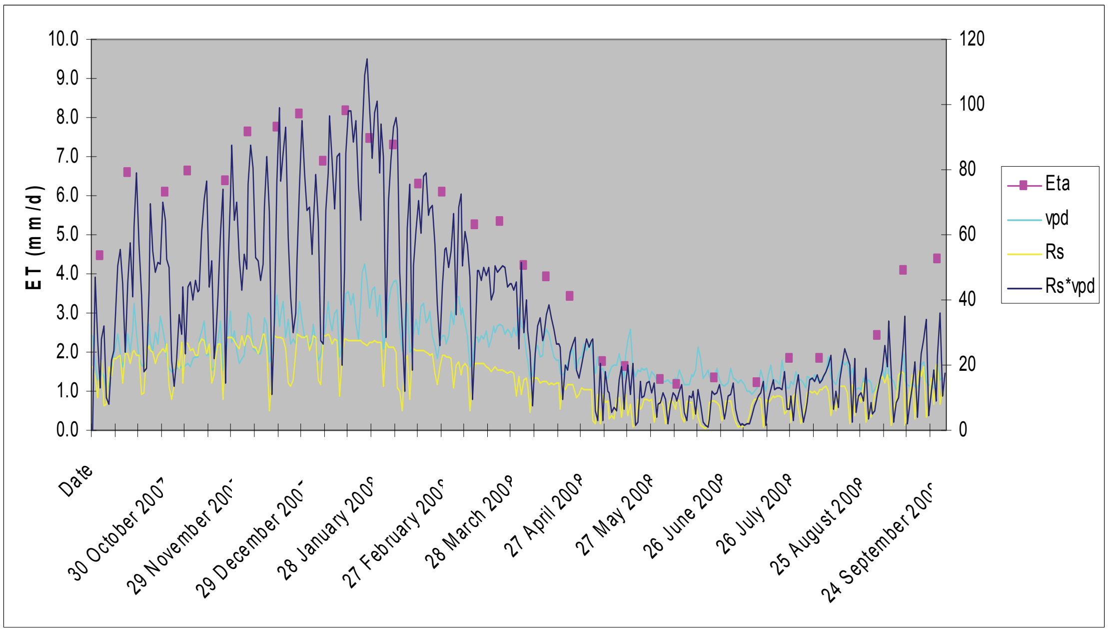

Figure 2.3.12: SEBS estimated daily ET (Eta) from an apple orchard, vapour pressure deficit (vpd), solar radiation (R_s) (secondary Y axis) and the product of solar radiation and vapour pressure deficit (R_s*vpd) (secondary Y axis)

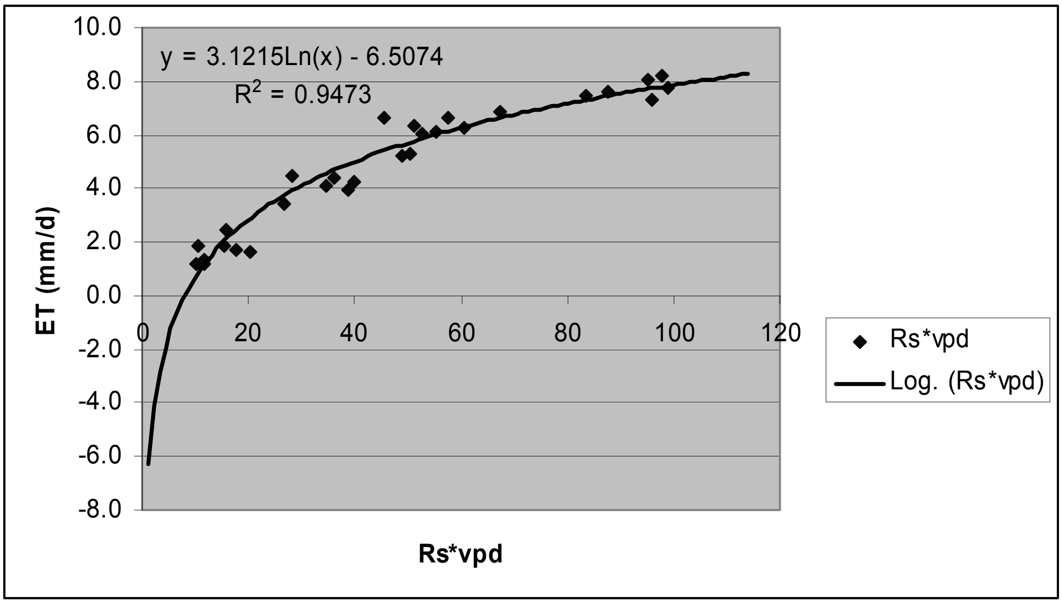

Figure 2.3.13: Relationships derived for estimating daily total evaporation (ET) rates from the product of solar radiation and vapour pressure deficit (R_s*vpd)

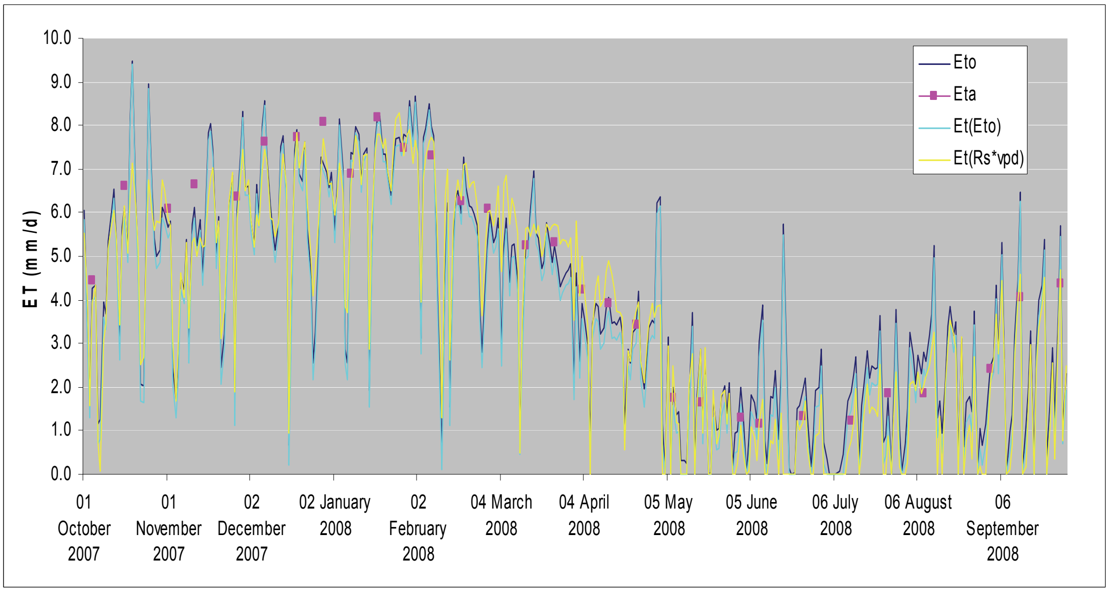

Figure 2.3.14: SEBS estimated daily ET (Eta) and reference evaporation (ETo) as measured at the apple orchard.

*ET (ETo) and ET(Rs*vpd) refers to the total evaporation calculated as a function of reference evaporation and the product of solar radiation and vapour pressure deficit respectively.*

MODIS images for the 17 and 20 November 2008 (DOY 322 & 325) were obtained and processed using the methodology detailed in Chapter 2.3. The results of energy balance fluxes, evaporative fractions and daily evaporation at the field validation site are shown in Figures 2.3.15 & 2.3.16.

It must be reiterated that the resolution of the MODIS pixel was 1000 m and due to landscape heterogeneity a mixed pixel effect may be coming into play, so it is probable that the energy balance fluxes calculated using the SEBS model are also influenced by surrounding pixels. Nevertheless, although there is some discrepancy between the energy balance fluxes, on the whole, there appears to be a good correlation between the field measurements and the field measurements especially on 20 November (DOY 325) where the field measured evaporation and the SEBS estimate evaporation were very similar. On 17 November (DOY 322), a lower energy day there was a bigger difference between the evaporation estimates. Further processing would be required to get a quantitative estimate of the accuracy of the SEBS model with the field measured values, however, the outlook is promising given the results reported on here.

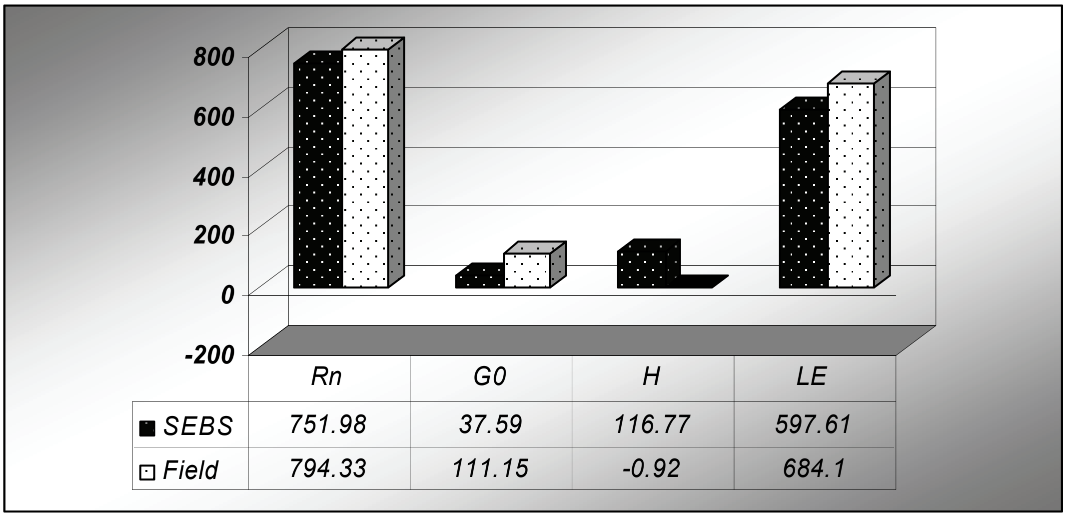

a

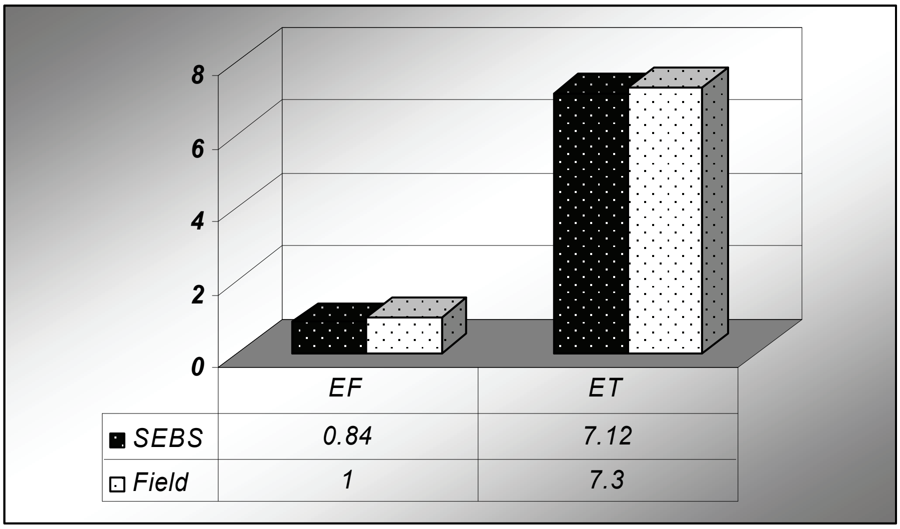

b

Figure 2.3.15: SEBS ET estimates compared with field measurements on 20 Nov 2008 (DOY 325). a. Instantaneous energy balance fluxes, b. Evaporative fraction and daily ET

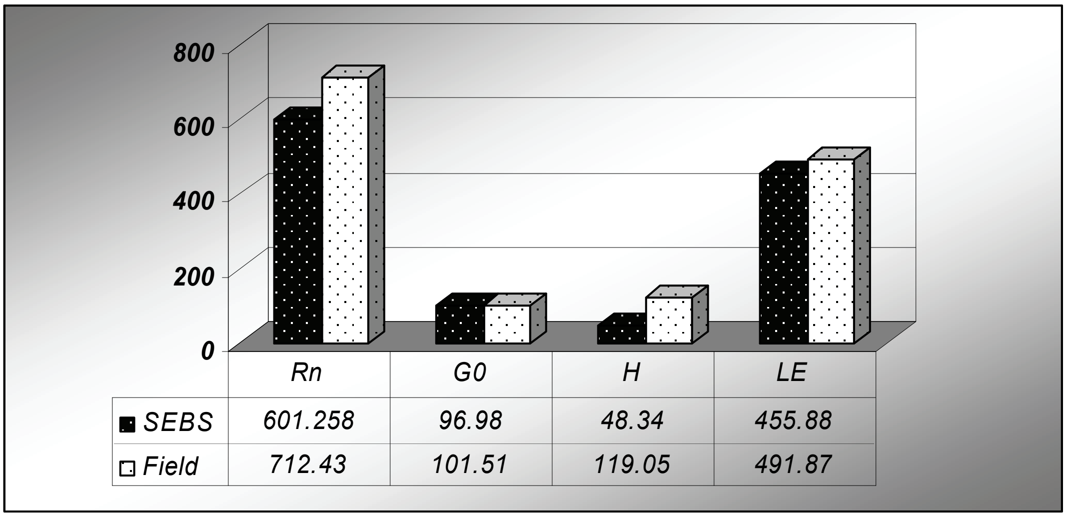

a

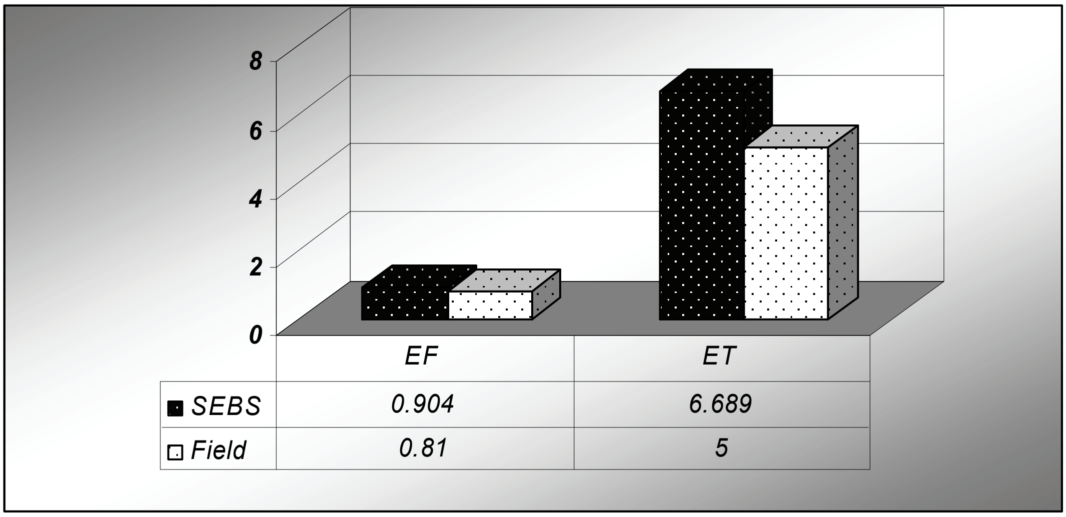

b

Figure 2.3.16: SEBS ET estimates compared with field measurements on 17 Nov 2008 (DOY 322). a. Instantaneous energy balance fluxes, b. Evaporative fraction and daily ET.

2.3.7 Conclusion

If the total volume of water calculated to have evaporated from the G10K catchment (1.397 km^3) is compared with the total amount of rain which is estimated to have fallen for the catchment (0.771 km^3) it appears that the methodology used to estimate total evapotranspiration for the study period has overestimated what occurs in reality. Until the validation has been carried out, it is difficult to draw conclusions as to where the potential errors may be occurring but the following possibilities are presented:

1. *Additional parameterization is needed for the study area*

   The NDVI was used to model surface roughness, canopy height and displacement height. According to Su (2009b), for areas with high vegetation (trees and bushes), where NDVI is low, calculated roughness length is also low resulting in a lower sensible heat flux and a higher evapotranspiration. If roughness length could be obtained from another source, this might lead to a lowering of the evapotranspiration at least for the three landuse classes with the highest mean evapotranspiration (see Table 2.3.3) which would also have the highest expected height of vegetation.

2. *Errors in atmospheric correction*

   Difficulties in obtaining reliable atmospheric correction input data were alluded to in section 2.3.2: Satellite data selection, acquisition and preparation. If this input data was incorrect, the reflectance data may not have been correctly adjusted for the effects of the atmosphere leading to incorrect albedo and NDVI values which in turn would influence the evapotranspiration estimation.

3. *Better interpolation of weather station data is required*

   One weather station was selected to represent an entire climatic zone as illustrated in Figure 2.3.3. In reality, this is not the case as spatial variations of surface characteristics which have a large influence on the near-surface weather conditions (Voogt, 2006). Ideally, accurately interpolated meteorological data for each pixel would be the most appropriate since the energy balance is calculated on a pixel by pixel basis.

4. *The model has not been implemented correctly*

   Currently there are limited skills in South Africa for remote sensing estimation. The SEBS model is freeware and although the developers are very helpful and correspondence by e-mail took place frequently, it is possible that in the absence of direct supervision, errors in its execution may have occurred.

The issue of resolution and landscape heterogeneity should also be discussed here. In section 2.3.2 it was stated that MODIS data is not suitable for quaternary catchments because of the coarse 1000 m resolution. When looking at legal compliance of water users to water use legislation, the pixel resolution needs to be appropriate to the size of the agricultural field or farm. Gibson (2003) reports on the issue of appropriate resolution by citing some examples:

1. Errors along landcover boundaries may be compounded because a substantial proportion of the signal, apparently coming from a land area represented by a specific pixel, actually comes from that pixel's neighbours (Townshend *et al.*, 2000). This results in a tendency for misclassified pixels to form chains along the boundaries of homogeneous patches.

2. Smith *et al.* (2002) conducted a study to evaluate the impact of patch size and scene heterogeneity on accuracy of classification in landcover mapping. According to Smith *et al.* (2002), landscape characteristics that have been hypothesized to contribute to pixel misclassification include high landcover heterogeneity, small patch size and convoluted shapes, all of which result in pixels being harder to classify. They concluded that as heterogeneity increases, the probability of misclassifying pixels increases, while as patch size increases, the probability decreases.

3. In the late 1980s a series of papers was published that discussed images in terms of spatial autocorrelation between pixels. For example, homogeneous areas were seen as having high spatial autocorrelation (neighbouring pixels were similar) such that a coarse spatial resolution (i.e. large pixel size) would be appropriate, whereas heterogeneous areas were seen as having low spatial autocorrelation (neighbouring

pixels dissimilar) so a fine spatial resolution (i.e. small pixel size) would be needed. (Curran & Atkinson, 1999)

Although the above refers to classification procedures, the principles hold true for allocating an evapotranspiration value to one irregularly shaped parcel of land when the pixel resolution is large. If this principle is applied to the G10K catchment it may be concluded that the 1000 m pixel resolution is more appropriate in the low lying areas where extensive dryland agriculture is practised than in the heterogeneous, topographically varied landscape of the Bo-Piketberg where a variety of different land uses occur over a short distance. However, if highlighting the variation of evapotranspiration within the catchment is the prime purpose, MODIS at 1000 m resolution is appropriate.

2.4 Soil moisture

2.4.1 Introduction to soil moisture quantification

Information about the distribution of surface soil moisture is important for a number of applications including the precision management of agriculture and natural resources, as well as for understanding land-atmosphere interactions (Rahman *et al.*, 2008). It is often difficult and impractical to map soil moisture in the field over large regions (Svoray & Shoshany, 2004; Western *et al.*, 2004). Due to the high spatial and temporal variability and, consequently, the cost of direct monitoring by means of field observations, as well as the extended time scales involved, a means of remote monitoring of soil moisture variability would be ideal for long-term soil moisture status assessment. Images of radar backscatter from orbiting satellites have been used extensively in an attempt to map surface soil moisture (Rahman *et al.*, 2008; Álvarez-Mozos *et al.*, 2005; D'Urso & Minacapilli, 2006; Turesson, 2006; Zribi *et al.*, 2005a; Zribi *et al.*, 2005b; Holah *et al.*, 2005; Svoray & Shoshany, 2004; Western *et al.*, 2004).

The aim of this component of the study was to test a variety of soil moisture quantification algorithms and to determine their accuracy in providing soil moisture measurements over time. Two different sources of synthetic aperture radar (SAR) data from orbiting satellites were obtained. These are dual-polarimetric images provided by the ASAR (Advanced Synthetic Aperture Radar) instrument on board the Envisat satellite, as well as fully polarimetric data provided by the PALSAR (Phased Array type L-band Synthetic Aperture Radar) sensor on board the ALOS (Advanced Land Observing Satellite) satellite. The Envisat and ALOS data was provided by the European Space Agency (ESA).

2.4.2 *Satellite image data obtained*

Synthetic aperture radar systems are designed to transmit either vertically polarized or horizontally polarized radiation (or sometimes both). Likewise, the radar can receive either vertically or horizontally polarization (or both). The planes of transmitted and received polarization are designated by the letters H and V for the horizontal and vertical cases, respectively. Thus the polarization of a radar image can be HH, for horizontal transmit, horizontal receive, VV for vertical transmit, vertical receive, HV for horizontal transmit vertical receive, and *vice versa* (Canada Centre for Remote Sensing, 2006).

Four Envisat ASAR images, captured in dual polarization mode, were received. The sensor configuration for the Envisat scenes is displayed in Table 2.4.1. As mentioned in the introduction, the ALOS PALSAR scene was captured in fully polarimetric mode implying that HH, HV, VH and VV were captured. The scene was captured on 1 April 2007.

TABLE 2.4.1: SENSOR CONFIGURATION FOR ENVISAT DATA USED FOR THE STUDY

ORBIT	TRACK	DATE CAPTURED	POLARIZATION	INCIDENCE ANGLE RANGE	TIME OF OVERPASS	PASS
17374	286	2005-06-26	HV HH	19.2-26.7	21:21:18-21:21:33	Ascending
17417	329	2005-06-29	HV HH	31.0-36.3	21:26:56-21:27:12	Ascending
24180	78	2006-10-15	VV VH	26.0-31.4	08:05:29-08:05:44	Descending
24388	286	2006-10-29	HV HH	19.2-26.7	21:21:13-21:21:28	Ascending

2.4.3 *Field-based soil moisture measurements*

The agricultural fields on the farm Mouton's Valley are the subject of precision agriculture practices. These practices include the measurement of soil moisture content at different depths of the soil profile by using neutron probes. These measurements are taken once a week and the data is stored in a database spanning back to March 2006. The measurements taken at the times closest to the time of image capture was taken on 2006-10-15 and 2006-11-02. The soil moisture measurements could then be used as input into linear regression models with the aim of quantifying soil moisture estimates, even over fields for which soil moisture measurements were unavailable.

2.4.4 *Data preprocessing*

The specific Envisat datasets obtained for the study was captured in alternating polarization image mode with the digital numbers of this product being in units of amplitude. These were converted to radar backscatter σ^0 using the following equation:

$$\sigma^0 = \frac{\langle A^2 \rangle}{K} \sin\alpha$$

where A is the pixel intensity in amplitude values, K is an external calibration constant and α is the distributed incidence angle. The external calibration constant and the distributed incidence angles for each image and consequent conversion of amplitude to radar backscatter was performed by using the PSINGEST function implemented in PCI Geomatica's SAR Polarimetry Workstation software. The calibrated radar backscatter data was then converted to logarithmic (or decibel) scale with the aim of reducing the dynamic range of pixel values, which is more convenient for visual inspection and analysis. The power to decibel conversion is a logarithmic conversion where:

$$\sigma^0(dB) = 10\left[\log(\sigma^0)\right]$$

The ALOS scene for the study area was obtained as a geocoded, ellipsoid corrected product. Image processing included the importing of the product in PCI Geomatica SAR Polarimetry Workstation (SPW) software and converting units of amplitude to radar backscatter. The data was converted to linear scale as opposed to decibel scale for input into multiple-polarization models for soil moisture quantification. With the above mentioned image processing being performed, the data could now be used for further image processing and analysis with the aim of quantifying soil moisture content in the study area.

2.4.5 Soil moisture quantification using SAR data

According to Álvarez-Mozos *et al.* (2005) the principle of radar-based soil moisture estimation relies on the existing relation between the backscattering coefficient σ^0 (in dB) and the dielectric properties of the observed soils. The dielectric properties of the observed soils are directly related to the moisture content of soils. Various authors describe the relationship between the radar backscattering coefficient (σ^0) and dielectric constant (ε) to parameters including soil moisture content (Dabrowska-Zielinska *et al.*, in press; Turesson, 2005; Álvarez-Mozos *et al.*, 2005; Moran *et al.*, 2005). The measurement of soil moisture using radar remote sensing is based on the large contrast between the dielectric properties of dry soil ($\varepsilon \approx 2.5$ to 3.5) and water ($\varepsilon \approx 80$) (Narayanan & Hirsave, 2001; Moran *et al.*, 2000; Engmen & Chauhan, 1995; Moran *et al.*, 2005). As the soil water content increases, the dielectric constant increases from approximately 2.5-3.5 when dry to about 25-30 under saturated conditions. This translates to an increase in reflected power by almost 8 dB for wet soil compared to dry soil.

Various models have been proposed for the quantification of soil moisture content including the use of linear regression models (Svoray & Shoshany, 2004; Álvarez-Mozos *et al.*, 2005; Moran *et al.*, 2000) and multiple polarization models (Engmen & Chauhan, 1995; Western *et al.*, 2004). The following sections describe these models and present the result of the application of these models for quantification of soil moisture content.

2.4.5.1 Linear regression models

When using linear regression models for soil moisture quantification, one assumes a linear relationship between radar backscattering coefficient (σ^0) and volumetric soil moisture content. The linear relationship can be expressed as

$$\sigma^0 = a \times VSM + b$$

where VSM is the volumetric soil moisture content, the slope coefficient *a* is related to the signal's sensitivity to change in soil moisture concentration, and the intercept coefficient *b* represents the backscatter of dry soil.

The field data was used as input into the model with the aim of estimating of *a* and *b* coefficients. The values for *a* and *b* were retrieved by linear regression analysis on the fields with known moisture content values. The volumetric soil moisture content could be derived by solving for VSM using the radar backscatter, and *a* and *b* coefficients as input. If one assumes that the signal's sensitivity to change in soil moisture concentration (coefficient *a*) and the backscatter of dry soil (coefficient *b*) does not change between datasets, the same coefficient values can be applied to all the datasets. However, such an assumption would only be valid if the sensor configuration does not change between image acquisitions.

The results of the linear regression analysis on the image data are displayed in Figure 2.4.1. They depict estimated soil moisture values in volumetric percentage. Visual inspection of the results indicates a fairly obvious flaw in radar remote sensing data for soil moisture quantification, mainly due to the radar image geometry. Due to the side-looking geometry of the radar sensors, mountainous regions show severe image distortions known as layover and foreshortening. These areas have a severe effect on radar image interpretability. In particular, anomalously high backscatter values are recorded on the ridges of mountains, which is not necessarily a true reflection of the backscatter values for a particular land surface. Additionally, no means of retrieving true backscatter values from these areas exists. Consequently, these areas should be masked out of algorithms aiming to quantify soil moisture content in mountainous regions.

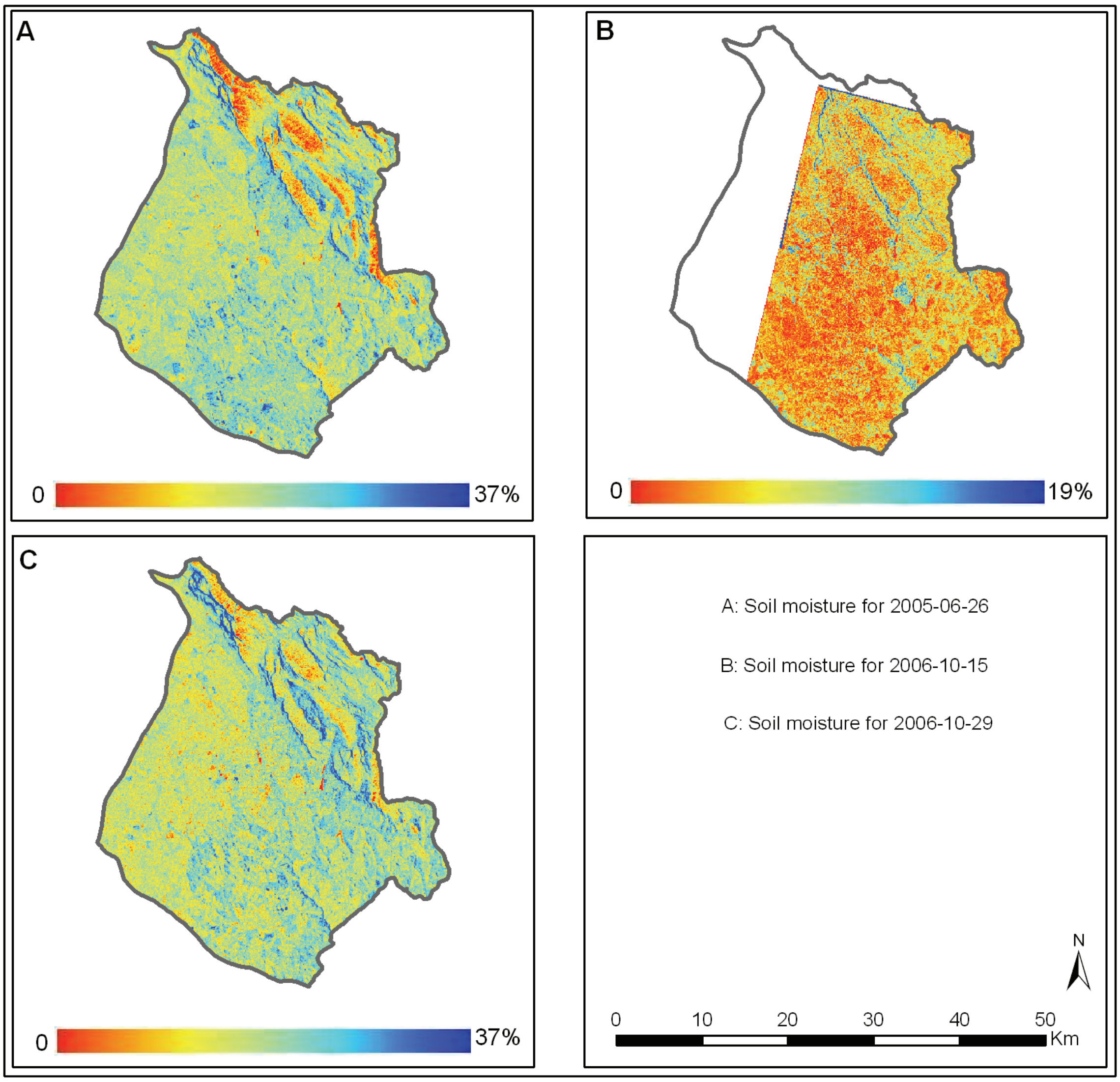

Figure 2.4.1: Soil moisture (in volumetric percentage) as quantified by linear regression models

It is difficult to assess the accuracy of the linear regression models for soil moisture quantification since distributed ground truth is unavailable. Additionally, the soil moisture measurements are not captured on a continuous basis, meaning that soil moisture readings at the exact instant of satellite overpass were not available. These factors combine to produce large uncertainties with regards to the reliability of the results. To assess if soil moisture patterns compare with the rainfall patterns for the period during which the data was captured, 1 km rainfall grids were obtained from the ARC-ISCW. The rainfall grids (Figure 2.4.2) represent the cumulative rainfall over a 10-day period, including the date of image capture.

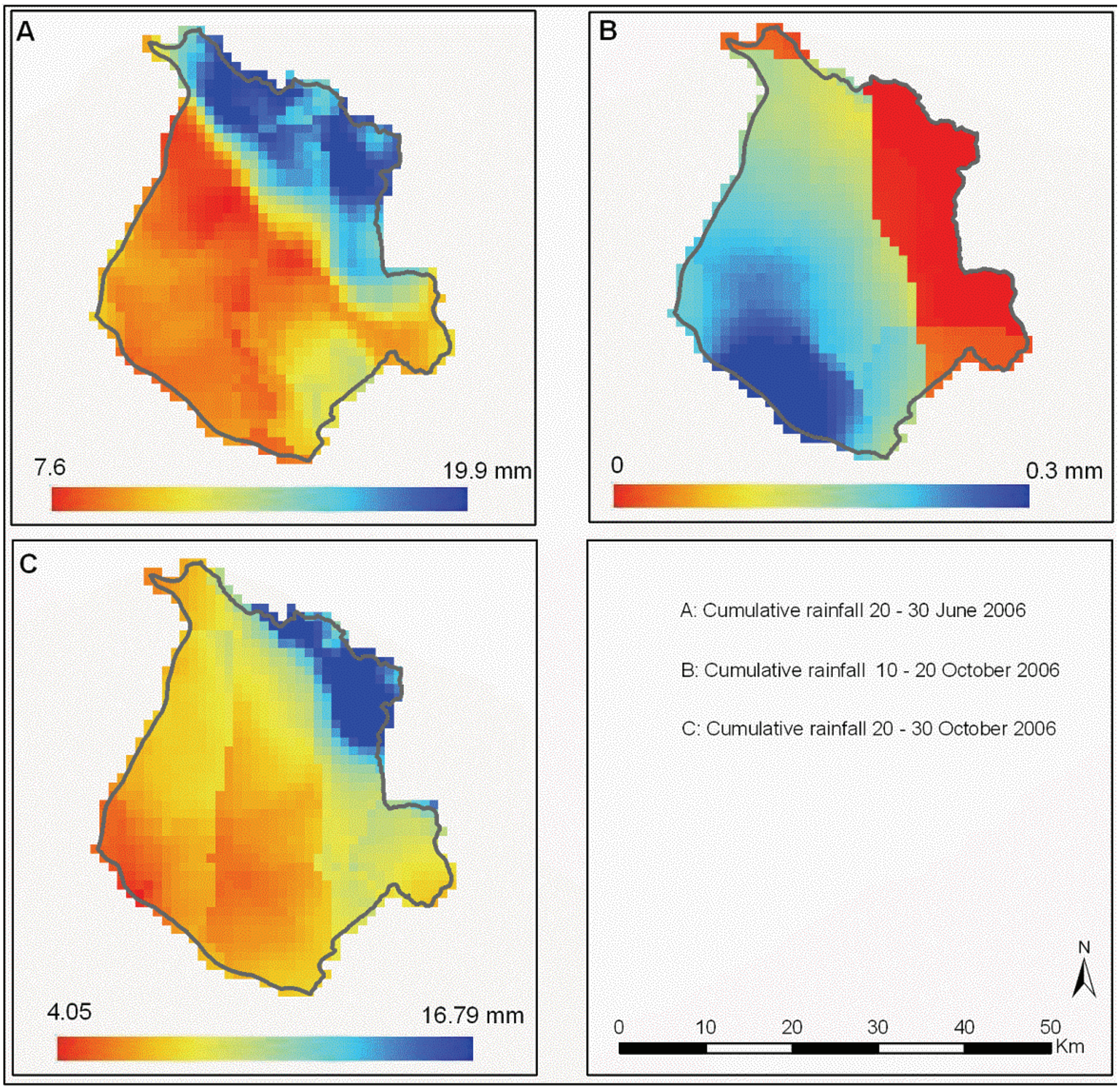

Figure 2.4.2: ARC-ISCW cumulative rainfall grids over a 10-day period

Comparing the rainfall grids with the soil moisture values calculated using linear regression models one achieves at least a qualitative assessment of the accuracy of the model to quantify soil moisture content. The maximum cumulative rainfall per pixel for the period 20-30 June is reported to be 19.9 mm while the maximum volumetric soil moisture is calculated to be 37% for the image captured during this period (2005-06-26). This is in sharp contrast with the soil moisture values obtained for the image captured on 2006-10-15 (maximum of 19%) where the maximum cumulative rainfall is recorded at 0.3 mm. An increase in rainfall for the period 20-30 October 2006 also led to an increase in volumetric soil moisture to a maximum of 37% calculated for the image captured on 2006-10-29. Interestingly, the 2006-10-15 soil moisture content image shows some agricultural fields with soil moisture values relatively higher than that of surrounding areas, possibly indicating that irrigation took place (Figure 2.4.3).

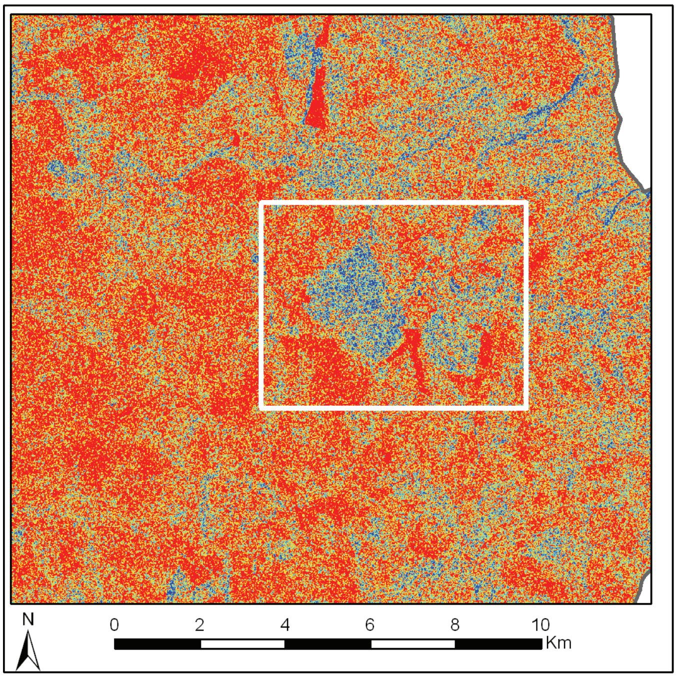

Figure 2.4.3: Irrigated fields (high soil moisture content) in contrast to surrounding areas with low soil moisture content

A well documented problem in the use of linear regression models for soil moisture quantification is that one assumes a linear relationship between soil moisture and radar backscatter, while in reality, radar backscatter is also influenced by surface roughness as well as by vegetation cover in the area of interest, both of which remain unaccounted for in this technique (Western *et al.*, 2004; Álvarez-Mozos *et al.*, 2005; Moran *et al.*, 2000; Moran *et al.*, 2005; Engmen & Chauhan, 1995; Dabrowska-Zielinska *et al.*, in press). The same researchers also state that, in some cases, the sensitivity of radar backscatter may be greater than the sensitivity to soil moisture, and should therefore be accounted for. The attenuation by vegetation is also expected to be significant due to the agricultural nature of the area of interest.

It is suggested that the strong interaction of the backscattered signal with soil as well as vegetation cannot be expressed by a simple linear function. In this regard, various authors describe the combination of microwave signatures at different frequencies and/or polarizations, which may provide additional information on soil and vegetation conditions which may prove to be more useful. The following section will address the limitations of linear regression models for soil moisture quantifications by describing multiple polarization data for surface soil moisture retrieval.

2.4.5.2 Multiple polarization models for soil moisture quantification

Because SAR is responding to several surface features which are usually unknown, it is necessary to use either several polarizations at one point in time, or alternatively, several images over time to develop reliable interpretation algorithms. Engmen & Chauhan (1995) state that, with models using multi-polarized radar data both soil moisture contents and surface roughness can be determined. Models have been developed for multi-frequency, multi-polarization SAR data which remove the need for prior information on roughness. One such a model, known as the Dubois model, relates two co-polarized backscatter responses σ_{vv}^0 and σ_{hh}^0 to the RMS surface height, the dielectric constant, the SAR wavelength, and local incidence angle. These equations are expressed as follows:

$$\sigma_{hh}^0 = 10^{-2.75} \frac{\cos^{1.5}\theta}{\sin^5\theta} 10^{0.028\varepsilon\tan\theta} (kh\sin\theta)^{1.4} \lambda^{0.7}$$

and

$$\sigma_{vv}^0 = 10^{-2.35} \frac{\cos^3\theta}{\sin^3\theta} 10^{0.046\varepsilon\tan\theta} (kh\sin\theta)^{1.1} \lambda^{0.7}$$

Where $k = \frac{2\pi}{\lambda}$, *h* is the rms surface height, ε is the dielectric constant, λ is the wavelength and θ is the local incidence angle. These equations were used to obtain estimates of dielectric constant and surface height by simultaneous solving of σ_{vv}^0 and σ_{hh}^0 (also known as inverse modelling) (Western *et al.*, 2004).

The soil moisture map derived using the Dubois Model and ALOS PALSAR data is displayed in Figure 2.4.4 indicating soil moisture content in volumetric percentage. Also presented is the cumulative rainfall over a 10-day period.

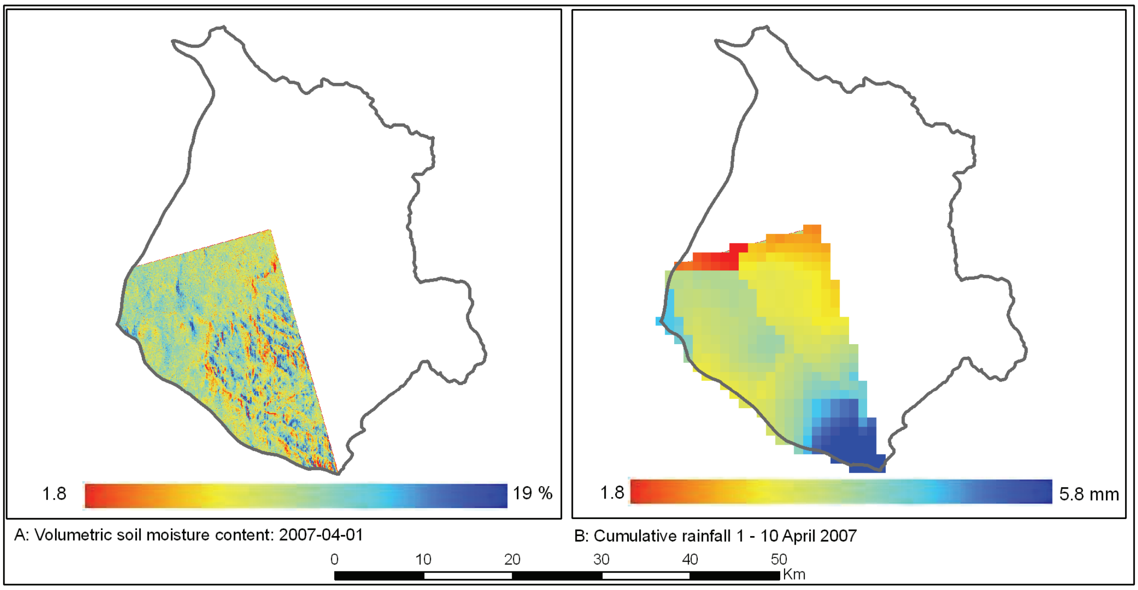

Figure 2.4.4: Soil moisture quantification using multiple polarization models (A) compared to rainfall (B)

Since detailed soil moisture measurements using ground-based techniques are unavailable at the time of image capture, it is difficult to assess the accuracy at which the moisture quantification was applied. However, visual inspection of the results once again indicates that the distortion effects due to topography may be influencing the results. Comparing the soil moisture values with rainfall over the period indicates a good qualitative assessment with a maximum cumulative rainfall over the 10-day period at 5.8 mm and the maximum volumetric soil moisture at 19%. This compares well with rainfall and soil moisture values achieved for the image captured on 2006-10-15 where the maximum cumulative rainfall was recorded at 0.3% and maximum volumetric soil moisture was calculated at 19%. Although one would expect lower volumetric soil moisture content for the image captured on 2006-10-15 (with maximum cumulative rainfall of 0.3%), one needs to consider the effect of anomalously high values recorded due to topographic effects as well as the effect of irrigated fields on the maximum volumetric soil moisture.

Multiple-polarization models provide the user with the opportunity to quantify soil moisture content within the scene in the absence of ancillary data on surface conditions, including surface roughness and vegetation descriptors. Furthermore, no initial field-based soil moisture measurements are needed for the estimation of soil moisture content in the area, as is the case with linear regression models. However, according to Western *et al.*

(2004) the Dubois model was developed for data with wavelengths ranging between 20.5 cm and 2.8 cm. On the other hand, the ALOS PALSAR data used in this process operates at a wavelength of 23.6 cm. Detailed ground-truth data will be needed to test the validity of the model at this wavelength. Additionally, Western *et al.* (2004) state that surface roughness values should range between 0.3 and 3 cm while the local incidence angles should vary between 30 and 65°. Although the surface roughness estimates for the data remain in the 0.3-3 cm range, the local incidence angles, derived using a 20 m digital elevation model as input, are below the 30° threshold for large portions of the scene. Despite these limitations, the derived volumetric soil moisture estimates range between 1.8 and 19% which seems consistent with soil moisture ranges derived using linear regression models and correlates well with the cumulative rainfall figures for the study area. However, the valid ranges for wavelength and incidence angles associated with the Dubois model combine to produce large uncertainties with regards to the reliability of the results. Therefore, field-based ground-truth data is needed to test the validity of the Dubois model when applied to ALOS PALSAR data.

2.4.6 Concluding remarks

Soil moisture variability is an important factor for many applications including precision agriculture and hydrological models. Radar imagery for the quantification of soil moisture content is the focus of many research programmes, and the results indicate that the data can be used with various levels of success. In general, SAR systems show a relatively high sensitivity to soil moisture due to the large contrast in the dielectric constant of dry and wet soils at microwave frequencies. Consequently, much hope has been put in the capability of SAR sensors to quantify soil moisture content. However, according to Wagner & Pathe (2005), despite extensive efforts by the science community, soil moisture retrieval from SAR imagery can still be considered to be in an experimental stage.

According to Wagner & Pathe (2005), it is preferable to think of soil moisture as a process that requires monitoring over extended periods of time with sufficiently short repeat intervals. In fact, they mention that a single snapshot of soil moisture at a point in time is most likely of no particular relevance for any application. The aim of the soil moisture quantification for the Bo-Piketberg region is to analyze a time-series of datasets to derive a mean annual figure of soil moisture for each pixel. With currently available high resolution (12-20 m) radar data, the derivation of such a figure is not possible. This is due to image data being captured at infrequent intervals and at a variety of incidence angles and polarizations, which implies that a single model cannot be consistently applied on the few available datasets. However, new SAR sensors are being developed and launched on a continuous basis and it is believed that the consistent availability of SAR imagery at regular intervals will be a possibility in the near future.

According to Pathe & Wagner (2004) the current lack of operational soil moisture retrieval is one of the glaring deficiencies in earth observation. Fortunately much progress has been made and it can be expected that within the next ten years remotely sensed soil moisture data with spatial resolution of 25-50 m will become routinely available. One of these research programmes (known as SHARE) aims at enabling an operational soil moisture monitoring service for the Southern African Development Community (SADC) region by using ASAR Global mode data in combination with ERS/METOP scatterometer data to build a 1 km soil moisture product. The aim is to publish the data on a weekly basis, meaning that the derivation of a mean annual figure of soil moisture for regional applications becomes more feasible.

2.5 Surface runoff

2.5.1 Introduction

Runoff is a major component of the hydrologic cycle. In context of this project it is defined as the part of precipitation collected from a drainage basin that appears at the outlet of the basin and includes surface runoff (overland flow), subsurface runoff (interflow) and baseflow (Batelaan, 2006).

As suggested in the literature review (WRC, 2006) remote sensing can be used to produce input for refining runoff predictions and runoff potential. Some recent studies have been successful in using remotely sensed data exclusively to predict surface runoff, though never at the level of accuracy that can be achieved from direct in-stream measurements (Bjerklie *et al.*, 2003). Remotely sensed data can successfully be used in the calculation of river discharge, prediction of surface water runoff and the production of runoff potential maps (WRC, 2006).

The aim of this component of the study was to calculate runoff for the study area to feed into the water balance equation. From the water balance equation an indicator of catchment stress could be developed, quantification of water use being the final objective. During methodology development, various models were considered (WRC, 2007b) but the GIS-based WetSpass model (Batelaan & De Smedt, 2001) was selected for use.

2.5.2 *Suggested methodology*

2.5.2.1 Hydrograph baseflow separation

Separation of streamflow hydrographs into baseflow and surface runoff components is often used to estimate the groundwater contribution to streamflow. Hydrograph separation techniques have been used to quantify the groundwater component of hydrologic budgets and to aid in the estimation of recharge rates (Sloto & Crouse, 1996).

Sloto & Crouse (1996) developed a program called HYSEP that uses a mathematical technique for separation of a streamflow hydrograph. HYSEP includes three methods of hydrograph separation that are referred to in literature as the fixed-interval, sliding-interval, and local-minimum methods (Sloto & Crouse, 1996). Daily mean stream discharge is used as input to the program. The program describes the frequency and duration of measured streamflow and computed baseflow and surface runoff. Output from the program includes tables, graphs, and data files.

Although streamflow along the Berg River is measured, the stretch through the G10K catchment is mostly ungauged, with streamflow being measured at input to the catchment at DWAF station G1H031 where flow records have been collected since 1974. At stream gauging station G1H023 at the outflow of the Berg River from G10K into catchment G10M, only water levels are measured. Figure 2.5.1 shows the location of these flow gauging stations as well as monthly streamflow at G1H031. Monthly data for hydrological years 2005/6, 2006/7 and 2007/8 were analyzed. Daily average streamflow data from

G1H031 for the same period have been used as input to the HYSEP program for hydrograph baseflow separation. DWAF streamflow data can be downloaded from *http://www.dwaf.gov.za/hydrology/cgi-bin/his/cgihis.exe/station*.

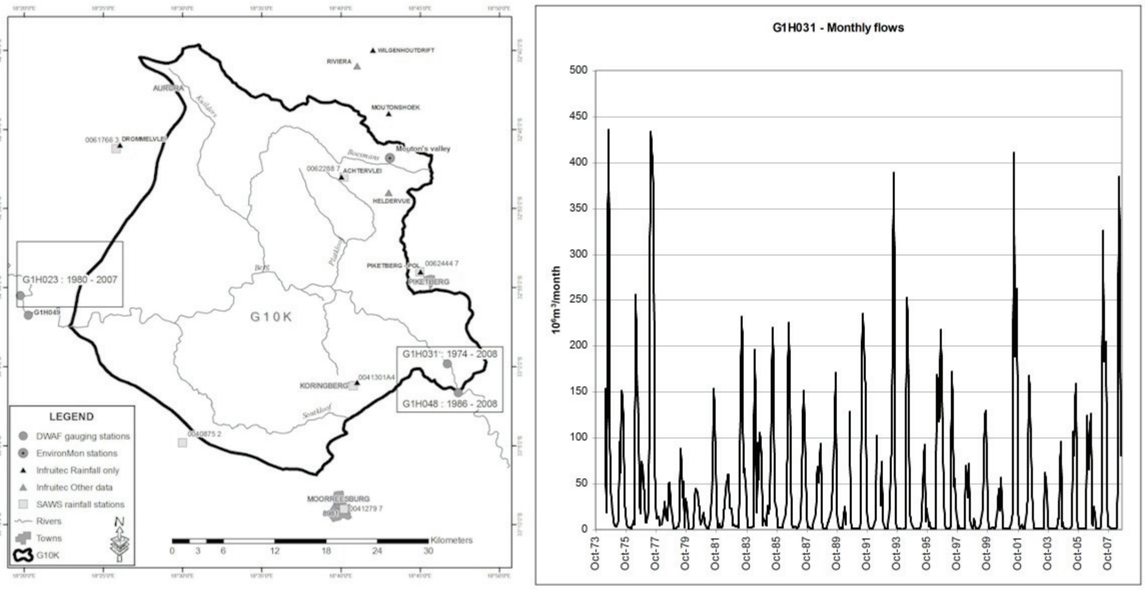

Figure 2.5.1: Location of streamflow gauges in G10K with streamflow at G1H031

2.5.2.2 WetSpass modelling

WetSpass, an acronym for Water and Energy Transfer between Soil, Plants and Atmosphere under quasi Steady State, integrates a water balance in a geographical information system (GIS) (Batelaan & De Smedt, 2001). By using long-term average standard hydrometeorological parameters as inputs, the model simulates the temporal average and spatial differences of surface runoff, actual evapotranspiration, and groundwater recharge. Details of the WetSpass model can be found on the enclosed CD. In the WetSpass model the study area is treated as a grid of raster cells, with every raster cell subdivided into a vegetated, bare soil, open water and impervious surface fraction. Independent water balances are calculated for each fraction on a seasonal basis, which allows the model to account for sub-cell land cover heterogeneity.

The WetSpass model simulates runoff per grid cell in two stages: firstly potential surface runoff is calculated based on vegetation type (for the vegetated fraction only), soil texture (for vegetated and bare soil fractions), slope and groundwater saturated areas (only for the vegetated fraction). In stage two, the potential surface runoff is adjusted for recharge areas taking the seasonal precipitation intensity in relation to the soil infiltration capacity into account. In groundwater discharge areas all potential runoff is assumed to contribute to surface runoff, while in infiltration areas only high intensity storms will generate surface runoff (Batelaan & De Smedt, 2007). The WetSpass model was adapted in ArcView to produce monthly runoff figures using monthly precipitation data.

2.5.3 Results

The results of the hydrograph baseflow separation analysis for DWAF flow gauging station G1H031 at the inflow to the G10K catchment using HYSEP can be seen in Figure 2.5.2. Figure 2.5.2(a) details the fixed-interval method, Figure 2.5.2(b) shows seasonal distribution of baseflow and runoff, Figure 2.5.2(c) pictures the sliding-interval method and Figure 2.5.2(d) shows results from the local-minimum method. Baseflow and runoff for three hydrological years are shown in Table 2.5.1. It is important to note that this represents the runoff at entry to the G10K catchment. Outflow from the catchment has not been measured in terms of streamflow, merely water level, and this can be seen in Figure 2.5.3 which compares the water level at G1H031 (inflow) and G1H023 (outflow). The base level of the river seems to have increased by at least 1 m, but appears to experience smaller peaks for high flow in winter months.

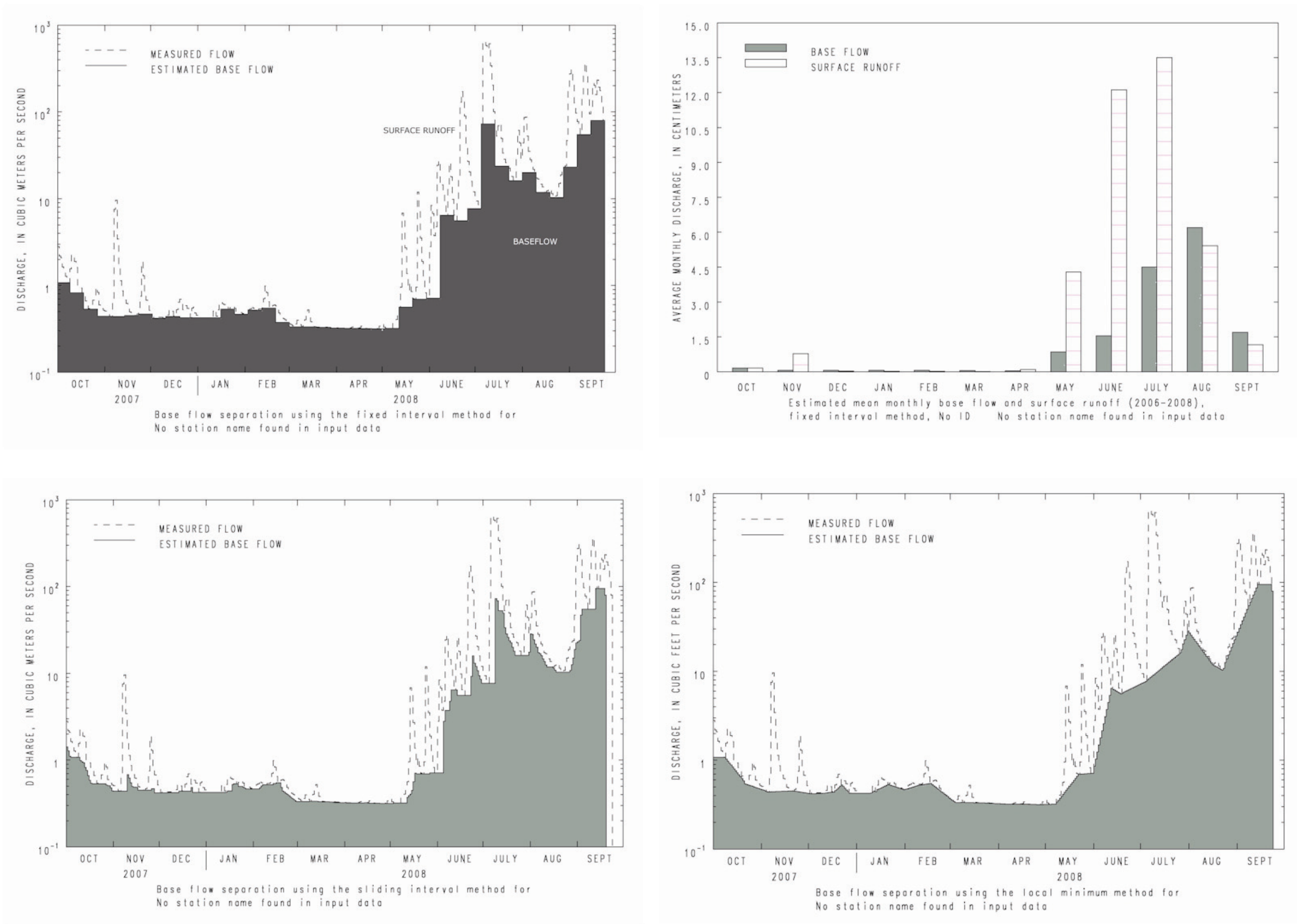

Figure 2.5.2: Hydrograph analysis for G1H031 for hydrologic year 2007/8:

(a) fixed-interval method; (b) seasonal distribution; (c) sliding interval method and (d) local-minimum method

Table 2.5.1: Hydrograph separation results

Method	Mean stream-flow (m³/s)	Mean base-flow (m³/s)	Mean surface runoff (m³/s)	Total stream-flow (m)	Total base-flow (m)	Total surface runoff (m)	BF/ stream-flow (%)	Base-flow (m³/s/km²)
2005/6								
Fixed	13.17	4.11	9.06	0.353	0.110	0.243	31.22	0.003496
Sliding	13.17	4.24	8.93	0.353	0.114	0.239	32.22	0.003608
Local-minimum	13.17	3.44	9.73	0.353	0.092	0.261	26.10	0.002924
2006/7								
Fixed	27.17	7.48	19.70	0.729	0.201	0.528	27.51	0.006358
Sliding	27.17	7.88	19.29	0.729	0.211	0.518	29.01	0.006705
Local-minimum	27.17	6.48	20.69	0.729	0.174	0.555	23.85	0.005512
2007/8								
Fixed	29.18	8.66	20.52	0.769	0.228	0.541	29.68	0.007365
Sliding	27.92	7.71	20.21	0.728	0.201	0.527	27.62	0.006558
Local-minimum	29.18	7.43	21.75	0.769	0.196	0.573	25.46	0.006317

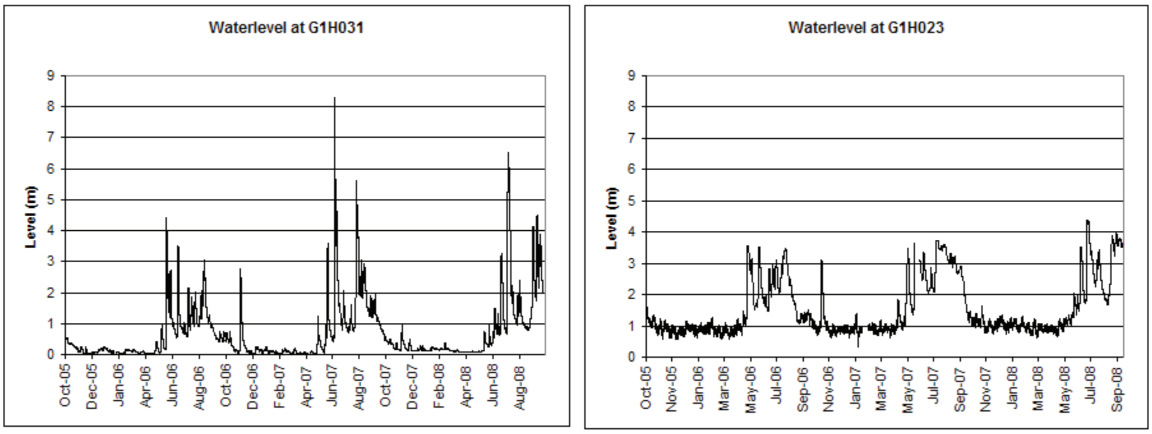

Figure 2.5.3: Comparison of waterlevels in Berg River at inflow (G1H031) and outflow (G1H023) to G10K catchment

Figure 2.5.4 shows the temporal variation in total monthly runoff estimated with the modified WetSpass model. The cumulative monthly runoff ranges from 0 to 650 mm/yr with an average runoff of 42.7 mm/yr. The original simulated WetSpass model simulated runoff ranges from 0 to 557 mm/yr with an average runoff of 63.01 mm/yr. In Table 2.5.2 the values obtained through modelling are compared to results from WR90.

Table 2.5.2: Comparison of runoff from WetSpass with WR90

Option	MAP (mm)	Mean Runoff (mm)	Coefficient
WetSpass monthly	612.00	42.70	0.070
WetSpass annual	612.00	63.01	0.103
WR90	381.85	21.40	0.056

Since runoff is a function of the precipitation, which is one of the great uncertainties in the calculation of the total water balance as described in section 2.1 on precipitation, the mean monthly modelled runoff was compared to rainfall, both the mean for the catchment, as well as point values at Mouton's Valley rainfall station. The result is reflected in Figure 2.5.5. Runoff varies between 5.3-7.5% of rainfall on a grid by grid basis, and between 2.0-7.3% as compared to Mouton's Valley rainfall.

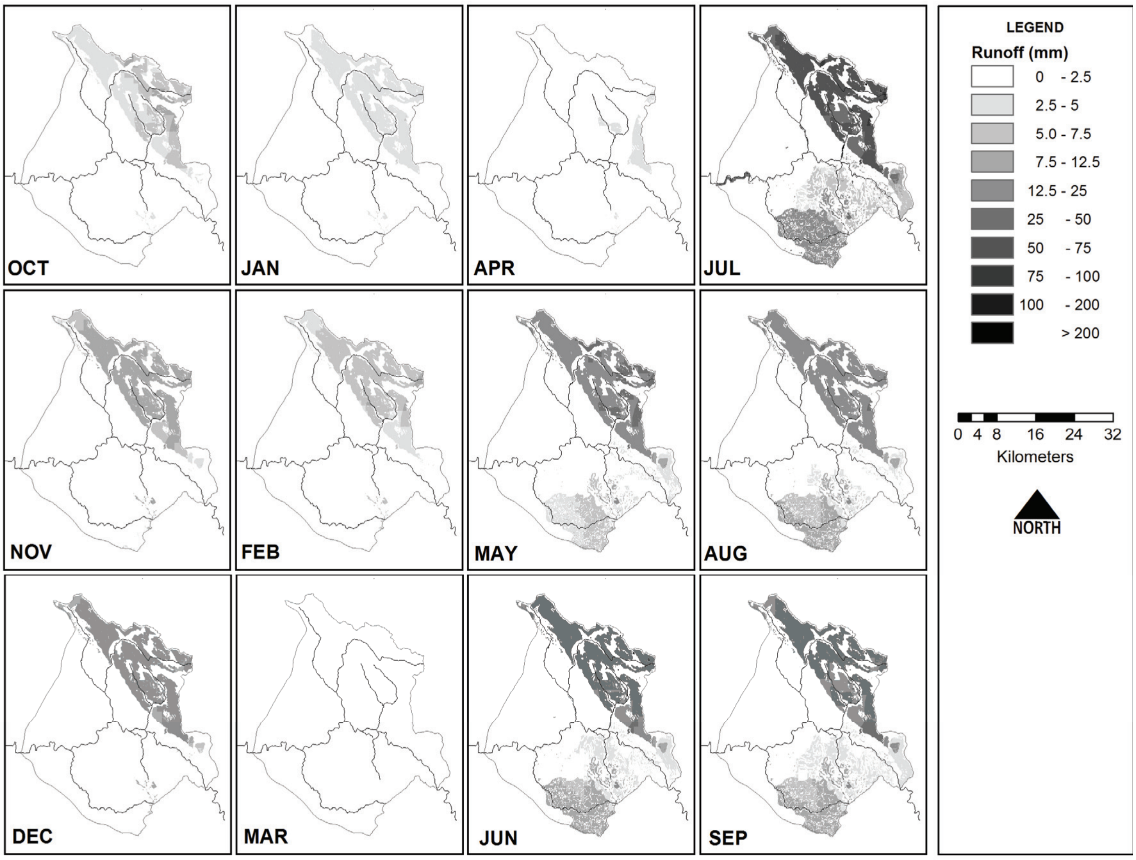

Figure 2.5.4: Temporal variation of runoff modelled with WetSpass

2.5.4 Discussion

The runoff calculated using the hydrograph baseflow separation represents flow into the G10K catchment. The higher water level at inflow to G10M indicates that there is a gain of surface water flow in catchment G10K. According to the WetSpass model, this figure represents 1.59-2.35 m^3/s. Errors in the model can be attributed to uncertainties in the complexity of the model-data input such as uncertainties in landcover, soil classifications, slope and especially precipitation maps. The natural water balance in this particular catchment is modified by extensive irrigation from pumped groundwater and dams.

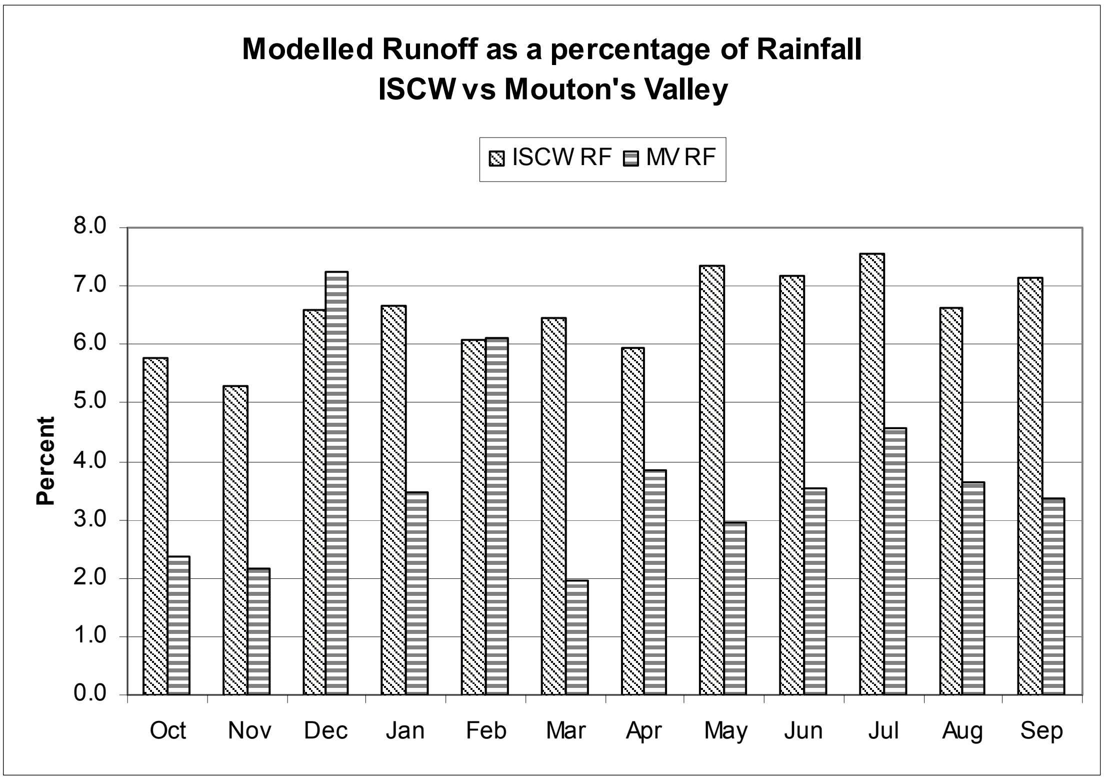

Figure 2.5.5: Comparison of monthly runoff to monthly precipitation

Notwithstanding these shortcomings, the WetSpass model introduces the concept of modelling the runoff in the catchment in a spatial, distributed way, which can be validated with the necessary field data. Generally, average annual estimates are more reliable than monthly or daily estimates of baseflow or surface runoff. One of the major difficulties during this study was the lack or real surface runoff volumes.

2.6 Groundwater

2.6.1 Introduction

Qualitative and quantitative information on aquifer recharge rates and storage are needed to manage groundwater resources. Recharge is regarded as the entry into the saturated zone of water made available at the water table surface, together with the associated flow away from the water table within the saturated zone (Freeze, 1969).

The use of remote sensing has affected the way in which natural resources on the earth's surface, and water resources in particular, can be managed. Despite the fact that groundwater is a subsurface resource that cannot directly be measured by remote sensing, the opportunity for using this innovative technology in combination with GIS is immense as groundwater management systems, especially in developing nations, are often severely limited by the lack of adequate data (Jha & Chowdary, 2006). Remote sensing has the general advantage of providing a spatially distributed measurement on a temporal basis and a link must be established between the surface observation and the subsurface (groundwater) phenomena (Jackson, 2002).

The aim of this section of the project is to generate a spatially distributed recharge layer to be used in the water balance equation in order that water use (or over-use) of water resources within a catchment may be determined. This information will assist decision makers of additional allocations in the water licensing process.

2.6.2 Methodology

A conceptual model of the geology and hydrogeology of the area was constructed. This assisted in the understanding of recharge and discharge areas. Using remote sensing based analysis, geological structure was investigated using lineament mapping. This conceptual model was used in the construction of a numerical model. Three main recharge zones were identified, named "Sand", "TMG" and "Malmesbury".

Based on a hydrocensus within the pilot study area, a number of boreholes were selected for continual water level data logging and chemical sampling. Chloride, oxygen (O^{18}) and deuterium (H^2) isotope contents were analyzed. The chloride mass balance (CMB) method was used to estimate and characterize recharge on a local and regional scale by using the chloride concentration in rainfall and comparing it to that of groundwater chloride concentration. Since chloride in rainfall was only measured at three locations, with a single sample at two of the sites, it was decided to adopt the approach applied by Adams (2004) to generate a chloride in rainfall surface. Based on a linear regression the relationship between chloride and the amount of rainfall occurring near the coastal sites of South Africa at a distance >15 km away from the coastline, chloride in precipitation can be estimated. The relationship provides a best estimate of chloride in rainfall in the absence of data (Adams, 2004). Caution is advised when using the CMB method for this study area where the precipitation comes from a frontal system generated over the southern Atlantic ocean (Van Wyk, 2009) and fog/mist is very prevalent (Adams, 2004; Roets *et al.*, 2008).

The stable isotopes oxygen-18 (O^{18}) and deuterium (H^2) were used to differentiate between water that recharged directly to the saturated zone from precipitation infiltrating through the unsaturated zone and water that could have undergone evaporation prior to recharging through some form of runoff infiltration. The isotope approach gives a qualitative indication of recharge processes. Both rainfall and groundwater samples were analyzed for the stable isotopes O^{18} and $H^2$and compared to results found during the CAGE study (Hartnady & Hay, 2000) carried out in the adjacent E10 catchment, to determine recharge characteristics. Isotope samples were only collected for the pilot study area, which falls exclusively in the TMG recharge zone. This is regarded as the main recharge area for the study area.

Estimating recharge by correlating water levels, rainfall and aquifer storage was identified as a promising method for application to the G10K catchment. Bredenkamp *et al.* (1995) has shown that the cumulative rainfall departures (CRD) and saturated volume fluctuation (SVF) methods are probably the most successful in estimating recharge in South Africa (Adams, 2004). The SVF method was used to estimate storage coefficients and recharge. The CRD method was used to estimate the recharge rates to the aquifers. A limitation in using these two methods is the absence of long-term groundwater level data.

The WetSpass model developed by Batelaan & De Smedt (2001, 2007) was also implemented. In this model recharge is calculated as the residual of a water balance in which precipitation is the principal input. Runoff and evapotranspiration are calculated as a function of landuse, soil, slope and potential evapotranspiration (sections 2.3, 2.4 & Appendix II). The resultant recharge layer is used as input to a MODFLOW model. A modification to the MODFLOW package, called SEEPAGE, has been developed which has the function of more effectively identifying discharge (Batelaan & De Smedt, 2004). As described in Appendix II, the WetSpass model has been modified to generate monthly recharge grids from monthly variable input datasets, one of these being the groundwater level which varies and is used as input to potential storage in the WetSpass model. One of the outputs from the WetSpass recharge calculation is the delineation of discharge areas.

2.6.3 Conceptual model

Based on the geology and hydrogeology of the study area a conceptual model was constructed (Figure 2.6.1). Three recharge zones have been identified: Cenozoic sands to the northwest, the TMG in the northeast and the Malmesbury group in the southern part of the study area. In Figure 2.6.1, the hydraulic conductivity (m/day) of the formations in the study area reflects their water-bearing capacity.

The Sand recharge zone, made up of the sandy soil of the Sandveld group, could be regarded as a primary aquifer. However, infiltration is slow, and evaporation through the unsaturated zone takes place. Groundwater quality is poor (up to 1000 mS/m) and groundwater levels are shallow (<3 mbgl).

Hartnady & Hay (2000) state that the TMG constitutes the "Table Mountain Superaquifer" consisting of the Peninsula aquifer (Peninsula and Pakhuis formations), Piekenierskloof aquifer and Nardouw Aquifer with intervening aquitard units. Figure 2.6.2 shows a cross-section through the TMG. This "super-aquifer" has been identified as the main recharge area for the study area. Estimates by specialists of recharge to the TMG (Parsons, 2002) vary from 2-43% depending on precipitation. These estimates of recharge percentages linked to precipitation can be found in Table 2.6.1.

Extensive faulting is found in the sandstones of the TMG associated with higher recharge with expected infiltration up to 15% (Meyer, 2001). Lineament mapping (WRC, 2008b) indicated the correlation between higher yielding boreholes and lineaments/faults in the study area, which would be an indication of higher recharge potential.

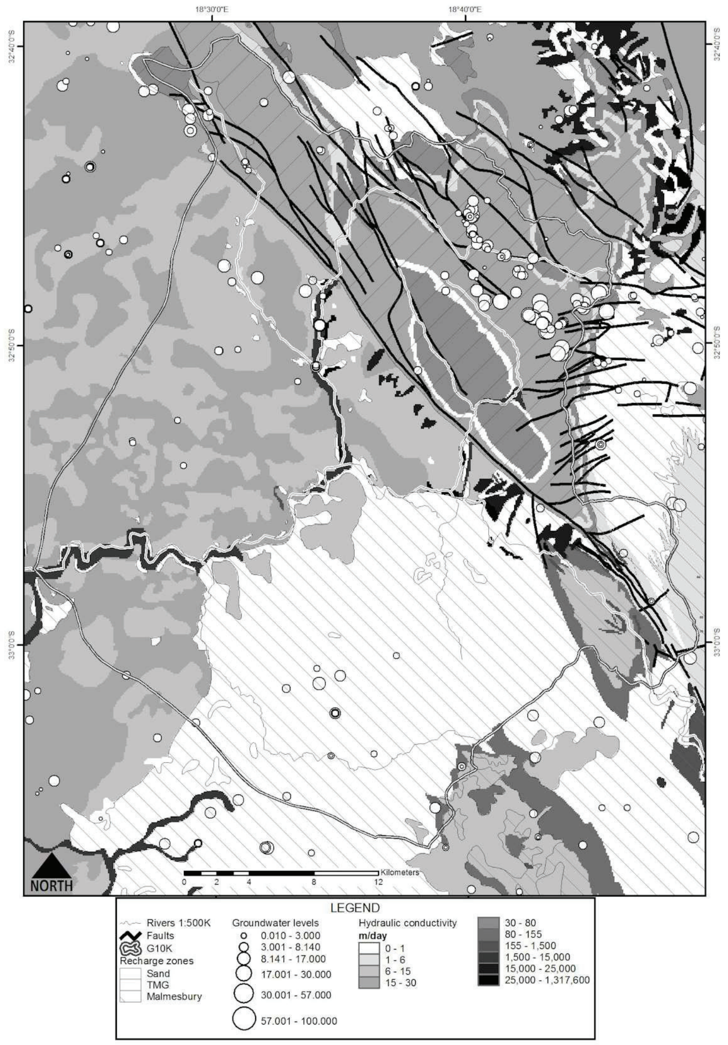

Figure 2.6.1: Conceptual model of the study area

Groundwater levels shown in Figure 2.6.1 were derived with Bayesian interpolation using Tripol with elevation as correlation value despite the fractured nature of the TMG aquifer, since there was a good correlation between groundwater levels and elevation (R^2 = 0.9575).

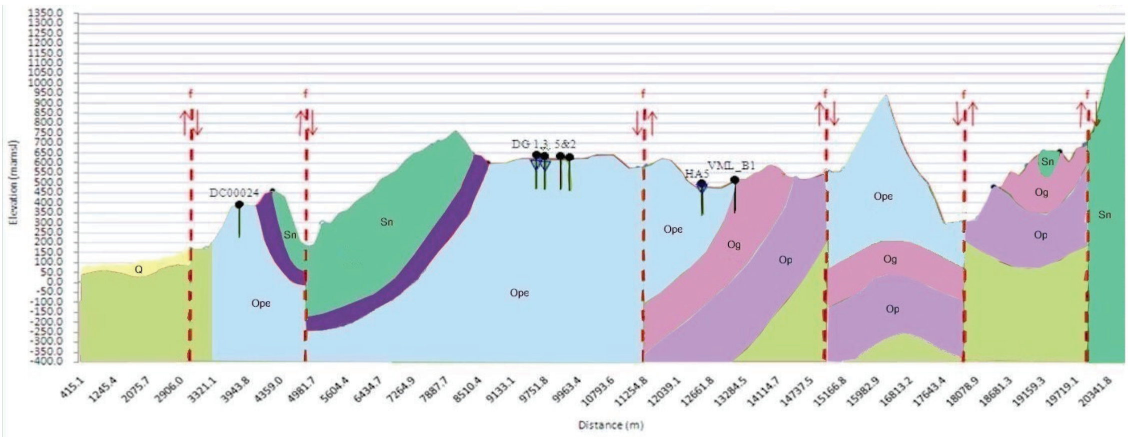

Figure 2.6.2: Cross-section of the geology of the TMG within the study area

TABLE 2.6.1: SURVEY OF ESTIMATES OF RECHARGE OF TMG AQUIFER SYSTEMS (AFTER PARSONS, 2002)

PARAMETER	RAINFALL (MM/A)		
	0-300	300-600	600+
Harmonic mean (%MAP)	5	11	21
Average (%MAP)	7	13	22
Respondents (n)	8	9	11
Minimum (%MAP)	2	6	12
Maximum (%MAP)	15	25	43

Groundwater exploitation in the Malmesbury Group is often problematic due to poor exposure and the largely argillaceous nature of the geology (Meyer, 2001), and within the study area the Malmesbury Group is regarded as a non-aquifer. Lineaments associated with high yielding boreholes in the southwest of the study area, as well as the location of multiple wet and dry pans, indicate that aquifers within the Malmesbury Group rocks are generally associated with faults and fractures. These aquifers tend to be confined or semi-confined (Colvin & Saayman, 2007).

This conceptual model will be used as input to a groundwater model constructed in MODFLOW.

2.6.4 Chloride Mass Balance

2.6.4.1 Rainfall evaluation

Rainfall chloride content was measured from rainwater collected at Excelsior, and at two DWAF rainfall gauging stations installed in the area. The chloride in rainfall was found to be higher than published values from literature where a value between 1.15-1.92 mg/l is suggested in the absence of measured chloride in rainfall based on average annual rainfall of 612 mm. Dry deposition of chloride was taken to be 10% of the rainfall chloride value as suggested by Xu & Van Tonder (2001). The average chloride in the rainfall samples was 4.75 mg/L. When the equation proposed by Adams (2004) for rainfall chloride was used, a spatially distributed layer was generated in GIS with a mean chloride value of 3.75 mg/L, minimum and maximum values were 2.76 and 7.5 mg/L (SD = 1.083).

2.6.4.2 Groundwater samples

The CMB method was applied to 36 sites from the hydrocensus (WRC, 2008a) as well as 63 samples from NGDB data (WMS). The descriptive statistics of the chloride concentrations in the groundwater are shown in Table 2.6.2.

TABLE 2.6.2: SUMMARY STATISTICS OF THE CHLORIDE CONCENTRATIONS (MG/L) FOUND IN THE GROUNDWATER SAMPLES OF THE NGDB AND HYDROCENSUS DATABASE

STATISTICS	CL NGDB	CL HYDROCENSUS
Count	63	36
Mean	1120	37
Standard Deviation	1363	18
Min	15	13
Max	4992	90
Harmonic Mean	98	30

The distribution of chloride in the groundwater of catchment G10K clearly indicates that lower concentrations occur in the high-lying TMG where the hydrocensus was carried out. The low-lying aquifers are characterized by highly saline groundwater, typically associated with the Malmesbury group and unconsolidated Tertiary age sands of the Sandveld Formation. The location of these three recharge zones can be seen in Figure 2.6.1 in the conceptual model.

2.6.4.3 Recharge estimation

The average, maximum and minimum chloride concentrations of the groundwater for the different recharge zones were used to determine the average, minimum and maximum rate of recharge. The chloride in precipitation grid previously prepared, plus average rainfall per recharge zone, was used to calculate recharge. The results are shown in Table 2.6.3.

TABLE 2.6.3: RECHARGE ESTIMATION USING THE CMB METHOD

RECHARGE ZONES	CL_{GW}			MAP	CL_{RF}	RECHARGE (MM/YR)			RECHARGE (%)		
	MEAN	MAX	MIN			MEAN	MIN	MAX	MEAN	MIN	MAX
Sand	1458	4993	50	491	3.2	1.19	0.35	34.57	0.24	0.07	7.04
TMG	68	90	13	983	5.3	84.28	63.68	440.84	8.57	6.48	44.85
Malmesbury	2030	3346	730	479	3.1	0.80	0.49	2.24	0.17	0.10	0.47

The chloride method was applied over the study area using GIS. Chloride concentration in groundwater grid was generated using 3D Analyst in ArcView. Recharge zones were used as soft clip polygons. Hydrocensus data fell exclusively in the TMG area. Using Spatial Analyst map calculator, grids were recalculated to give the estimated recharge in mm/year (Figure 2.6.3). The map gives an indication of the main recharge zones over the area, the highest recharge rates coinciding with areas of high elevation and fracturing.

The recharge determined using the CMB method reflects long-time recharge and gives an indication of recharge in the area. It is significant to notice that recharge to the Springfontein and Malmesbury Groups is low, below 5% with a maximum recharge of 44% in the TMG aquifer.

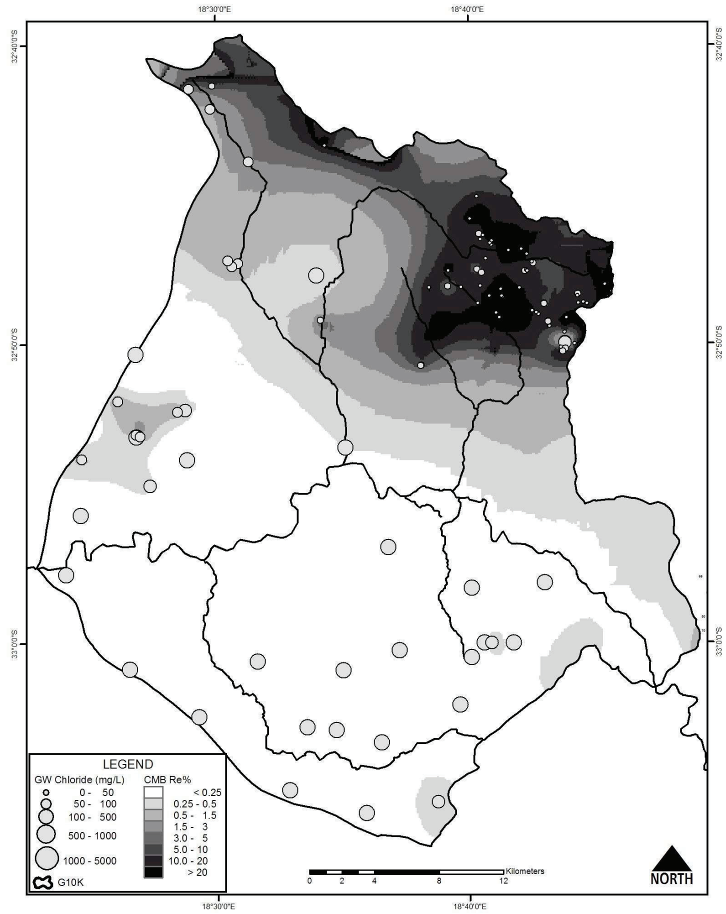

Figure 2.6.3: Annual recharge (%) for the G10K catchment using the CMB method

2.6.5 Stable Isotopes: oxygen-18 (O^{18}) and deuterium (H^2)

Craig (1961) showed that there was a correlation between D and O in precipitation waters world-wide with a best-fit line corresponding to $\delta D = 8\delta^{18}O + 10$, which is know as the global meteoric water line (GMWL). Different areas have their own distinctive local meteoric water lines (LMWL) and Diamond & Harris (1997) plotted a local meteoric water line (CMWL) for Western Cape precipitation ($\delta D = 6.2\delta^{18}O + 10.6$). Figure 2.6.4 shows a plot of the rainfall δD versus δ18O for the study area following the CMWL trend. The GMWL is also shown. Two samples, associated with two rainfall events, not plotting along the trend are marked in Figure 2.6.4 as “Exceptions” (29-07 and 3 August). The LMWL derived from precipitation data in the study area is similar to the CMWL for the Western Cape and is plotted in Figure 2.6.6 ($\delta D = 6.1183\delta^{18}O + 10.059$).

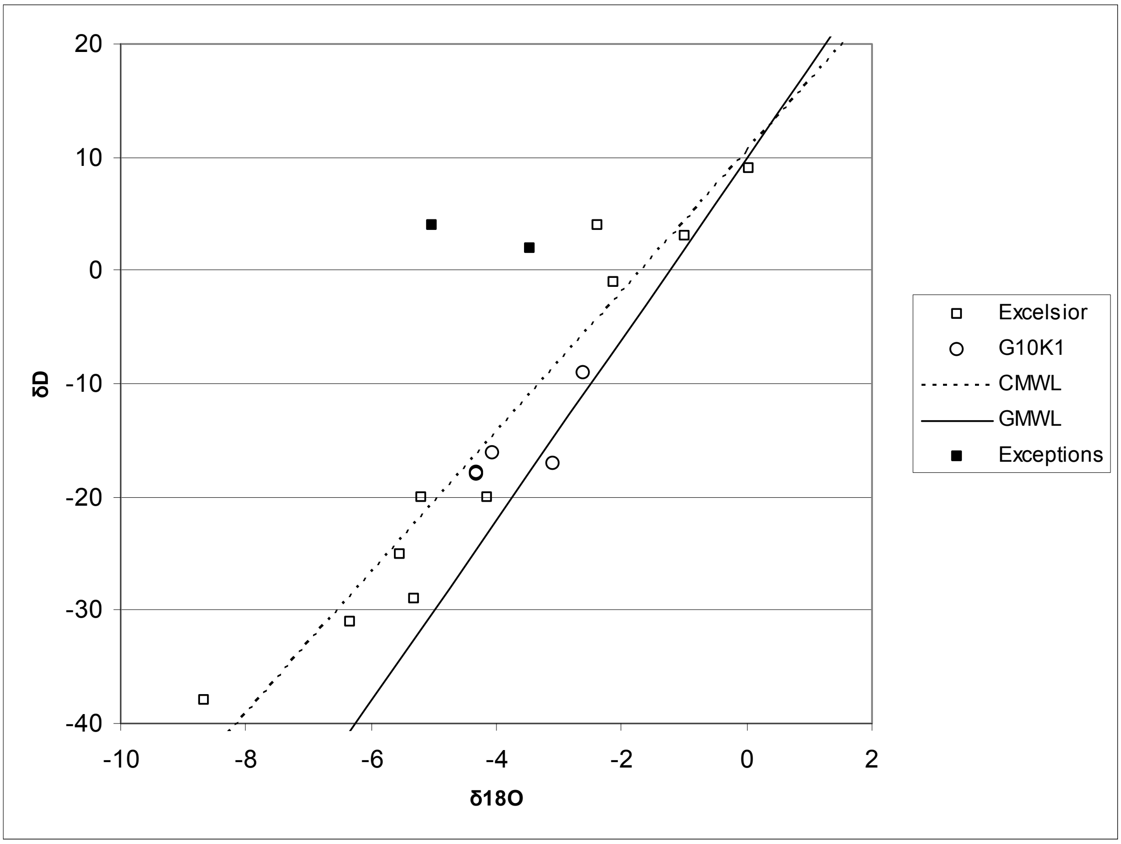

Figure 2.6.4: Plot of rainfall δD versus δ18O data

Isotope samples collected during the hydrocensus were predominantly from the Peninsula Formation (Ope) with a single sample from Graafwater (Og) and Piekenierskloof (Op) each. The spatial distribution of these samples is shown in Figure 2.6.5.

Evaporated water generally forms an array on a δD vs. δ^{18}O diagram, which has a shallower gradient than the LMWL along an Evaporation Line (EVAP) having a slope of 4 or 5 (Harris & Talma, 2002). The EVAP for groundwater samples from the TMG is depicted in Figure 2.6.6. There is no noticeable difference between samples from the Peninsula, Graafwater and Piekenierskloof. The slope of the EVAP for the study area is 4.35 indicating a change in isotope composition due to evaporation. However, there are samples that follow the LMWL closely indicating little or negligible enrichment by evaporation.

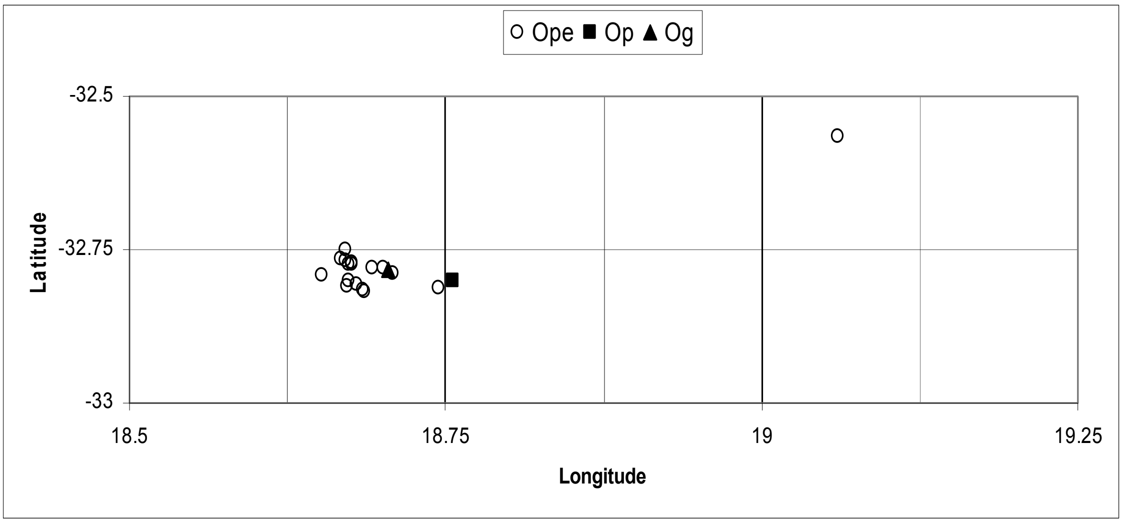

Figure 2.6.5: Spatial distribution of groundwater samples

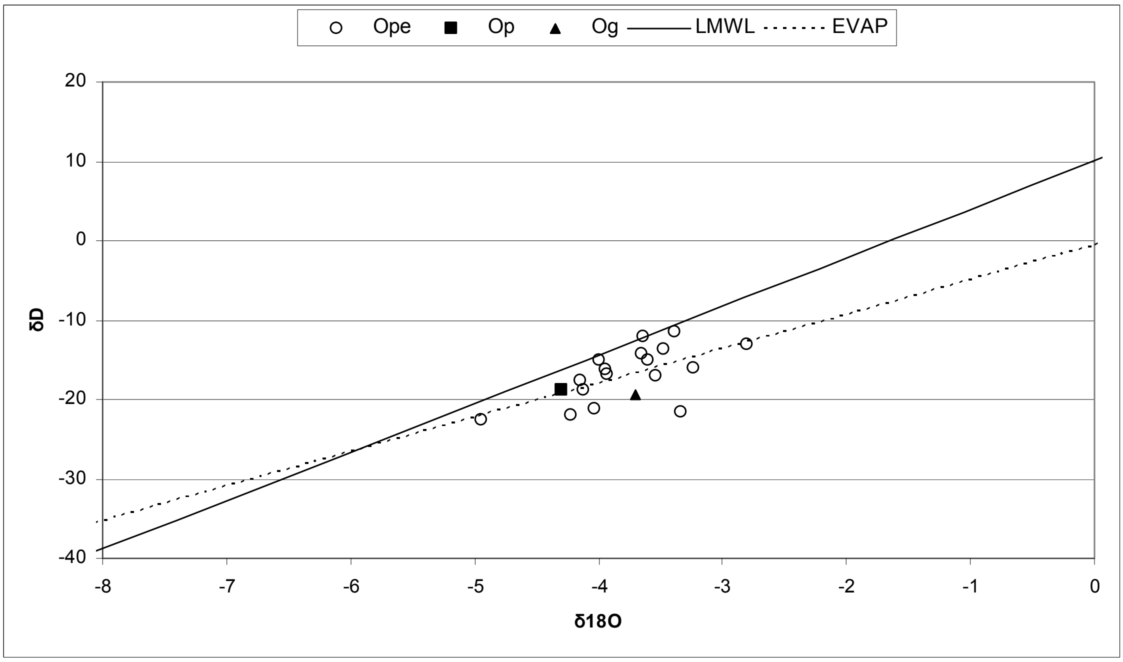

Figure 2.6.6: Plot of groundwater δD versus δ18O data

2.6.6 Physical methods

SVF and CRD simulations were developed for the TMG recharge zone based on information captured using the continuous loggers that were installed shortly after the completion of the hydrocensus of the pilot study area. Unfortunately only one year's worth of groundwater levels have been collected and the confidence level associated with the results of these physical methods is low.

2.6.6.1 The CRD method

Using the modified CRD method, as suggested by Xu & Van Tonder (2001), recharge for the study area was calculated at 11.1% (Figure 2.6.7). Storativity was assumed to be 0.0195, in line with parameters used by Hartnady & Hay (2000) in the CAGE study. Since no long-term data was available, the results reflect the current season only. The groundwater levels evaluated for this method came from a background borehole close to the catchment boundary where the local effect of pumping would not be significant. The recharge for this particular borehole, estimated with the CMB method, was 11.43%. According to Xu & Van Tonder (2001), most aquifers in South Africa are of a fractured nature with small storativities. Changes in groundwater levels in these aquifers would be very sensitive to recharge from rainfall, therefore simulation of water levels based on the CRD is less accurate.

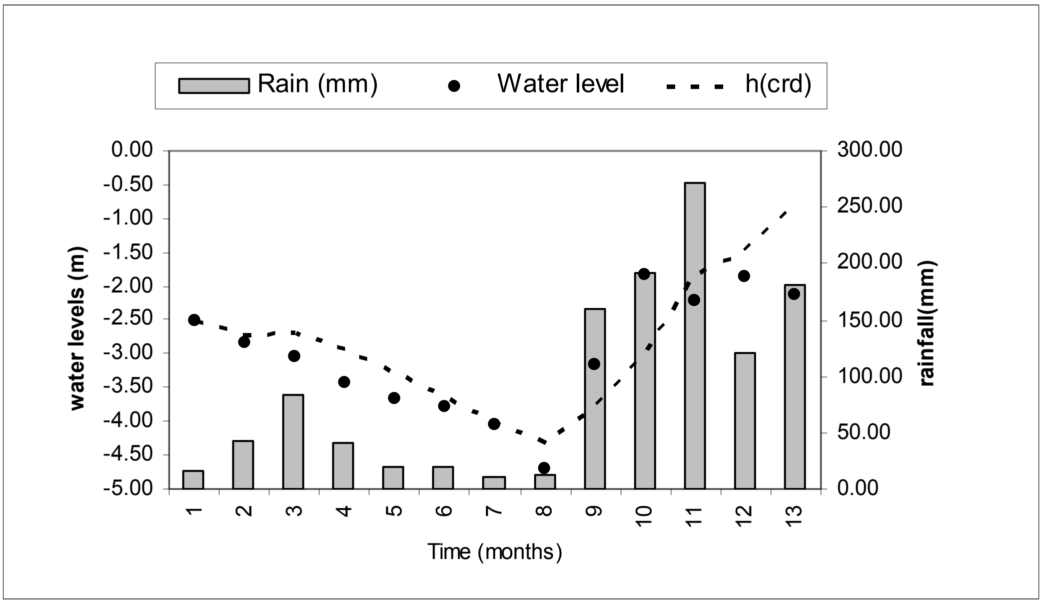

Figure 2.6.7: Simulation of groundwater fluctuation using the CRD method

2.6.6.2 The SVF method

Results from the SVF method based on groundwater levels in two boreholes within the TMG recharge zone are shown in Figure 2.6.8. The modelled recharge percentage was 10.5% using an S-value of 0.0135. Recharge values of respectively 11.43% and 19.74% were determined for these two boreholes using the CMB method.

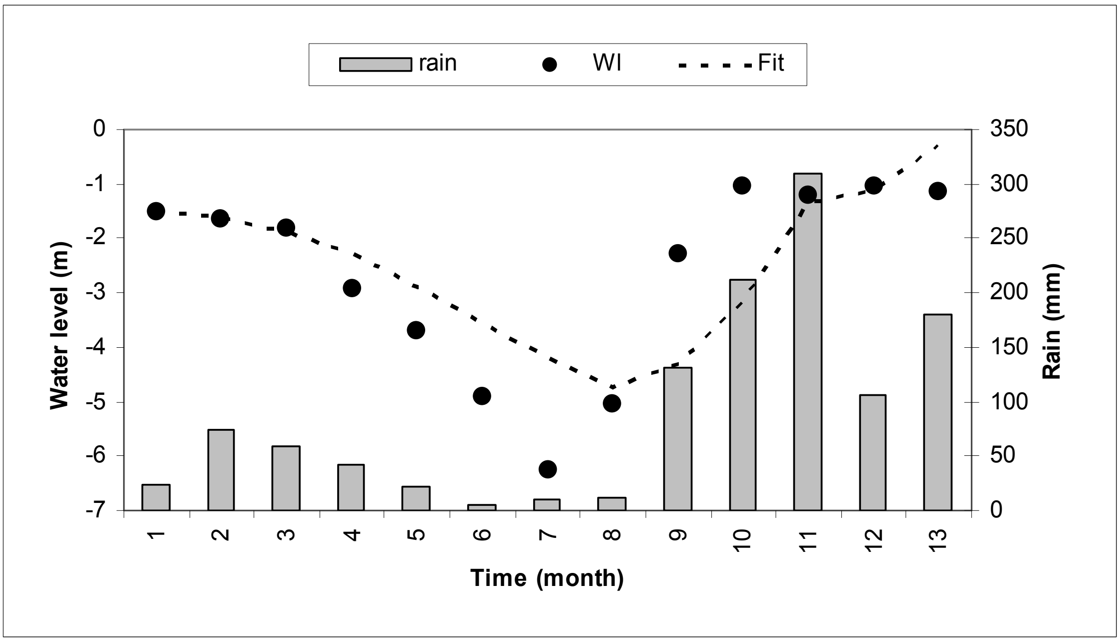

Figure 2.6.8: Simulation of groundwater fluctuation using the SVF method

2.6.7 WetSpass model

Recharge calculated using the WetSpass model is found in Table 2.6.4. The recharge percentages are higher than percentage calculated using other methods, but the mean recharge falls within the estimates stated in Table 2.6.1 and calculated using the CMB method.

TABLE 2.6.4: RECHARGE ESTIMATION USING WETSPASS

RECHARGE ZONES	MAP	RECHARGE (MM/YR)	RECHARGE (%)
Sand	491	66	13.4
TMG	983	327	33.3
Malmesbury	479	15	3.13

Due to the fact that the recharge is calculated as the residual of a water balance model, all other outputs need to be calibrated, in order for the recharge to be correct. Runoff and evapotranspiration are still under investigation. Yearly recharge results from WetSpass appear closer to accepted estimates than the cumulative monthly results, with summer results being predominantly negative and winter months positive. Negative recharge values indicate discharge zones. The monthly model overestimates recharge when recharge to the root zone becomes available to evapotranspiration and is termed storage. The storage is added cumulatively to recharge. This leads to over-accounting. If evapotranspiration is underestimated due to constraints in precipitation or potential evapotranspiration, the recharge will be overestimated. Figure 2.6.9 gives a reflection of the spatial distribution of the recharge as calculated by WetSpass.

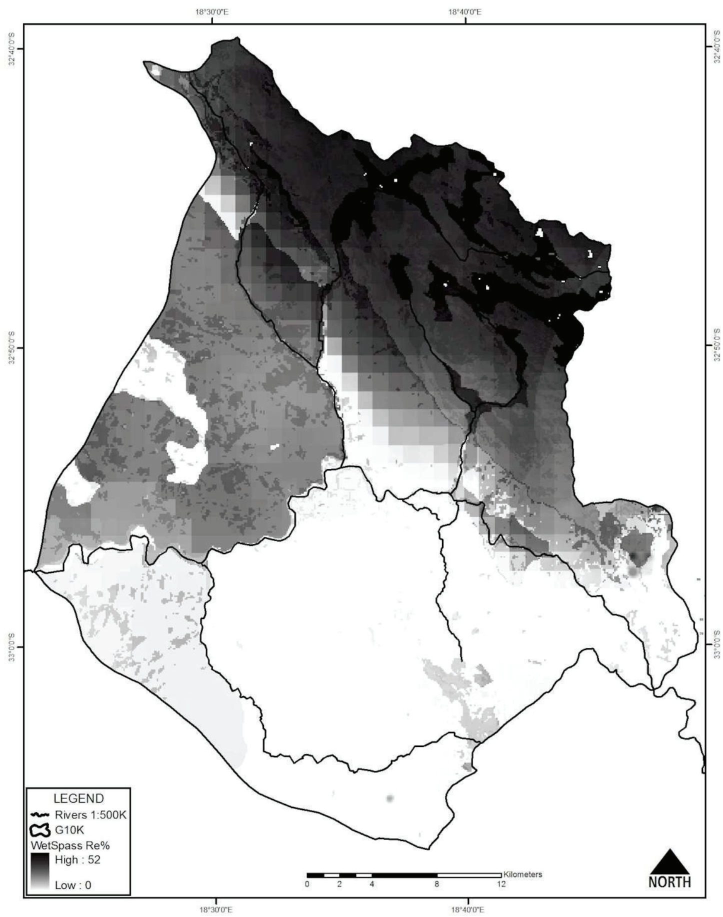

Figure 2.6.9: Annual recharge (%) for the G10K catchment using WetSpass

2.6.8 Discussion

Both CMB and WetSpass models predict low recharge in areas dominated by the Malmesbury group, with recharge predominantly predicted for the TMG area. Caution is advised when using the CMB method since the incoming rain has been generated over the ocean (Adams, 2004; Van Wyk, 2009) and in arid and semi-arid environments, recharge is essentially event driven. In hard rock aquifers, higher chloride values may indicate very old water, while low chloride groundwater is associated with active recharge. In addition, if there is runoff contributing to recharge over an area, the CMB method will underestimate recharge. The CMB method will always underestimate recharge in the alluvial aquifers; they are recharged during events of significant runoff (Adams, 2004).

The TMG group aquifer is assumed to be the major recharge zone for the study area, but the mechanism of recharge has not been clarified through the results achieved. The isotopic signature of the samples in the study area is very similar to those of a sample at Citrusdal.

It is well recognized that recharge is driven by single or multiple events and not annual averages. This is particularly true in arid and semi-arid environments. According to Parsons (2002: p. 97), "recharge estimation is thus prone to the fallacy of averaging". The WetSpass model tries to reduce this "fallacy of averaging" by using the precipitation fraction larger than infiltration in the modelling process. Recharge estimations in fractured aquifer systems are prone to error and groundwater modelling is required. Lack of suitable data is often the prime reason why recharge is not quantified. Errors in the model can be attributed to uncertainties in the complexity of the model-data input such as uncertainties in landcover, soil classifications, slope and especially precipitation maps.

The output from the WetSpass model needs to be used as input into a groundwater model, preferably MODFLOW. This process was completed but, due to a lack of input data, high-level modelling expertise and time, the MODFLOW model could not be calibrated fully (dry cells were being obtained). However, the lack of a fully functional and calibrated MODFLOW model was not deemed to negatively impact the overall outcome of the project results.

2.7 Dam volume calculations

2.7.1 Introduction

South Africa is categorized as a water scarce country, with a well-established commercial agriculture sector (Zietsman *et al.*, 1996). A problem arises in that a large proportion of farmers in the Southwestern Cape are reliant on irrigation water for farming practices. In an attempt to secure water supply in Botswana, farmers in rural areas construct small dams – 1000 m^3 to 100 000 m^3, which are largely unmonitored (Finch, 1997). In this context, Finch (1997) refers to "monitoring" as establishing the amount of water stored and assessing any declines in storage over time. This report highlights the need for water resource managers to have useful information regarding the spatial distribution of these resources and suggests the use of remote sensing as an appropriate tool for doing so.

In South Africa, it is the responsibility of the Department of Water Affairs and Forestry (DWAF) to obtain such information and to ensure compliance in water use regulations. Small dams are monitored on a case-by-case basis, but this is exceptionally time consuming and costly. In addition, water managers have to deal with complex issues related to data collection, staff capacity, communication and institutional fragmentation (Funke *et al.*, 2007). It is suggested that the Department needs less costly and time consuming means of obtaining and assessing information so as to manage systems better. It is possible that remote sensing technologies might prove an efficient means of monitoring water resources so as to alleviate some of the issues that inhibit efficiency, such as cost, accessibility, limited time and human resources.

2.7.1.1 Water Use Legislation – The Reserve

Under the National Water Act, monitoring of water resources incorporates licensing and target schemes, as well as water quality management at national, regional and local levels. One of the tools prescribed by the Act is the registration of water use, particularly at regional level (tier 2). Schedule 1 of the Act lists activities that require the registration of water use by means of a licence. Water storage, which is the focus of this report, is listed as one of these activities. The Act states that a licence is required for "any person or body storing water for any purpose (including irrigation, domestic supply, industrial use, mining, aqua culture, fishing, water sport, aesthetic value, gardening, landscaping, golfing, etc) from surface runoff, groundwater or fountain flow *in excess of 10 000 cubic metres* or where the *water area at full supply level exceeds 1 hectare* in total on land owned or occupied by that person or body and not in possession of a permit or permission" (DWAF, 2007).

Dams not licensed and registered to DWAF's inventory list would then be deemed illegal storage and should be addressed accordingly. The water user is expected to provide the location, nature and quantity of water use in the registration application process. According to DWAF (2007), if the water use is not registered, it is likely that DWAF will be unaware of the activity taking place, until such a time that the area is reviewed. Finch (1997) suggests that the construction of irrigation dams in rural areas goes largely unmonitored. This is cause for major concern in terms of establishing the Reserve and efficiently allocating water use to various sectors.

2.7.1.2 Aims

This section aims to use remote sensing to calculate the volume of water held in storage in farm dams. The steps to achieving this aim are listed as follows:

- Identify agricultural dams in the study area by classifying remotely sensed imagery within the Definiens™ software environment.
- Determine surface area of dams using Definiens™ software.
- Determine the volume of water stored in farm dams using a storage volume equation.
- Identify licensed and unlicensed dams using GIS cadastral information and DWAF's registration database.

2.7.1.3 Data

SPOT 5 data was selected for this study, as it is freely available for research purposes. It is also appropriate for this study since it offers high-resolution data that is likely to provide the most accurate results for the study. For the purposes of this study, the key features of SPOT 5 data include high resolution, capability of revisiting the scene at regular intervals and stereo imaging. The imagery was obtained from the Satellite Applications Centre (SAC). Given the reflectance characteristics of water, multispectral imagery is optimal in extracting surface water bodies. SAC distributes data in a GeoTIFF format for its generic nature and wide support of various GIS software (Lück, 2007). The imagery that covers the study area was acquired on 13/01/2007 and 12/03/2007. More recent imagery for this area is not available as yet.

2.7.2 *Definiens Software*

Although there may be a myriad of remote sensing software available for achieving the stated objectives, each with subjective benefits and shortcomings, this study will explore the use of the Definiens™ software. The key feature that is offered by Definiens™ is its semi-automatic classification capabilities in an object-oriented environment. Where other packages classify according to pixels, Definiens™ first segments the image into polygons (image objects) upon which classification is further conducted. Developing a model within this program may yield an efficient means of identifying and selecting water bodies from satellite images and if a suitable conversion formula is used, water storage may be determined.

In the Definiens™ environment, the first step of image analysis is segmentation. The image is divided into homogenous segments based on colour, scale, shape, compactness and smoothness. These segments can be merged or divided based on these parameters (Kressler *et al.*, 2005). The programme sets a context for the classification of the image, in that each object 'knows' its surrounding objects (Definiens™, 2000; Herald *et al.*, 2002). This hierarchical network is displayed in Figure 2.7.1.

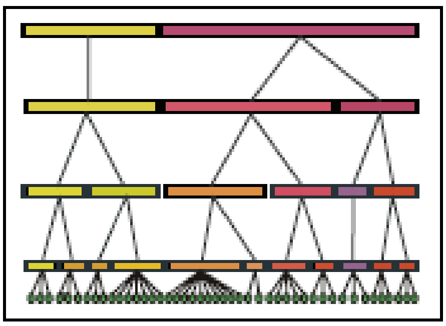

Figure 2.7.1: Hierarchical network of image objects

(Source: Definiens, 2000)

For example, an object at a given level is related to objects within the same level but also to objects in levels above and below it. Classification algorithms can be used with reference to this network. The classification process that will be followed in this study will only operate at one level so as to maintain a certain level of simplicity. Algorithms making use of brightness thresholds, distance relationships and the shape of features are means of classifying an image.

2.7.3 Methodology

2.7.3.1 Ground-truthing

Three farm dams have been surveyed in the Piketberg district to obtain bathymetric measurements that were necessary for validating remotely sensed data. Three dams were surveyed on farms in the Bo-Piketberg. These dams were chosen as they were relatively easily accessible and also had some form of craft available on site for use during field measurements. The same methodology was applied to all three dams as described below.

A small boat was used to traverse each dam. Measurements of the depth were recorded at approximately 10 m intervals along a predetermined transect. The co-ordinates at each measured point were also recorded using a hand-held Garmin GPS.

The recorded point data was uploaded to ArcMap™ to display the results on the SPOT XS image. In order to calculate values for the surface area of the respective dams, polygons were created by onscreen digitizing to represent the dams. Thereafter, triangulated irregular networks (TINs) were created for each dam to interpolate the bathymetry of the dams for a volume estimate. Using the digitized polygon as the water body surface layer and the TIN as the bathymetric interpolation layer, values for area were obtained using the ArcMap™ 3-D Analyst feature (Table 2.7.1).

TABLE 2.7.1: FIELD SURVEYED DAMS WITH THEIR CALCULATED SURFACE AREAS AND TIN DETERMINED VOLUMES

FARM DAM	SURFACE AREA (HA) ARCMAP™	VOLUME (M^3) FROM TIN
Dam A	5.497	239 166
Dam B	3.152	96 584
Dam C	12.942	316 749

A limitation in creating polygons in ArcMap™ with respect to calculating surface area is that the polygons do not take account of any rock outcrops or vegetation that may be present within the boundaries of the polygon. Onscreen digitizing may be a subjective approach to area estimation since the user decides which pixels to include in the creation of a polygon. This is particularly questionable for the polygon edges where dense vegetation may be misinterpreted as water and *vice versa*.

2.7.3.2 Object Oriented Classification

The focus of this section is to classify surface water bodies with a view to calculating their surface area. The main steps for each section are as follows:

- Apply the segmentation algorithm to the subset image.
- Develop a classification model within Definiens™ to identify farm dams based on various feature characteristics.
- Obtain the surface area of feature objects.

In order to process the image it was necessary to create smaller subsets of the image. Subsets were created in order to process an image since there were limitations on either the capacity of hardware capability and/or software such that Definiens™ was only able to process a limited number of image objects at a time.

The classification process within the object-oriented approach begins with segmentation. A multi-spectral segmentation algorithm was applied to the subset. The scale parameter was set to 10.

Various algorithms of band ratios were created and explored to obtain a relatively favourable result for the distinction of water bodies. A ratio of red to blue bands highlighted water bodies well, however, misclassifications were evident. This is to be expected with any classification approach and refinement of the classification is necessary. Other band ratios set to particular thresholds were used to classify variations of surface water for the interim classification. These variations were later assimilated to the 'water' class using a distance relational feature. Where linear features, such as roads, were misclassified with the initial band ratio, the asymmetry feature was used to correct for the misclassification. In addition, brightness thresholds were particularly useful in eliminating misclassifications on high slopes. Once a satisfactory result for surface water bodies was obtained, the water class was merged to create single image objects. These image objects could then be exported to ArcMap™ as a polygon shape file with associated area values.

The classification steps developed within Definiens™ are displayed in Figure 2.7.2.

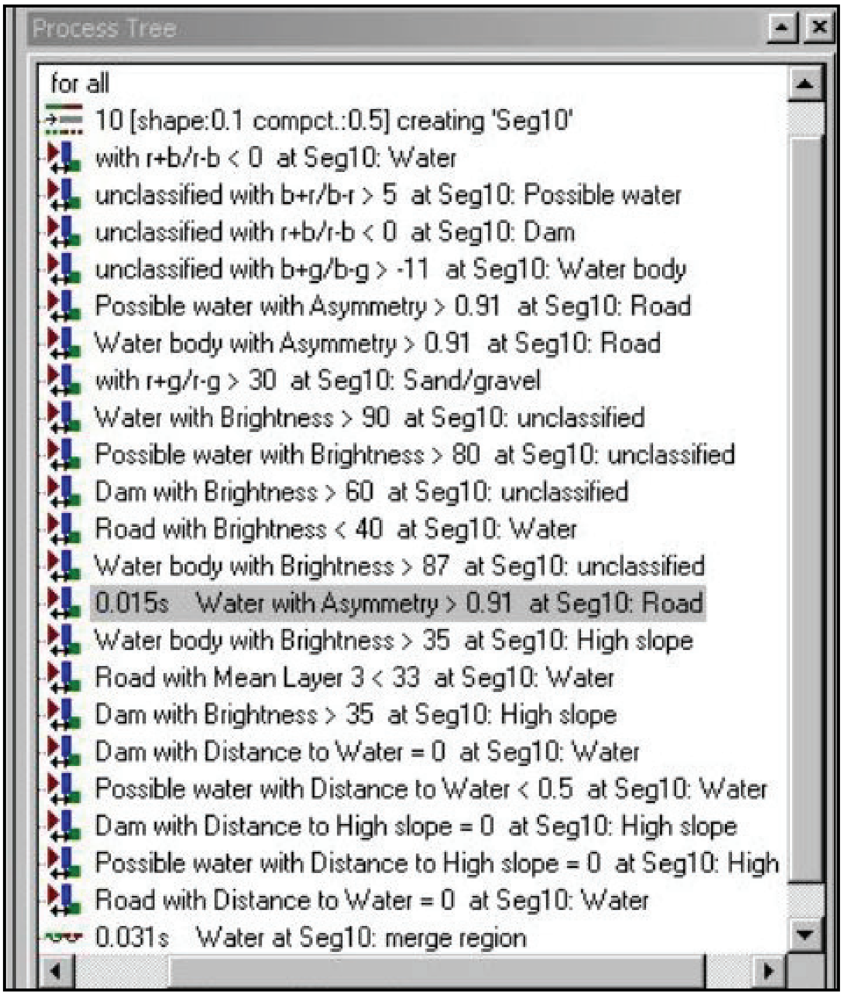

Figure 2.7.2: Process tree for Object Oriented Classification of Surface Water Bodies (Pilot Study Area)

The results of the object-oriented classification of farm dams in the study area were uploaded to ArcMap™, as can be seen in Figure 2.7.3.

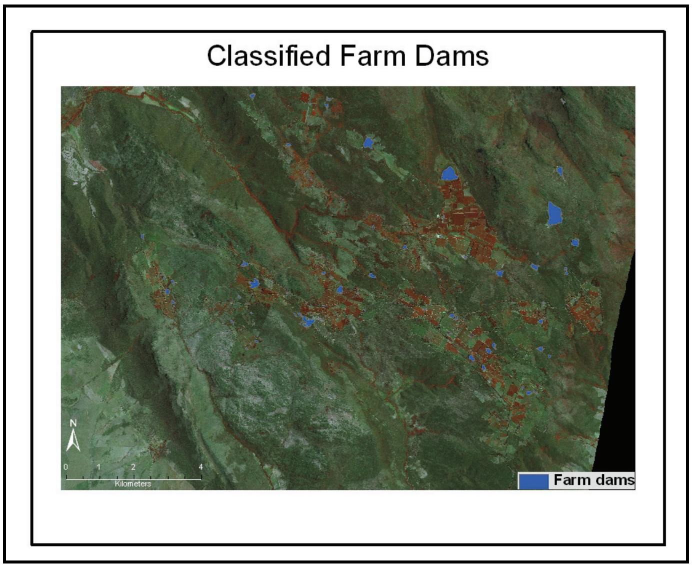

Figure 2.7.3: Object Oriented Classified of Farm Dams for Pilot Study Area

Of the three fieldwork sites, only the classification for Dam B is included in this report and is shown in Figure 2.7.4. The classification encompasses all the fieldwork data points. There appears to be a possibility that water in the north-north-west of the dam was not included in the classification.

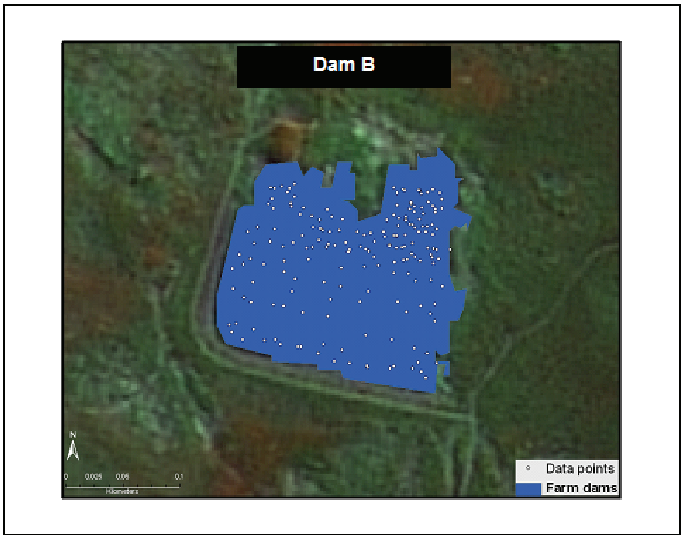

Figure 2.7.4: Field validation points for Dam B

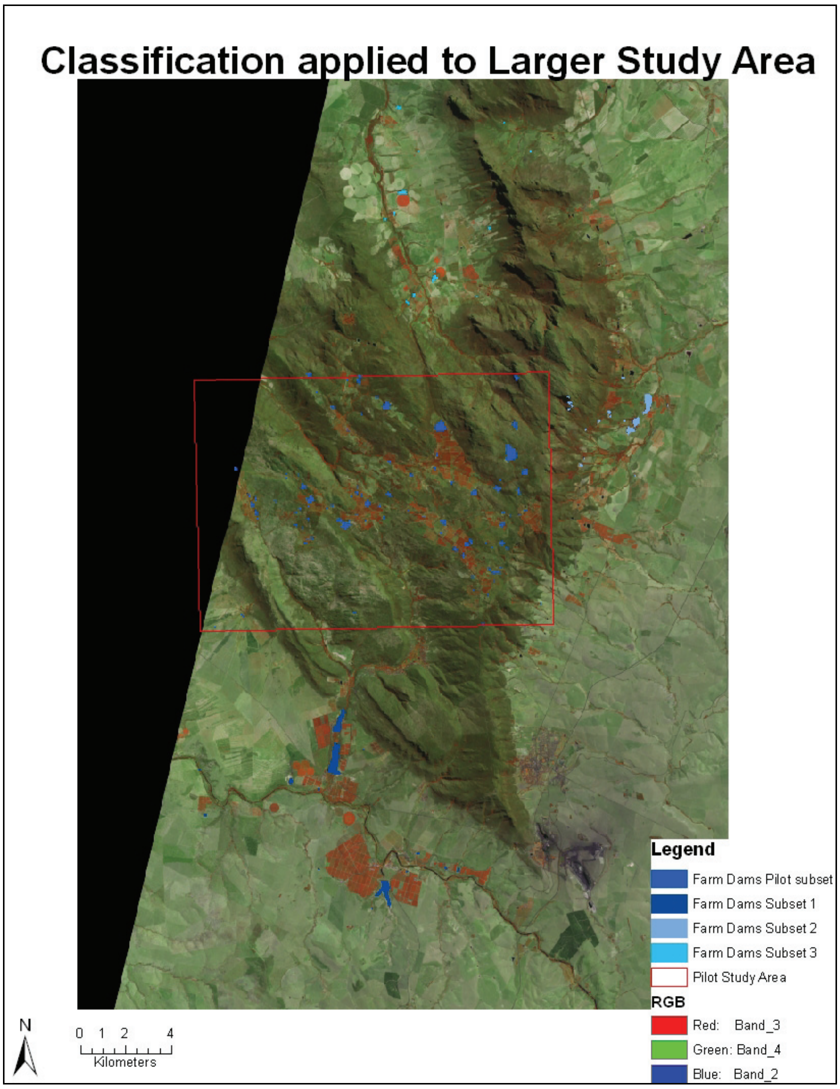

Figure 2.7.5: Classification of dams in the larger study area

The classification model developed for the pilot study area was run on three subsets within the larger study area. The result is displayed in Figure 2.7.5 where different shades of blue are used to illustrate farm dams in the various subsets. In each case, farm dams were generally well identified, however; some misclassifications were incurred. These were corrected for with relatively minor adjustments to the original process tree. For example, in the first subset, the river was identified as water and had to be excluded from the Farm Dam class. A ratio of length to width was used to classify the image objects forming part of the river.

In some areas of the second subset, parts of the farm dams were associated with the Potential Water class. By using a distance relationship, these objects were assimilated to the Farm Dam class. The length/width ratio and a blue to green band ratio were useful in modifying the third subset.

It was found that the model works well for the general identification of surface water bodies. However, it is necessary to modify the rule set as the areas of study differ. This is particularly necessary when dealing with a surface area (which affects volume) application as minor discrepancies can result in a significant difference in the value obtained for surface area.

2.7.3.3 Determining Volume Stored

Sawunyama *et al.* (2006) addressed a similar problem to that presented in this report, namely using Landsat data extracted from images covering Zimbabwe to identify small reservoirs used for domestic purposes and farming. The authors concluded that remote sensing is a way to improve water resource management given the constraints of time and cost. Sawunyama *et al.* (2006) reviewed existing area-capacity relationships and errors of dams and deemed it feasible to develop a model equation for estimating storage capacity of small reservoirs. The assumed general characteristics of the reservoirs in terms of topography, geology, size and maximum depths led to one general equation to establish capacity in terms of its relationship to surface area. This best-fit equation (Sawunyama *et al.*, 2006) is for the area-capacity relationship that will be used in this section and is given by:

$$\mathbf{C = 0.023 * A^{1.33} \; (R^2 = 0.95)}$$

where **C** is capacity in m^3 and **A** is area in m^2.

The relationship was validated by four independent reservoirs in the catchment. A t-test was conducted and that showed a strong correlation for surface area at 95% confidence interval. Possible reasons for error may be as a result of the coarse resolution of imagery used in this study, i.e. 30 m Landsat imagery. This report makes use of 2.5 m resolution imagery that should allow for more accurate results. The authors further note that vegetation in shallow water might account for the error, even though the error is considered minimal.

Similarly, Liebe (2002) developed a methodology that makes it possible to estimate storage volumes of reservoirs as a function of their surface area on the premise that knowledge of such a function allows calculating reservoir volumes on the basis of remotely sensed data. Liebe (2005) used 61 reservoirs which were precisely measured in the field and modeled to derive regularities and interrelations between the three variables 'area', 'depth', and 'volume'. Transferring their geometric properties into a generalized equation allowed the estimation of storage volumes based on surface areas. In combination with remotely sensed reservoir surface areas, this relation can be utilized to make reservoir volume inventories on regional or even higher level. The derived formula is given as:

Vol = 8.52 * Area$^{1.437}$ (10^{-3} m^3) (Van de Giesen et al, 2004)

Examples found in the literature provide positive responses to using remote sensing for determining dam capacity. However, challenges do exist in obtaining accurate results for identification and quantification of water bodies. Some issues to consider are reflectance, sedimentation and spatial resolution as these factors may contribute to data inaccuracies. For example, areas of high reflectance and/or sedimentation that should fall within a category classed as water may be inaccurately classified as a result of dissimilar pixel values. All things considered, this study attempts to obtain a relatively accurate result for water surface area and volume of water stored.

As described above, the 3-D analyst feature in ArcMap™ allows for the estimation of surface area and volume for interpolated features. The surface area value provides an input for the equations $C = 0.023 * A^{1.33}$ (Sawunyama *et al.*, 2006) (Figure 2.7.6) and **Vol = 8.52 * Area$^{1.437}$** (10^{-3} m^3) (Van de Giesen, 2004) (Figure 2.7.7) which are used to determine the volume of water stored in farm dams.

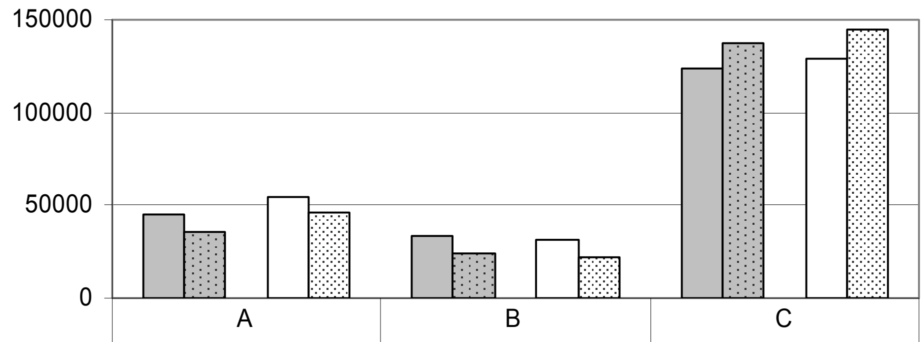

	A	B	C
Definiens area (m2)	45040	33310	124200
Definiens volume (m3)	35564	23810	137060
ArcGIS area (m2)	54970	31520	129420
ArcGIS volume (m3)	46355	22123	144774

Figure 2.7.6 : Volume results using the formula by Sawunyama et al. (2006) on surface area of dams mapped from satellite images (Definiens) and from the field survey data (ArcGIS).

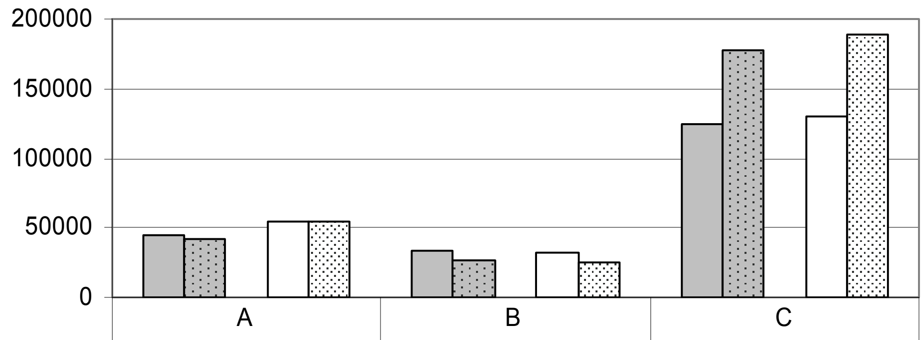

	A	B	C
Definiens area (m2)	45040	33310	124200
Definiens volume (m3)	41463	26877	178112
ArcGIS area (m2)	54970	31520	129420
ArcGIS volume (m3)	55208	24826	188967

Figure 2.7.7 : Volume results using the formula by Van de Giesen et al. (2004) on surface area of dams mapped from satellite images (Definiens) and from the field survey data (ArcGIS).

The methodology presented in this section takes into account ground truth data as well as object-oriented classification. The ground truth data was conducted to verify the classification to a certain extent. It requires the use of onscreen digitizing to obtain surface area values. The polygons created by onscreen digitizing give a satisfactory result, however, it is limited in that it does not account for vegetation or rock outcrops found in water bodies. Creating polygons in this manner has to be done on a case-by-case basis. This is suitable when only a few polygons are required but is not appropriate when attempting to quantify numerous dams across the study area. The object-oriented approach addresses this challenge, as the classification is semi-automatic. Although this sort of classification allows for the exclusion of rock outcrops, other misclassifications may occur.

2.7.4 Discussion

2.7.4.1 Surface area results

The classification process produced a satisfactory result in that it identified water bodies in the study area. Since the SPOT image used in this study was captured in January and March 2007 and fieldwork conducted between November 2007 and April 2008, a certain level of variation is to be expected, probably due to annual precipitation and vegetation growth. An improvement in the accuracy could be achieved if the fieldwork was conducted at the same time of year that the image was captured.

Differences in the fieldwork exercise to the object-oriented classified results are likely due to relatively higher rainfall in 2007 resulting in the farm dams being fuller than when the image was captured in 2005. An oddity in the classification was observed in the case of Dam A where part of the dam wall was classified as water.

A regression analysis was conducted for the respective surface area values obtained in ArcMap™ and Definiens™. Table shows that the values are not significantly different. All the standard deviations were low and fall within one standard deviation of the mean (Table 2.7.2). This means that there is great similarity between the values for surface area using Definiens™ compared to the value obtained by the fieldwork exercise.

TABLE 2.7.2: STANDARD DEVIATION FOR SURFACE AREA VALUES

FARM DAM	SURFACE AREA (HA) DEFINIENS™	SURFACE AREA (HA) ARCMAP™	STD. DEV.
Dam A	4.504	5.497	0.702157
Dam B	3.331	3.152	0.126572
Dam C	12.42	12.942	0.36911

In developing the classification process, it was realised that there is always a certain level of error particularly with regard to "mixed pixels" near the edges of the water bodies, for example, the partial misclassification of Dam A's wall. Areas of error that may exist, but are of no consequence, can be manually deleted from the result at the discretion of the user. It is noted that compensating for one misclassification may often lead to a misclassification of a different image object. Given the results of standard deviation, a subjective decision was made to keep the classification as is.

It is suggested that once specific areas of interest (e.g. dams of particular concern) have been identified, further refinement of the process can be made in order to obtain a more accurate result if necessary.

2.7.4.2 Volume results

The results of the various volume estimations (from field work using a TIN and formulae from the literature) are compared with the WARMS registered volumes for the selected dams and shown in Figure 2.7.8. It can be seen that contrary to expectations, there is better agreement between the WARMS registered value and the volumes calculated from the surface area to volume formulae, than between the WARMS registered value and the TIN calculated from field work. A couple of explanations for this are possible.

1) The volume obtained from the TIN is the closest to reality and the volumes registered in WARMS are too low and either a) WARMS volumes are coincidentally closer to the volumes calculated using the formula or b) the farmers have used a surface area to volume formula to calculate dam capacity for WARMS registration.
2) The WARMS registered values are correct as they may have been obtained from engineers when the dam was constructed and a) the surface area to volume

formulae (especially Van de Geisen *et al*, 2004) have performed well and b) there were inexplicable errors in the field survey data.

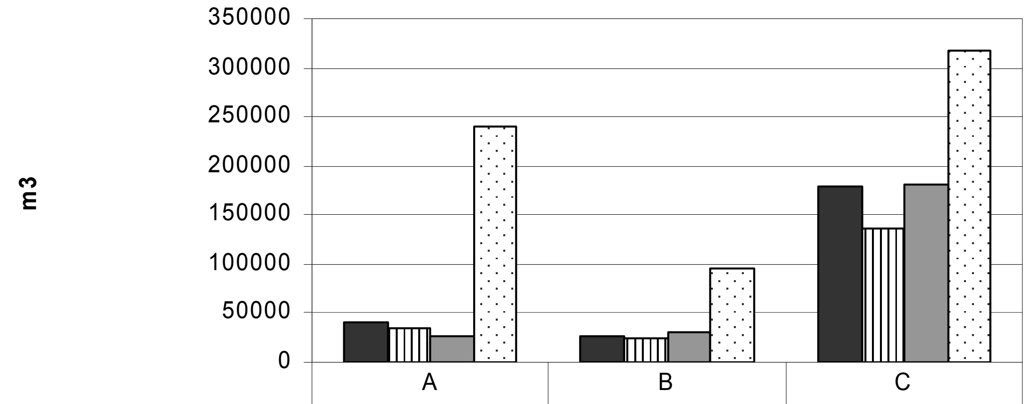

	A	B	C
Van de Giesen et al.	41463	26877	178112
Sawunyama et al.	35564	23810	137060
WARMS	27000	30000	182000
TIN	239166	96584	316749

Figure 2.7.8: Comparison of dam volumes calculated from field data using a TIN, the two formulae obtained from the literature and the volumes registered on the WARMS database.

It should also be stated that the formulae used were developed using relationships between surface area and dam volumes for specific regions and differences between regions (especially topographic differences) may result in different relationships being obtained. Liebe (2002) states that the relief plays an important role regarding (possible) dam construction. On the one hand, dam construction necessitates a certain landscape roughness. On the other hand, homogeneous relief properties are of great importance to the feasibility and success of a surface area to volume relationship. However, as long as the surface roughness is approximately constant, the presence of area volume relations is expected. In this context, "constant" refers to the surface undulating at a relative steady frequency and amplitude. If changes in roughness were identifiable, e.g. as they develop in areas with a significant change in geologies, splitting up the area into relatively homogeneous sub-areas is a reasonable means to (re-)achieve good area-volume correlations, if needed.

If this statement by Liebe (2005) is considered, applying one formulae across a catchment as diverse as G10K should not result in accurate volume calculations. If the topography of the study area used by Liebe (2002) (which was used to develop the Van de Giesen et al. (2004) formula) is compared with the G10K catchment, the is very apparent.

Table 2.7.3: Differences in topography between G10K catchment and the Ghanaian study area used by Liebe (2002)

	G10K	**Liebe (2002) study area**
Minimum elevation (m)	17	122
Maximum elevation (m)	1132	455
Mean elevation (m)	174	197
Standard deviation (m)	207	35.33
Average slope angle (°)	5.45	0.49
Total area (km²)	1260	8689

If an accurate estimation of dam volume is required, it is therefore necessary to work only within topographically homogenous areas, conduct extensive field surveys to establish the relationship (and therefore a formula) between surface area and volume and apply the formula to remaining dams in the area. It is possible that formulae may be used between regions that are homogeneously similar however, this would need to be tested.

2.7.5 Conclusion

This study found remote sensing, in the form of object-oriented classification, to be a reasonably accurate tool in identifying surface water bodies. A relatively simple classification process was developed so as to identify farm dams and obtain an estimate for surface area, a key input for volume. Data used for this study included high-resolution satellite imagery to generate a reasonably accurate result. This is important in context of this study as change in surface area has a direct effect on volume of water stored and consequently the legal status of water stored. The result for surface area was found to be satisfactory; however, there are other factors such as the level of sedimentation that the method does not take into account. At this stage sedimentation is not seen as a major limitation to the method since farm owners are required to register their dams at full capacity.

In order to obtain a value for water stored in farm dams, two capacity equations were used to convert surface area to volume. The equations make use of surface area and a constant as inputs so that implicit assumptions and errors may exist. The value generated using the equations may still provide a useful estimate for the amount of water stored however, more extensive field work and dam surveys would allow for the creation of a formula unique to the study area which could be applied across the catchment with more confidence.

This study concludes that in the context of illegal water use, using remote sensing as a tool to quantify water storage may be appropriate in identifying water bodies and generating an estimate of volume stored. It was found that the model works well for the general identification of surface water bodies. However, it is necessary to modify the rule set as the areas of study differ. This is particularly necessary when dealing with a surface area (which affects volume) application as minor discrepancies can result in a significant difference in the value obtained for surface area. There remain some uncertainties as to the assessment of the surface to volume conversions and further research is recommended.

Dams that have the potential to be in violation of the legislation should be dealt with on a case-by-case basis, using conventional methods.

3 WATER BALANCE RESULT – G10K CATCHMENT

The results presented in the previous section will now be combined and presented in three sections:

3.1 Annual water balance equation for the study area

3.2 Evapotranspiration differencing as an indicator of irrigation and/or recharge

3.3 Application of results to selected WARMS data to assess validity of methodology

3.1 Annual water balance equation for the study area

At catchment level, the water cycle can be represented by the water balance equation which is a simple statement of the law of mass conservation and is expressed as

Inflow = outflow ± changes in storage

or

$\Delta S = P - ET - Re - RO$

where ΔS is the change in water storage in the catchment, P is precipitation, ET is evapotranspiration, Re is groundwater recharge and RO is surface water runoff. In order to calculate annual ΔS for the catchment, an annual volume is required for each component of the water balance equation which was calculated in section 2.1. Simplistically put, at a catchment level, it can be determined whether a catchment is experiencing water stress on an annual basis by using the water balance equation. If $\Delta S > 0$ for a particular year, the catchment is not experiencing water stress, but if $\Delta S < 0$, water stress is occurring. If ΔS is calculated for a few years in succession, the overall water stress can be determined.

The limitations noted under the results of each of the individual components in sections 2.2 Precipitation, 2.3 Evapotranspiration, 2.5 Surface runoff and 2.6 Recharge should be considered. It was noted that, for various reasons, the precipitation for the study period was underestimated, evapotranspiration using the SEBS model appears to be overestimated, runoff is from an ungauged catchment and therefore unvalidated, recharge is overestimated due to underestimation of evapotranspiration in the WetSpass model, and therefore the result of combining the individual components of the water balance equation is not expected to reflect a real change in storage value. However, the exercise was completed to analyze whether any patterns and variations within the catchment could be discerned and explained.

ArcGIS Spatial Analysis was used to combine the results for the total study period (1 Oct 2007-30 Sept 2008) of P, ET, Re and RO for the G10K catchment according to the above equation and the result is shown in Figure 3.1.1.

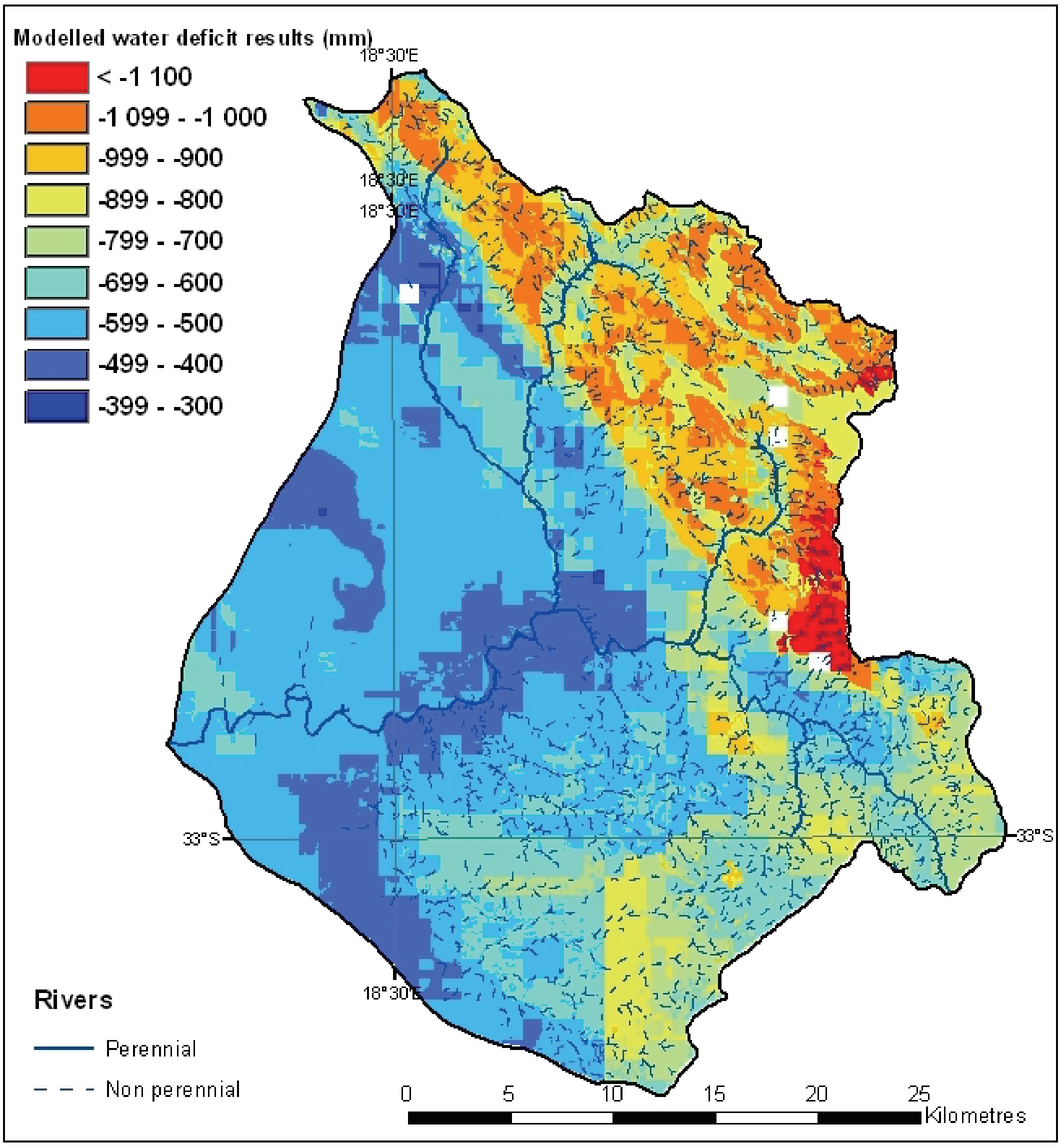

Figure 3.1.1: Results of applying the water balance equation to the modelled water balance components for the G10K catchment for the study period (1 Oct 2008-30 Sept 2008)

As expected, due to the underestimation of precipitation and the suspected overestimation of evapotranspiration, the G10K catchment shows a total water deficit for the study period across the entire catchment. Whilst there may not be much certainty in the absolute results of this method, it may be worth discussing the spatial variations across the catchment, as a relative rather than absolute result. Firstly, it can be noted that the deficit is highest in the elevated Bo-Piketberg area, despite the fact that this area receives the largest amount of rain in the catchment (section 2.2). This can be explained in two ways: 1) Evapotranspiration was estimated to be higher in the Bo-Piketberg than in any other part of the catchment (section 2.3), so even though in this area a lot of water entered the system, a lot of water also exited the system though evapotranspiration. 2) Due to the steep slopes in the mountainous area, runoff was modelled to be higher in this part of the catchment than anywhere else in the study area (section 2.5).

The water deficit increases from west to east across the catchment. This is in line with the climate zones in the catchment shown in Figure 1.2.3. The climate is described as semi-arid and cool to the west of the study area and humid subtropical and warm in the eastern regions of the study area.

Since there are many uncertainties associated with the input data into the water balance equation it may be more useful to create a unitless index to assess the spatial variables across the catchment rather than to look at absolute values. For this purpose, the concept of the normalized difference storage index (NDSI) was coined, where

$$NDSI = (P - u)/(P+u)$$

where P = precipitation
u = ET+Re+RO

where ET is actual evapotranspiration, Re is recharge and RO is runoff.

Simplistically put,
NDSI = (inflow-outflow)/(inflow+outflow)

which should result in a value of between -1 and 1 with a negative value meaning a decrease in storage (more outflow than inflow) and a positive value meaning an increase in storage (more inflow than outflow). The higher the positive value, the larger the increase in water stored, and the higher the negative, the larger the decrease in water storage. This is shown in Figure 3.1.2.

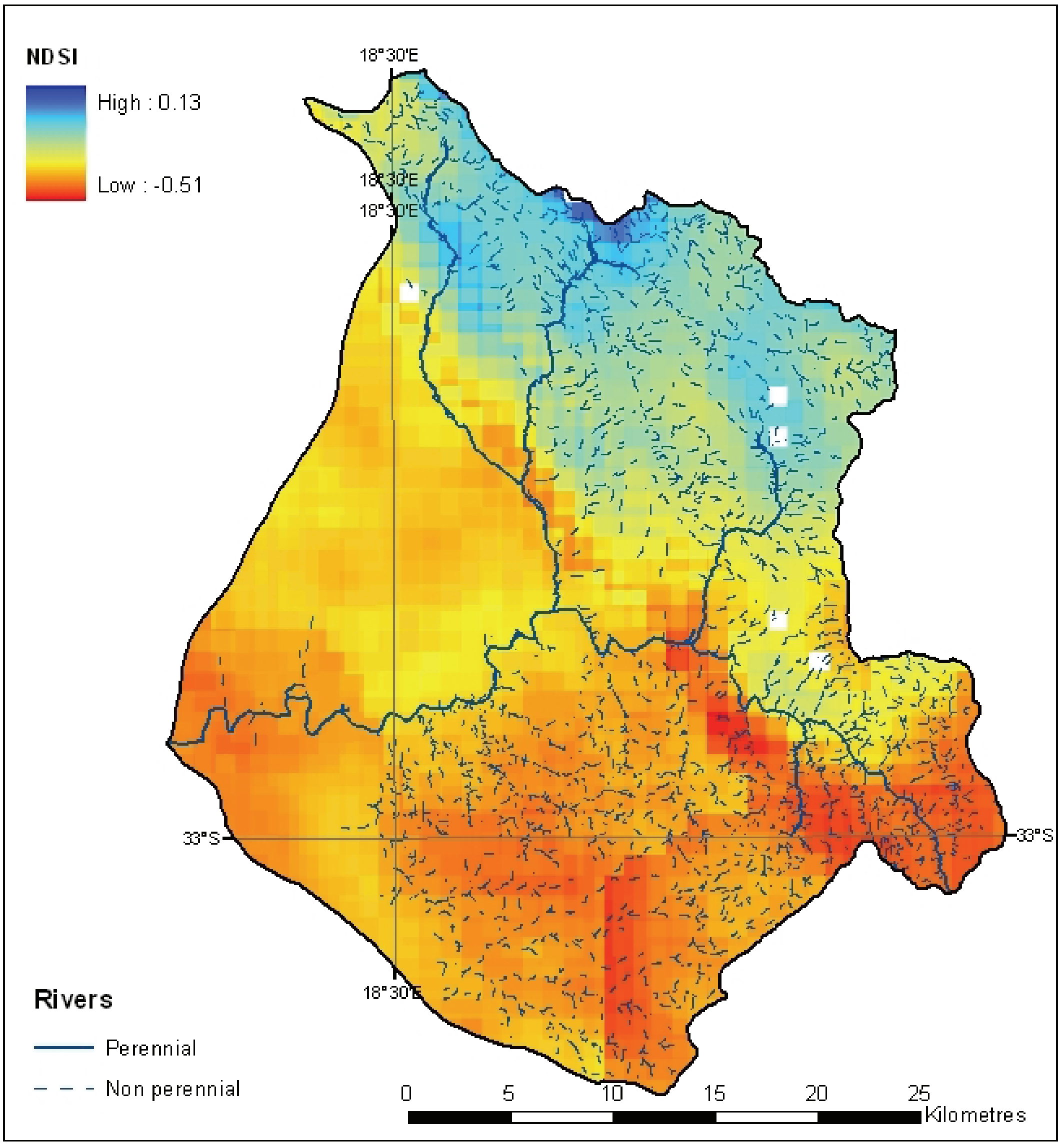

Figure 3.1.2: The normalized difference storage index for G10K catchment for the study period

When the results in Figure 3.1.2 are examined, a very different scenario is presented. The Bo-Piketberg no longer shows the highest water deficit as the high rainfall has a normalizing effect. As with the result of the water balance equation, the water balance deficit index shows a similar southwest to northeast trend across the catchment with lower values in the southwest. On the low-lying areas, the water deficit index mirrors the Moorreesburg Formation (see Figure 1.2.2), also reflected by the higher drainage density and the presence of pans in the southernmost regions of the catchment (see Figure 1.2.5).

Whilst the Bo-Piketberg shows highest water usage (Figure 3.1.1), it is not necessarily experiencing the highest water stress as there is less outflow per unit precipitation in this area than in other parts of the catchment. The value of using the NDSI is thus illustrated as a useful tool to highlight areas of relative water stress within a catchment.

3.2 Differencing of evapotranspiration results as an indicator of irrigation and/or recharge

Actual evapotranspiration was calculated using two different models in this project and gave very different results.

SEBS: The first method was the SEBS model (section 2.3) which is based on the energy balance equation where the constraining factor is radiation and measured precipitation is not used in any way to constrain the results of the model. The result for estimation of actual evapotranspiration using the SEBS model for the one-year study period is shown in Figure 3.2.2 and Figure 3.2.3.

WetSpass: The second method of calculating evapotranspiration used for this project is as a step in the WetSpass model used to determine surface runoff and groundwater recharge, reported in sections 2.5 and 2.6, respectively. The result for estimation actual evapotranspiration using the WetSpass model for the one-year study period is shown in Figure 3.2.2 and Figure 3.2.3. In WetSpass the total actual evapotranspiration is the sum of interception, transpiration and the evaporation from bare soil and open water. Evapotranspiration is simulated using climatic data and parameterized values for vegetation from landuse and soil characteristics. Parameterized values for Leaf Area Index and Canopy Height have been superseded by remote sensing data. Mean annual potential evaporation of open water (A-pan evaporation) is used as a point of departure and its use is well motivated by Schulze & Maharaj (2007).

For vegetated areas, transpiration is calculated. In vegetated groundwater discharge areas, the actual transpiration is equal to the reference transpiration, since there is no limitation of soil water presence. In vegetated areas where the groundwater level is below the root zone, the actual transpiration is influenced by the groundwater level and soil characteristics. For bare soil surfaces, evaporation is based on potential evaporation and available soil water. For open water, potential evaporation is used.

A constraining factor in the evapotranspiration calculation is the accuracy of the distribution of vegetated, bare soil and impervious surfaces for each raster cell per landuse class. Water available for evapotranspiration is always constrained by the precipitation remaining after runoff has been calculated and potential evaporation. Figure 3.2.1 shows a comparison of the use of A-pan evaporation as input potential evapotranspiration vs. the Penman-Monteith approach as a reference for crop potential evaporation, with monthly modelled evapotranspiration values varying by 1-6 mm. Table II.1 in Appendix II documents the constraints the WetSpass model operates under. This constrained model appears to function effectively under humid conditions (Batelaan & De Smedt, 2007).

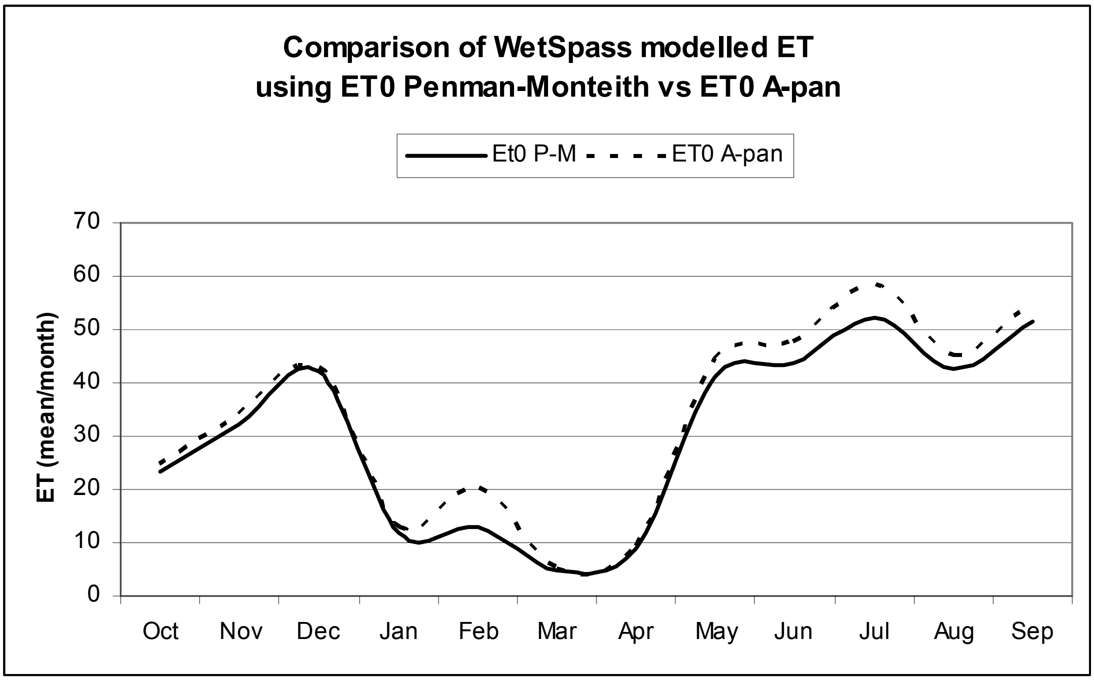

Figure 3.2.1: Comparison of WetSpass modelled ET constrained by A-pan evaporation vs. Penman-Monteith Potential evapotranspiration

Therefore, if the assumption is made that both models have been implemented correctly with accurate input data, then it is envisaged that the difference between the SEBS modelled evapotranspiration and the WetSpass modelled evapotranspiration can be explained by irrigation from stored water sources (dams), precipitation incorrectly partitioned to runoff, or additional water entering the catchment as recharge via fractured systems. At this point it should be stated that it may be incorrect to make this assumption on the basis of the results from sections 2.3, 2.5 and 2.6, however, in the interests of showing the monthly results for each method and to demonstrate the methodology, the monthly WetSpass evapotranspiration results were subtracted from the monthly SEBS evapotranspiration results and are displayed in Figure 3.2.2.

It can be seen in Figure 3.2.2 that the results of the methods paint two very different scenarios. If the results of the SEBS model are examined, it can be seen that evapotranspiration is highest in the summer months and lowest in the winter months. This would make sense in an environment with unlimited water supply. Spatially across the G10K catchment, the elevated areas experience more evapotranspiration than the low-lying areas. This is in line with the constraining factor of radiation which is higher in elevated areas (Barry & Chorley, 1987).

If the results of the WetSpass model are examined, the opposite trend can be seen. Evapotranspiration is shown to be lowest in the summer months as if there is low rainfall, there is very little water available for evapotranspiration, regardless of the energy available. Conversely, in the winter, there is plenty of water available to evapotranspiration and a higher evaporation rate is estimated. Spatially across the catchment the lowest evapotranspiration is found in low-lying areas, with elevated areas showing a higher value due to higher precipitation at elevated areas. An anomalous band of high evapotranspiration appears at the border of the mountaineous area with low-lying areas associated with the higher bare-soil evapotranspiration, slope, soil and landcover where the resolution of the different input datasets influences the result. Discharge areas along the southeast of the study area show high evapotranspiration values in months with high precipitation.

The differing resolutions of the input datasets are apparent in the level of detail visible. In the SEBS model a pixel resolution of 1000 m is inherited from the input MODIS level 1B data and a blocky effect is noted. The WetSpass model had input data of differing resolution ranging from 90-1000 m (from interpolated point data to MODIS input) and as land use is an input into the model, high evapotranspiration is noted at areas mapped as water bodies on the land use map.

It must be re-iterated that the WetSpass model was developed with long-term average data in mind. The fact that a monthly landuse parameter dataset was not created, but a seasonal dataset used, may influence the results obtained with respect to the relationship of vegetated area to bare soil as well as the fraction of precipitation greater than infiltration for soils.

If the difference between the two methods is examined on a month by month basis with the assumption that both models were implemented correctly, it can be seen that for the summer months, more water is evapotranspired for the catchment than is available from the precipitation which fell on a month to month basis. In the winter months, as radiation decreases, and precipitation increases, the results of the two models converge and fluctuate around zero in May, become negative during the wettest months of winter (June & July) and fluctuate around zero again for August and September. An interpretation of these results in terms of the water balance is that for the months where ET difference is greater than zero (summer months) water from stored water sources (dams) is used as irrigation or water from outside the catchment is supplementing the water supply to natural vegetation, e.g. recharge through fracture systems or groundwater is being tapped by deep-rooted vegetation. Conversely, where the ET difference is positive, there is excess water available for that time period and the additional water will either contribute to runoff or recharge.

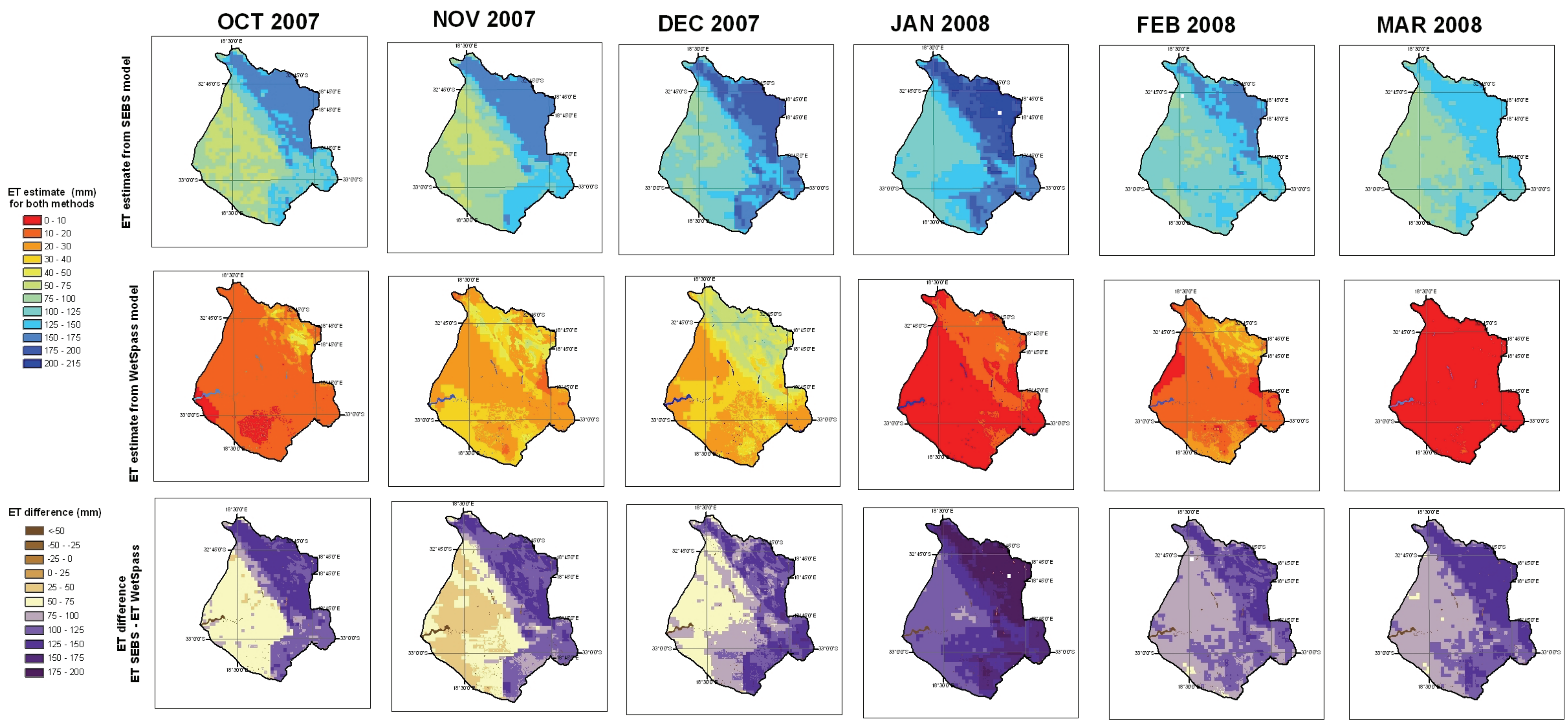

Figure 3.2.2: Comparison of SEBS modelled ET and WetSpass modelled ET, with ET difference for summer

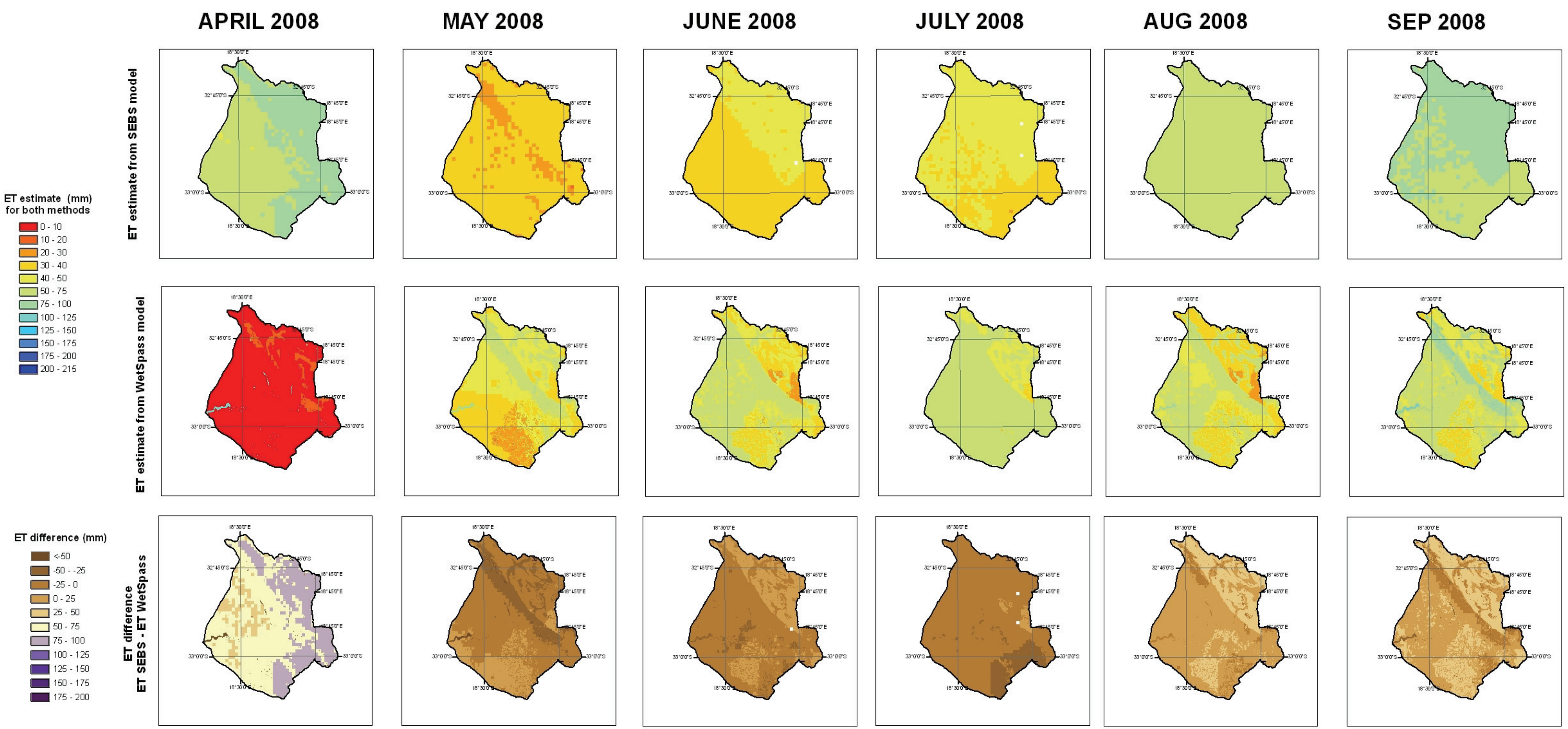

Figure 3.2.3: Comparison of SEBS modelled ET and WetSpass modelled ET, with ET difference for winter

3.3 Application of results to selected WARMS data to assess validity of methodology

Under the terms of the National Water Act (Act 36 of 1998), DWAF have been given the authority to gather information needed for the optimal management of water resources. The registration of water use is required to enable DWAF to manage water resources, ensure fair allocation, protect the environment and charge for water resources. Registration of water use is captured in the Water Authorization Resource Management System (WARMS).

All water users who do not receive their water from a service provider, local authority, water board, irrigation board, government water scheme or other bulk supplier and who are using water for irrigation, mining purposes, industrial use, feedlots, or in terms of a General Authorization, must be registered. This covers the use of surface and groundwater. Registration also applies to all existing lawful use.

When trying to link WARMS data to cadastral farm data or coordinates in the WARMS records, certain inconsistencies may be found. WARMS relies on information supplied by the customer regarding spatial location of registration. Registration of the water source is not necessarily linked to an individual water source, but rather to the water use per farming unit, which means that more than one water source may be linked to a single registration, or there may be multiple registrations per farming unit, one for each type of water source. Cadastral information regarding the water source may not be accurate as a farming unit can consist of multiple portions, not necessarily adjacent, with registration being linked merely to one of many portions. This and subdivisions of cadastral portions may cause problems. Care must be taken to use the same farm data from the Surveyor General as was used by DWAF.

DWAF is currently busy with a programme of validation and verification of all WARMS records where inaccuracies are sorted out.

To illustrate the application of the results to the WARMS database, three different areas in the catchment will be considered:

3.3.1 The Bo-Piketberg where the majority of dams were mapped (section 2.2)
3.3.2 Irrigated agriculture adjacent to the Berg River
3.3.3 Dryland agriculture where non-perennial pans are found

3.3.1 The Bo-Piketberg

The National Water Act states that a licence is required for "any person or body storing water for any purpose (including irrigation, domestic supply, industrial use, mining, aqua culture, fishing, water sport, aesthetic value, gardening, landscaping, golfing, etc) from surface runoff, groundwater or fountain flow *in excess of 10 000 cubic metres* or where the *water area at full supply level exceeds 1 hectare* in total on land owned or occupied by that person or body and not in possession of a permit or permission" (DWAF, 2007).

In section 2.7 the results of dam volume calculations were given. It can be seen in Figure 2.7.5 that there is a plethora of small dams, especially in the elevated Bo-Piketberg. However, in terms of the above paragraph, only dams with a storage volume of greater than 10 000 m^3 need to be registered so smaller dams can be excluded from this analysis. In Figure 3.3.1, the dam storage volumes described in section 2.7 are shown against the dam storage volume registered in WARMS. The challenges facing WARMS users can be seen by looking at Figure 3.3.1. There are very few cases where even the dam location in WARMS matches reality. It can also be seen that there are cases where 1) there is a WARMS registration on a property but no dam was mapped, or 2) only dams smaller than 10 000 m^3 were mapped. In the former case, it is possible that the dam is located on another portion of the farm which is not necessarily adjacent. In the case of the latter, it is possible that the volumes of many small dams (total surface area in excess of 1 ha) have been registered in WARMS, and to determine which small dams and on which farm portion they were registered is extremely difficult.

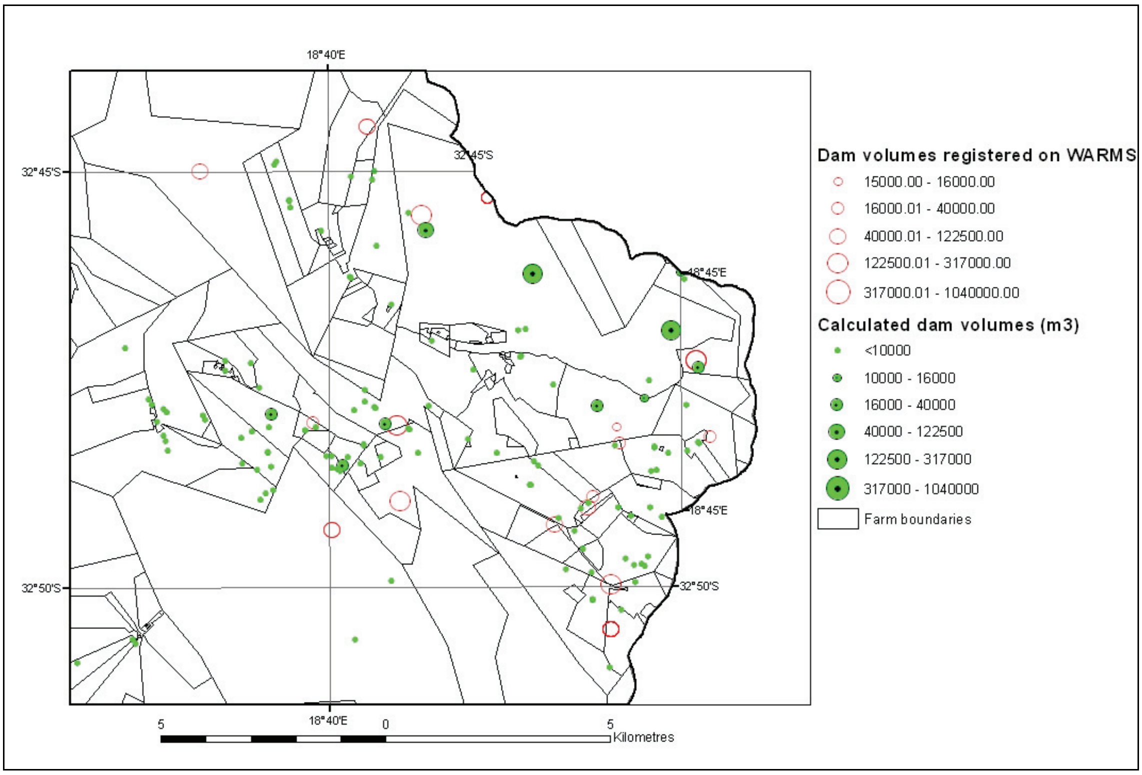

Figure 3.3.1 Calculated dam volume storage and dam volume storage from WARMS database

Note that dams < 10 000 m³ do not need to be registered hence the greater number of dams mapped than registered on WARMS.

3.3.2 Irrigated agriculture adjacent to the Berg River

The next area considered is adjacent to the Berg River to the south of the Bo-Piketberg. According to the WARMS database (Figure 3.3.2), irrigation of this region is from rivers and dams.

If zonal statistics in ArcGIS Spatial Analyst are applied to the water balance (see Figure 3.1.1) and the farm boundaries dataset, the mean water balance (mm) for each farm can be determined. This can then be converted to a volume of water usage per farm (Figure 3.3.3) using the formula:

Volume water usage per farm (m^3) = (Mean water use per farm (mm)/1000)*farm area (m^2)

If Figure 3.3.2 and 3.3.3 are compared, it can be seen that the difference in water usage between farms in this area is almost indistinguishable with the area of the farm being the factor which determines total water use per farm rather than the use of irrigation. This is due to 1) the incorrect assumption that the water balance equation resulted in an accurate assessment of water use per pixel, and 2) the resolution of the input data. The 1000 m pixel resolution of the MODIS data used in evapotranspiration estimation is having a moderating effect on local variations of the results. If the level of detail in the NDVI in Figure 3.3.2 is examined, local variations between farms and even within farms can be discerned. The coarser MODIS resolution does not allow for the same detection of variation.

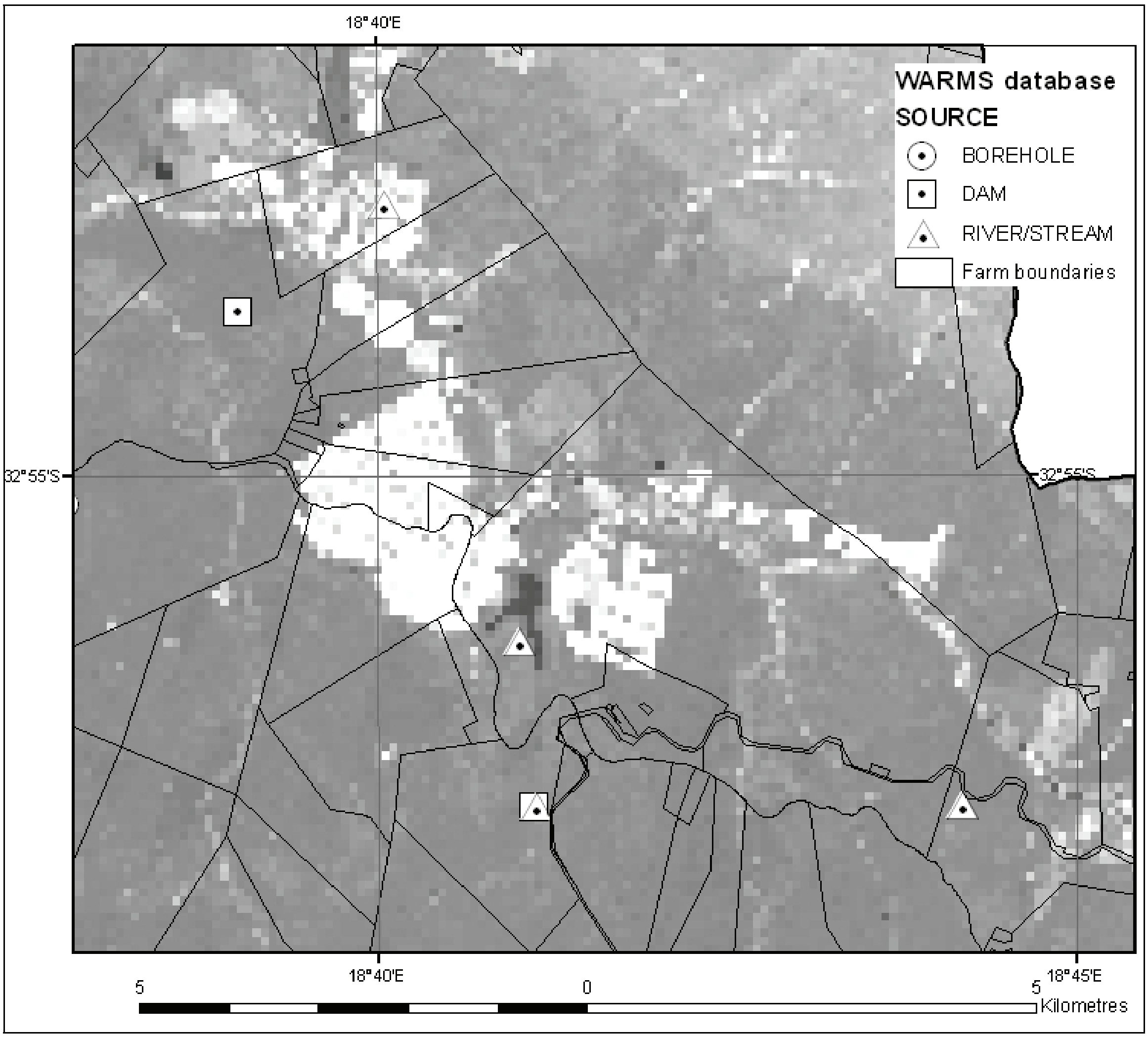

Figure 3.3.2: Source of water registered on WARMS database with the NDVI from an ASTER image (29 Feb 2008) used as a back drop. Irrigated agriculture is clearly visible in white

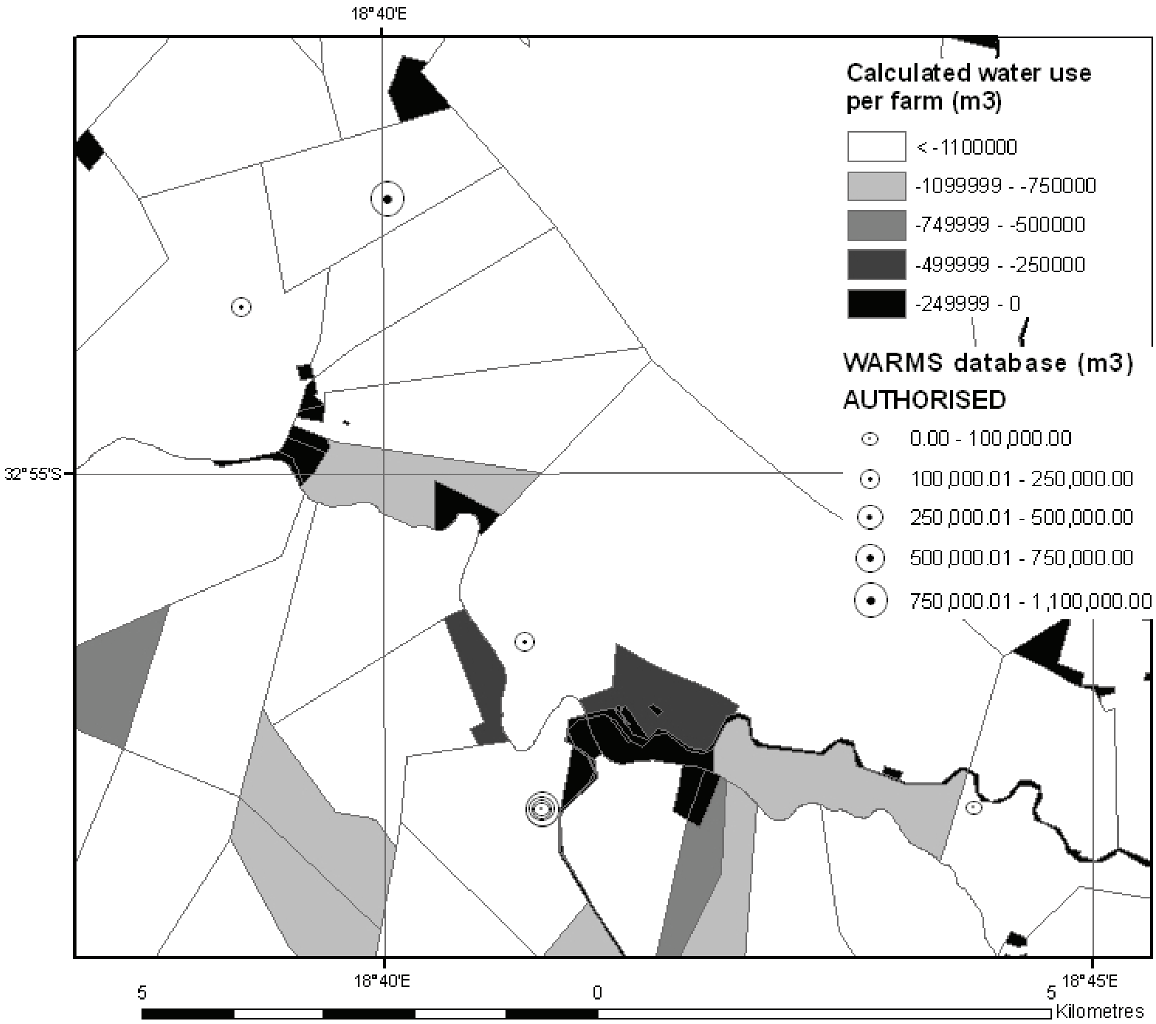

Figure 3.3.3: Volume water usage per farm as calculated from the results shown in Figure 3.3.2. Water use values indicated as negative (low values equal high water use)

3.3.3 Dryland agriculture where non-perennial pans are found

If the land use map shown in Figure 1.2.6 is examined, it can be seen that in the southern parts of the study area dryland agriculture occurs and the presence of small non-perennial pans is noted. The dryland agricultural status is corroborated by the fact that there are no WARMS registrations in that region (Figure 3.3.4). Similarly to the case of irrigated agriculture adjacent to the Berg River, the volume water usage per farm was calculated. It can be seen in Figure 3.3.4 that water usage is high despite the fact that no irrigation is recorded to take place in the area. Once again this points to an incorrect water balance result.

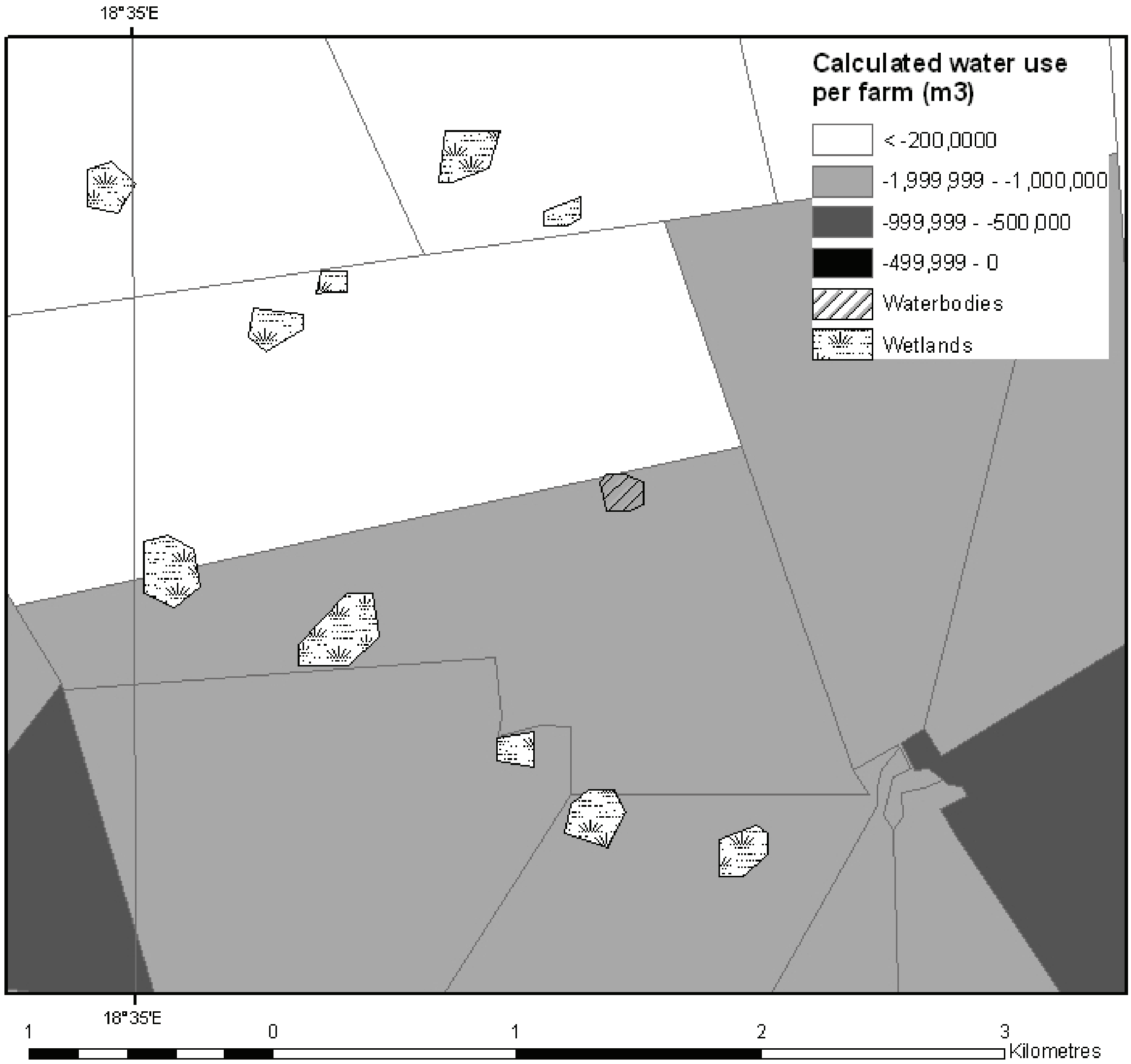

Figure 3.3.4: Volume water usage per farm as calculated from the results shown in Figure 3.1.1. Water use values indicated as negative (low values equal high water use)

4 DISCUSSION

The methodology developed for this research project relied on the spatial calculation of each component of the water balance equation across the G10K catchment and once this was completed the results for the study period were combined in a water balance equation. Because each component of the water balance was calculated independently (with the exception of runoff and recharge which were calculated using the same WetSpass model), there were no opportunities for the model to self-correct and allow for closure of the water balance equation. This could be seen as both a strength and a weakness of the methodology as the model is not forced to close at the expense of one of the components.

A brief discussion of each component will now be given but more information is found under the relevant sections of the report.

Rainfall (section 2.2)

It was found that for the G10K catchment, there is a good correlation between the total measured rainfall for the study period and the ARC-ISCW interpolated grid values, and as expected, the correlations are more variable at a monthly time scale. The spatial rainfall pattern provided by the ARC-ISCW interpolated rainfall grids appears to be sound, however, it is apparent that there is a significant underestimation of rainfall in the G10K catchment as a result of: 1) underestimation of rainfall in ARC-ISCW interpolated grid; 2) random and systematic errors in the collection of rainfall; and 3) the as yet unquantified contribution of condensation to precipitation. This reiterates the previous reports of uncertainties in rainfall measurements (Schulze, 2007; Rubel & Hantel, 2001, in Adams, 2004).

Evapotranspiration (section 2.3)

Using the SEBS model to estimate daily evapotranspiration and then upscaling daily evapotranspiration to monthly and annual evapotranspiration using relative and potential evapotranspiration appears to have overestimated evapotranspiration for the study period if the results are compared with the rainfall results. Since the evapotranspiration results have only been validated for an irrigated apple orchard and not other land use types, it is difficult to draw conclusions as to where possible errors may be occurring but the possibilities include: 1) the need for additional parameterization specific to the study area for the accurate estimation of roughness lengths; 2) errors in atmospheric correction due to difficulties in obtaining input data for the SMAC model; 3) the lack of interpolated weather station data; or 4) errors in implementing the model due to the absence of direct supervision. Furthermore, the issue of image resolution and landscape heterogeneity may also be impacting on the accuracy of results. The 1000 m pixel resolution of MODIS data makes it unsuitable for quaternary catchments and the heterogeneous landscape in the Bo-Piketberg compounds this.

Soil moisture (section 2.4)

Soil moisture quantification for the Bo-Piketberg region as a time-series analysis to derive a mean annual figure of soil moisture for each pixel could not be done due to the lack of availability of high resolution (12-20 m) radar data, so soil moisture could not be used in the water balance equation. Although the methodology to determine soil moisture for images obtained appears to be successful for the G10K catchment, a single snapshot of soil moisture at a point in time is most likely of no particular relevance for any application (Wagner & Pathe, 2005).

Runoff (section 2.5)

The runoff calculated using the hydrograph baseflow separation represents flow into the G10K catchment. The higher water level at inflow to G10M indicates that there is a gain of surface water flow in catchment G10K. Errors in the model can be attributed to uncertainties in the complexity of the model-data input such as uncertainties in landcover, soil classifications, slope and especially precipitation maps. The natural water balance in this particular catchment is modified by irrigation from pumped groundwater and dams. Notwithstanding these shortcomings, the WetSpass model introduced the concept of modelling the runoff in the catchment in a spatial, distributed way, which can be validated with the necessary field data. Generally, average annual estimates are more reliable than monthly or daily estimates of base flow or surface runoff. One of the major difficulties during this study was the lack of real surface runoff volumes.

Recharge (section 2.6)

Due to the fact that the recharge is calculated as the residual of a water balance model in WetSpass, all other outputs need to be calibrated, in order for the recharge to be correct. Yearly recharge results from WetSpass appear closer to accepted estimates than the cumulative monthly results. The monthly model overestimates recharge when recharge to the root zone becomes available to evapotranspiration and is termed storage as the storage is added cumulatively to recharge, leading to over-accounting. If evapotranspiration is underestimated due to constraints in precipitation or potential evapotranspiration, the recharge will be overestimated.

Both CMB and WetSpass models predicted low recharge in areas dominated by the Malmesbury group, with recharge predominantly predicted for the TMG area. Caution is advised when using the CMB method since the incoming rain has been generated over the ocean (Adams, 2004; Van Wyk, 2009) and in arid and semi-arid environments, recharge is essentially event driven as it is recognized that recharge is driven by single or multiple events and not annual averages which gives rise to the saying: "recharge estimation is thus prone to the fallacy of averaging" (Parsons, 2002). The WetSpass model tries to reduce this "fallacy of averaging" by using the precipitation fraction larger than infiltration in the modelling process. Recharge estimations in fractured aquifer systems are prone to error and groundwater modelling is required. Lack of suitable data is often the prime reason why recharge is not quantified. Errors in the model can be attributed to uncertainties in the complexity of the model-data input such as uncertainties in landcover, soil classifications, slope and especially precipitation maps.

Dam storage (section 2.7)

Remote sensing, in the form of object-oriented classification, was used to identify surface water bodies. A relatively simple classification process was developed so as to identify farm dams and obtain an estimate for surface area, a key input for volume. In order to obtain a value for water stored in farm dams, a capacity equation was used to convert surface area to volume. The equation makes use of surface area and a constant as inputs so that implicit assumptions and errors may exist. The use of high resolution data is important as change in surface area has a direct effect on volume of water stored.

4.1 Uncertainties and limitations

The uncertainties and limitations encountered during this research project can be categorized into four sections:

1) Accuracy, availability and accessibility of input data

The fact that this study was not based on historic data but relied on data being captured during the course of the study, meant that it was not known *a priori* exactly what data would be captured during the course of the study area and because of this, some of the data expectations were not met. For example, soil moisture could not be calculated for the catchment, and evapotranspiration had to be estimated at 1000 m resolution instead of the 15 m resolution as had been anticipated in Deliverable 3 (WRC, 2007b).

The accuracy of weather station data was called into question with rainfall (section 2.2) being the major point for concern with irregularities in radiation data also being reported (section 2.3). The lack of models to interpolate hourly weather station data may also have added to inaccuracies in the evapotranspiration estimates.

The size of the datasets that needed to be downloaded and processed was also problematic at times. In the evapotranspiration component alone, over 7 GB of MODIS data had to be downloaded from the internet. Processing the high resolution SPOT data for dam surface area classification (section 2.7) was also a challenge and the SPOT image had to be subdivided into smaller datasets and processed separately.

The selection of the study area should perhaps have been done by the researchers rather than involving DWAF. DWAF was consulted in the selection of the study in order to select a study area that was currently relevant to them but as a result, a relatively ungauged catchment was selected rather than one with many existing records. Although rain gauges and borehole loggers were installed during the course of the project, the lack of long-term data was significant especially in the runoff and recharge components.

2) Heterogeneity of the study area

The heterogeneity of the study area has been reported on throughout this report. The catchment is diverse in terms of climate, geology, landuse, topography, hydrology and geohydrology. This has impacted the research in two ways. Firstly, from a remote sensing perspective (reported on in section 2.3.7) and secondly because the methodologies used in this research are untested in South Africa. Because the methodologies are new in South Africa, it would have been better to have applied them to a less diverse catchment where implementation and validation would have been easier. The methodologies could then subsequently be applied to a more complex catchment such as the G10K.

3) Skills shortage (supervisory level) in South Africa

To the knowledge of the researchers, some of the methodologies (e.g. SEBS and WetSpass) used in this project have been untested in South Africa (at date of writing). Although much appreciated support was obtained from many quarters (see Acknowledgements) there remains a shortage of skills at supervisory level for these specific methodologies. Progress was therefore often slower than anticipated.

4) Models and software

The models and software used for this research presented their own individual challenges. The SEBS model was constantly being adjusted and updated throughout the course of the project and the final version was received less than a month before the project due date. The WetSpass model produces sixty temporary grids as part of the processing steps. This puts pressure on computer storage space especially when the grid is being run on a monthly basis. The Definiens model used to map dams was difficult to learn to use and was very computer resources intensive.

For many of the models, there are many processing steps along the way and the potential for incorrectly entering data (typing errors) becomes an issue. As far as possible, scripts were written to streamline the process; however, automating the process further would minimize the potential for errors of this nature.

Besides the difficulties outlined above a great deal has been learnt about the detailed modelling of the components of the water balance equation. The uncertainties encountered during the estimation of the water balance, are summarized in Table 4.1. It must also be noted that many of the models that were used for the project such as SEBS and Wetspass are freely available and thus have wide usability. The knowledge gained by the project team needs to be built upon and these models need to be promoted nationally through workshops and training sessions. The benefits from using such models far outweigh the initial challenges encountered.

TABLE 4.1: SUMMARY OF UNCERTAINTIES IN CALCULATING WATER BALANCE COMPONENTS

WATER BALANCE COMPONENT	KNOWN CAUSE OF UNCERTAINTY	POSSIBLE CAUSE OF UNCERTAINTY
Precipitation	• ISCW interpolated grid underestimated rainfall for study area	• Turbulent effect of the wind • Rain gauge errors • Unknown contribution from fog
Evapotranspiration	• Limited atmospheric correction data • Meteorological data is not interpolated across study area	• Additional parameterization needed for study area • Model may have been incorrectly implemented
Soil moisture	• Lack of field validation data	•
Runoff	• Modelled results dependent on accuracy of input data sets • Ungauged catchment – results could not be validated	• Resolution of cell sizes of input data sets • Incorrect assumptions in implementing model
Recharge	• Limited validation points • Modelling needed to verify results	•
Dam storage	• Satellite image acquired at different time of year to field validation • Topography of study different to topography where formulae developed	• Field survey methods • Correctness of WARMS registration

4.2 WARMS

The inconsistencies encountered when trying to link WARMS data to cadastral farm data or coordinates in the WARMS records were highlighted in section 3.3. DWAF are currently busy with a programme of validation and verification of all WARMS records where inaccuracies are sorted out. Once this is complete, it may be possible to simply compare results of future water use studies with WARMS data to highlight water use offenders, but until that time, working with WARMS data remains difficult.

5 CONCLUSION

At catchment level, the water cycle can be represented by the water balance equation which is a simple statement of the law of mass conservation and is expressed as

$$\Delta S = P - ET - Re - RO$$

where ΔS is the change in water storage in the catchment, P is precipitation, ET is evapotranspiration, Re is groundwater recharge and RO is surface water runoff. In order to calculate annual ΔS for the catchment, an annual volume is required for each component of the water balance equation. Each component of the water balance equation was calculated on a monthly basis and for the total study period (1 Oct 2007-30 Sept 2008) for the G10K catchment with varying success. For various reasons, precipitation appears to have been underestimated, evapotranspiration overestimated, and recharge overestimated. As expected, due to the underestimation of precipitation and the suspected overestimation of evapotranspiration and recharge, the G10K catchment shows a total water deficit for the study period across the entire catchment.

Whilst there may not be much certainty in the absolute results of this method, the spatial variations within the catchment were highlighted through the creation of a normalized difference storage index (NDSI). The NDSI is a unitless index designed to assess the spatial variability across the catchment rather than to look at absolute values. Results for the NDSI range from -1 to 1, where the higher the positive value, the larger the increase in water stored, and the higher the negative, the larger the decrease in water storage. If the results of the water balance equation and the NDSI are compared, it can be seen that whilst the Bo-Piketberg shows highest water usage, it is not necessarily experiencing the highest water stress as there is less outflow per unit precipitation in this area than in other parts of the catchment. The value of using the NDSI is thus illustrated as a useful tool to highlight areas of relative water stress within a catchment.

Actual evapotranspiration was calculated using two different methods in this project – the SEBS model (unconstrained by precipitation) and the WetSpass model (constrained by precipitation). It was envisaged that the difference between the SEBS modelled evapotranspiration and the WetSpass modelled evapotranspiration can be explained by irrigation from stored water sources (dams), precipitation incorrectly partitioned to runoff, or additional water entering the catchment as recharge via fractured systems.

The evapotranspiration differencing was done on a month by month basis on the assumption that both models were implemented correctly. The interpretation of the results in terms of the water balance showed that for the months where ET difference is greater than zero (summer months) water from stored water sources (dams) is used as irrigation or water from outside the catchment is supplementing the water supply to natural vegetation, e.g. recharge through fracture systems or groundwater is being tapped by deep-rooted vegetation. Conversely, where the ET difference is positive, there is excess water available for that time period and the additional water will either contribute to runoff or recharge.

Finally, the results of the water balance equation and dam water storage calculation were compared with the WARMS database for different parts of the G10K catchment. The problems with using the WARMS data were highlighted especially as one farming unit can extend over cadastral boundaries. It was found that very seldom does the dam location in WARMS match reality. This is confounded by the fact it is possible that the summed volumes of many small dams (with total surface area in excess of 1 ha, required to be registered in terms of legislation) have been registered on the property in WARMS but to determine which small dams and on which farm portion they were registered is extremely difficult. Zonal statistics were used to calculate the water use per farm (volume) in an irrigated area adjacent to the Berg River and in an area of dryland agriculture. It was found that the difference in water usage between farms in these areas was almost indistinguishable with the area of the farm being the factor which determines total water use per farm rather than the use of irrigation. This is due to 1) the incorrect assumption that the water balance equation resulted in an accurate assessment of water use per pixel, and 2) the resolution of the input data.

In conclusion, it can be said that the application of the water balance equation to the G10K catchment did not determine the level of legal compliance of water users to legislation. However, if the uncertainties and limitations encountered in the course of the research project are considered and acted upon, it is may be possible that at least parts of the methodology may be relevant at a later stage for water use determination.

Finally, the capacity building component of the research project cannot be overlooked. New methodologies, untested in South Africa, were applied to the study area with many challenges encountered. There is much hope that, as remote sensing technology develops and remotely sensed data becomes available at a higher spatial and temporal resolution, the full potential of these models will be able to be fully tested, and if proven accurate, could possibly be used operationally in the future.

6 RECOMMENDATIONS

Uncertainties in data accuracy, availability, and accessibility have been reported difficulties for the duration of this research project. The accuracy of weather station input data mostly affects the precipitation and evapotranspiration estimation components of the water balance equation. Accuracy assessments of rainfall gauges in different settings are needed in order to determine the order of magnitude to which they underestimate actual precipitation. Usually precipitation is the only inflow in a water balance equation and if the estimate is incorrect, all other components of the water balance are likely to be calculated incorrectly. Many research projects would benefit from a study of this nature. On the same theme, the amount precipitation from fog can also be significant to the water balance, depending on the environment. Methods for quantifying this amount especially in arid and semi-arid areas would be helpful.

Accurate spatial interpolation techniques for hourly weather station data would also be helpful in the estimation of evapotranspiration. Remote sensing techniques calculate evapotranspiration on a pixel by pixel basis but weather station data occurs only at point locations. Accurately interpolating these data across a study area will greatly enhance the results of evapotranspiration estimation.

Accuracy assessment for the soil moisture component of the study could not be performed since distributed ground truth data at the time of image capture was unavailable. Field validation for this component is important since one of the models used for estimating soil moisture content was designed for different ranges of parameters such as incidence angle and wavelength. Field validation will enable the identification of errors in these models which may result in refinement of the models which will lead to an increase in the accuracy of the results of soil moisture quantification.

The availability of high resolution remotely sensed data was also a reported problem. Evapotranspiration was estimated using the 1000 m level 1B MODIS data; however, if MODIS data products are used, the resolution could be improved to 250 m which may make it suitable for farm scale evapotranspiration determination. Higher resolution

MODIS data products could also be used to estimate vegetation parameters for the WetSpass model, improving the spatial variability of the results.

In addition to the field validation results that were reported, the results of the SEBS model should be validated for multiple land use types. This would give an indication of the accuracy of the results or if and where errors are occurring. The validation may show that extra parameterization is needed for the study area which would involve the creation of an accurate detailed landuse map with associated roughness parameters.

The results of the recharge calculated using the WetSpass model should be validated using MODFLOW. The results of evapotranspiration using WetSpass need to be investigated to find the source of the lower than expected values. It is possibly a result of precipitation values or because of the coarse resolution vegetation cover input data.

In a study which uses complex models with many input datasets and values, the potential for typing errors becomes quite large. Automating the input of data as far as possible is recommended to avoid this type of error.

Future remote sensing projects which aim to test new methodologies should use study areas which are homogeneous, well researched and have plenty of historic data available. This will allow for easier understanding of processes and validation will consequently be much easier and less costly.

More time and thought should be spent on the design of projects such as this one. Perhaps the concept of seeding funds should be considered where funds are made available to investigate the methodologies available and possible study areas. In this way, better informed decisions can be made regarding the choice of study area, the type and cost of validation instrumentation needed, and the appropriate capacity building requirements (which may not necessarily be a degree from a tertiary institution) can be motivated for and a budget assigned.

It is recommended that this project be extended to include a more homogeneous study area, i.e. the Sandveld on the Western Cape coast. It is relatively homogeneous area and extensive data exists for the area. There is also a flow gauging station at Het Kruis. In addition the Department of Agriculture is also running the SEBAL model for this area. This future study should include groundwater modelling with MODFLOW and should include linkage with high level institutions and specialists. The results and skills then need to be transferred via workshops and courses.

7 REFERENCES

Acocks, J. P. H., 1988. Veld Types of southern Africa. Botanical Research Institute, Pretoria, RSA. *Botanical Survey of South Africa Memoirs*, 57. pp. 146.

Adams, S., 2004. Groundwater recharge assessment of the basement aquifers of central Namaqualand. Ph.D. thesis. Cape Town: University of the Western Cape.

Allen, R. G., Pereira, L. S., Raes, D. & Smith, M., 1998. Crop evapotranspiration: guidelines for computing crop water requirements. *FAO Irrigation and Drainage Paper 56*, Rome, 300 pp.

Álvarez-Mozos, J., Casali, J., González-Audícana, M. & Verhoest, N. E. C., 2005. Correlation between ground measured soil moisture and RADARSAT-1 derived backscattering coefficient over an agricultural catchment of Navarre (North of Spain). *Biosystems Engineering*, 92: 119-133.

ARC-ISCW, 2005. Ten Daily Rainfall Estimate Grids. Grid metadata

ARC-ISCW, 2007. Köppen Climate Classification System. Shapefile metadata.

Barry, R. G. & Chorley, R. J., 1987. Atmosphere, Weather and Climate. 5th Edition. Methuen and Co. Ltd.: London.

Barry, R. G., 1992. Mountain weather and climate. 2nd ed. Routledge, London.

Batelaan, O., 2006. Phreatology: Characterizing groundwater recharge and discharge using remote sensing, GIS, ecology, hydrochemistry and groundwater modeling. Ph.D. thesis, Vrije Universiteit Brussel.

Batelaan, O. & De Smedt, F., 2001. WetSpass: a flexible, GIS based, distributed recharge methodology for regional groundwater modelling. In: Gehrels, H., Peters, J., Hoehn, E., Jensen, K., Leibundgut, C., Griffioen, J., Webb, B. & Zaadnoordijk, W-J. (eds). Impact of Human Activity on Groundwater Dynamics. IAHS Publ. no. 269, Wallingford UK, pp11-17.

Batelaan, O. & De Smedt, F., 2004. SEEPAGE, a new MODFLOW DRAIN Package. *Ground Water*, 42: 576-588.

Batelaan, O. & De Smedt, F., 2007. GIS-based recharge estimation by coupling surface-subsurface water balance. *Journal of Hydrology*, 337: 337-355.

Bjerklie, D. M., Moller, D., Smith, L. C. & Dingman, L., 2005. Estimating discharge in rivers using remotely sensed hydraulic information. *Journal of Hydrology* 309: 191-209.

Blight, G. E., 2002. Measuring evaporation from soil surfaces for environmental and geotechnical purposes. *Water SA*, 28(4): 381-394.

Bredenkamp, D., Botha, L. J., Van Tonder, G. J. & Janse van Rensburg, H., 1995. Manual on qualitative estimation of groundwater recharge and aquifer storativity, based on practical hydro-logical methods. Water Research Commission, TT 73/95. ISBN 1 86845 1763.

Canada Centre for Remote Sensing, 2006. Tutorial: Radar Polarimetry. [online]. Available at URL http://www.ccrs.nrcan.gc.ca/resource/tutor/polarim/index_e.php. [Accessed August 2006]

Colvin, C., & Saayman, I., 2007. Challenges to groundwater governance: a case study of groundwater governance in Cape Town, South Africa. *Water Policy 9 Supplement*, 2: 127-148.

Craig, H., 1961. Isotopic variation in natural waters. *Science*, 133: 1702-1703.

Crosby, C. T. 1996. SAPWAT 1.0 – A computer program for estimating irrigation requirements in Southern Africa. WRC Report No. 379/1/96. Water Research Commission: Pretoria.

Crosby, C. T. & Crosby, C. P., 1999. SAPWAT – A computer program for establishing irrigation requirements and scheduling strategies in South Africa. WRC Report No. 624/1/99. Water Research Commission: Pretoria.

Curran, P. J. & Atkinson, P. M., 1999. In Stein, A., van der Meer, F. & Gorte, B. (eds*) Spatial Statistics for Remote Sensing*, pp. 115-133. Dordrecht: Kluwer Academic Publishers.

Dabrowska-Zielinska, K., Inoue, Y., Kowalik, W. & Gruszczynska, M., in press. Inferring the effect of plant and soil variables on C-band and L-band SAR backscatter over agricultural fields, based on model analysis. *Advances in Space Research*.

Definiens, 2000. Definiens User Guide – take the plunge.

Department of Water Affairs and Forestry (DWAF), 2007. WARMS – Water Use Registering and Licensing. Available at URL: http://www.dwaf.gov.za/Projects/WARMS/default.asp [Accessed 15 March 2008].

Diamond, R. E. & Harris, C., 1997. Oxygen and hydrogen composition of Western Cape meteoric water. *South African Journal of Science*, 93: 371-374.

D'Urso, G. & Minacapilli, M., 2006. A semi-empirical approach for surface soil water content estimation from radar data without a-priori information on surface roughness. *Journal of Hydrology,* 321: 297-310.

DWAF & DFID, 2005. Water and Forestry Support Programme – Water Resource Management Component. Undertake an Assessment of the Lawfulness of Registered Water Use in the Mhlathuze River Catchment. Report no: WFSP/WRM/CON2002.

Engmen, T. E. & Chauhan, N., 1995. Status of microwave soil moisture measurements with remote sensing. *Remote Sensing of Environment,* 51: 189-198.

ESRI. 2006. ArcGIS Desktop Help.

Fairbanks, D. H. K., Thompson, M. W., Vink, D. E., Newby, T. S., van den Berg, H. M. & Evereard, D. A., 2000. The South African Land-cover Characteristics Database: a synopsis of the landscape. *South African Journal of Science*, 96: 69-82.

Fetter, C.W., 2001. Applied hydrogeology – 4th ed. Prentice-Hall, Inc., New Jersey.

Finch, J. W., 1997 Monitoring Small Dams in Semi-arid Regions using Remote Sensing and GIS, *Journal of Hydrology*, 195: 335-351.

Freeze, R. A., 1969. The mechanism of natural ground-water recharge and discharge 1. Onedimensional, vertical, unsteady, unsaturated flow above a recharging or discharging groundwater flow system. *Water Resources Research*, 5 (1): 153-171.

Funke, N., Oelofse, S.S.H., Hattingh, J., Ashton, P.J. & Turton, A. R., 2007. IWRM in Developing Countries: Lessons from the Mhlatuze Catchment in South Africa, *Physics and Chemistry of the Earth*, 32: 1237-1245.

Gibson, L.A., 2003. The detection of wetlands using remote sensing in Qoqodala, Eastern Cape. M.Sc. dissertation. University of Cape Town.

Haasbroek, P. D., 2008. Personal communication with Lesley Gibson.

Haasbroek, P. D., 2009. Incorrect rainfall measurements due to different windspeeds and raindrop sizes. Preliminary unpublished report. ARC-ISCW, Pretoria.

Hailegiorgis, W. S., 2006. Remote Sensing analysis of summer time Evapotranspiration using SEBS algorithm: a case study in Regge and Dinklel, The Netherlands. M.Sc Thesis. International Institute for Geo-information Science and Earth Observation.

Harris, C. & Talma, A. S., 2002. The application of Isotopes and Hydrochemistry as exploration and management tools. In: A Synthesis of the Hydrogeology of the Table Mountain Group – Formation of a Research Strategy. Pietersen, K. & Parsons, R. (eds). WRC TT 158/01. Water Research Commission, Pretoria.

Hartnady, C. J. H. & Hay, E. R., 2000. Reconnaissance investigations into the development and utilization of Table Mountain Group Artesian groundwater, using the E10 catchment as a Pilot Study Area. Final Report prepared for the Department of Water Affairs and Forestry. Umvoto Africa/SRK Consulting Joint Venture, Cape Town.

Herald, M., Scepan, J., Muller, A. & Günther, S., 2002. Object-oriented mapping and analysis of urban land use/cover using IKONOS data, Proceedings of 22nd EARSEL Symposium "Geoinformation for European-wide integration": Prague.

Holah. N., Baghdadi, N., Zribi, M., Bruand, A. & King, C., 2005. Potential of ASAR/ENVISAT for the characterization of soil surface parameters over bare agricultural fields. *Remote Sensing of Environment*, 96: 78-86.

Jackson, T. J., 2002. Remote sensing of soil moisture: implications for groundwater recharge. *Hydrogeology Journal,* 10: 40-51.

Jarmain, C. & Mengistu, M.G., 2009. Validating energy fluxes estimated using the Surface Energy Balance System (SEBS) model for a small catchment. WRC Consultancy Report K8/824. Water Research Commission, Pretoria.

Jia, L., Su, Z., Hurk, B. V.d., Menenti, M., Moene, A., Bruin, H. A. R. D., Yrisarry, J. J. B., Ibanez, M. & Cuesta, A., 2003. Estimation of sensible heat flux using the surface energy balance system (SEBS) and ATSR measurements. *Physics and Chemistry of the Earth*, 28: 75-88.

Jin, X., Wan, L. & Su, Z., 2005. Research on evaporation of Taiyuan basin area by using remote sensing. *Hydrology and Earth System Sciences Discussions*, 2: 209-227.

Jha, M. K. & Chowdary, V. M., 2006. Challenges of using remote sensing and GIS in developing nations. *Hydrogeology Journal,* 15: 197-200.

JPL, 2009. SWIR- ASTER User Advisory. [online]. Available at URL: http://asterweb.jpl.nasa.gov/swir-alert.asp [Accessed 30 March 2009]

Kellgren, N., 2002. Applicability of Remote Sensing Techniques to Groundwater Exploration in Semi-Arid Hard Rock Terrain, Goteborg, Sweden. Phd. Thesis, Chalmers University of Technology.

Kustas, W. P., Norman, J. M, Anderson, M. C. & French, A. N., 2003. Estimating subpixel surface temperatures and energy fluxes from the vegetation index-radiometric temperature relationship. *Remote Sensing of Environment*, 85: 429-440.

Kriek, 2005. Manual for the Training of DWAF Regional Officers. Course notes from course on Water Resource Management, September 2005.

Kressler, F. P., Steinnocher, K. & Kim, Y., 2005. Enhanced semi-automatic image classification of high-resolution data, In: Proceedings of the IGARSS 2005 Symposium. Seoul, Korea. July 25-29, 2005.

Liang, S., 2001. Narrowband to Broadband Conversions of land surface albedo I: Algorithms. *Remote Sensing of the Environment*, 76(2): 213-238.

Liebe, J. 2002. Estimation of water storage capacity and evaporation losses of small reservoirs in the upper east region of Ghana. Diploma Thesis. Geographische Institute der Rheinischen Fiedrich-Wilhelms-Universität Bonn.

Linacre, E., 1992. Climate data and resources: a reference and a guide. Routledge, London.

Lück, W., 2007. SPOT 5 National Mosaic Production and Accuracy Report. Eastern South Africa: CSIR.

Lynch, S. D., 2004. *Development of a Raster Database of Annual, Monthly and Daily Rainfall for Southern Africa*. Water Research Commission, Pretoria, RSA, WRC Report 1156/1/04. pp. 78.

Lynch, S. D. & Schulze, R. E., 2007. Rainfall Database. In: Schulze, R. E. (Ed). 2007. South African Atlas of Climatology and Agrohydrology. Water Research Commission, Pretoria, RSA, WRC Report 1489/1/06, Section 2.2.

Meyer, P. S., 2001. An Explanation of the 1:500 000 General Hydrogeological Map Cape Town 3317. May 2001. Department: Water Affairs and Forestry, South Africa.

Mora, F. & Iverson, L. R., 1998. On the sources of vegetation activity variation, and their relation with water balance in Mexico. *International Journal of Remote Sensing*, 19(10): 1843-1871.

Moran, M. S., Hymer, D. C., Qi Jand Sano, E. E., 2000. Soil moisture evaluation using multi-temporal synthetic aperture radar (SAR) in semiarid rangeland. *Agricultural and Forest Meteorology*, 105: 69-80.

Moran, M. S., McElroy, S., Watts, J. M. & Peters-Lidard, C. D., 2005. Radar remote sensing for estimation of surface soil moisture at the watershed scale [online]. Available at http://www.tucson.ars.ag.gov/unit/Publications/PDFfiles/1566.pdf. [Accessed November 2006].

Műnch, Z., 2004. Assessment of GIS-interpolation techniques for groundwater evaluation: a case study of the Sandveld, Western Cape, South Africa. M.Sc. dissertation, University of Stellenbosch.

National Water Act (36 of 1998). Republic of South Africa.

National Water Resource Strategy (NWRS), 2004. Republic of South Africa.

Narayanan, R. M. & Hirsave, P. P., 2001. Soil moisture estimation models using SIR-C SAR data: a case study in New Hampshire, USA. *Remote Sensing of Environment,* 75: 385-396.

Parodi, G., 2008. SEBS for ILWIS OPEN 3.4: An interface for Surface Energy Balance in ILWIS Open Source (Jul 2007). Presented at: S. E. B. Models of Agricultural Areas from Earth Observation Data", Lima, Perú, 13 March 2008.

Parsons, R., 2002. Recharge of Table Mountain Group Aquifer Systems. In: A Synthesis of the Hydrogeology of the Table Mountain Group – Formation of a Research Strategy. Pietersen, K. and Parsons, R. (eds). WRC TT 158/01. Water Research Commission, Pretoria.

Pathe, C. & Wagner, W., 2004. Soil moisture estimation on a regional scale using Envisat ASAR wide swath images ? Proceedings of the 2004 Envisat & ERS Symposium, Salzburg, Austria 6-10 September 2004.

Pidwirny, M., 2006. "Climate Classification and Climatic Regions of the World". Fundamentals of Physical Geography, 2nd Edition. Date Viewed 31 March 2009 http://www.physicalgeography.net/fundamentals/7v.html

Pike, A., 2008. Hydrology in South Africa. (Notes prepared by Dr G. A. Kiker). [online]. Available at www.beeh.unp.ac.za/pike/hydroEngineers/Hydrological%20Process-Infiltration-Runoff.ppt

Pike, A. & Schulze, R. E., 1995. AUTOSOILS: A Program to Convert ISCW Soils Attributes to Variables Usable in Hydrological Models. Department of Agricultural Engineering, University of Natal, Pietermaritzburg, RSA (Also updates).

Quibell, G., 2005. Verifying existing lawful water use. Unpubl Powerpoint Presentation.

Rahman, H. & Dedieu, G., 1994. SMAC: a simplified method for the atmospheric correction of satellite measurements in the solar spectrum. *International Journal of Remote Sensing*, 15(1): 123-143.

Rahman, M. M., Moran, M. S., Thoma, D. P., Bryant, R., Holifield Collins, C. D., Jackson, T., Orr, B. J. & Tischler, M., 2008. Mapping surface roughness and soil moisture using multi-angle radar imagery without ancillary data. *Remote Sensing of Environment,* 112: 391-402.

Ritter, M. E., 2006. The Physical Environment: an Introduction to Physical Geography. [online]. Available at http://www.uwsp.edu/geo/faculty/ritter/geog101/textbook/title_page.htm [Accessed 31 March 2009].

Roets, W., Xu, Y., Raitt, L. & Brendonck, L., 2008. Groundwater discharges to aquatic ecosystems associated with the Table Mountain Group (TMG) aquifer: A conceptual model. *Water SA,* 34: 77-88.

Savage, M. J, Everson, C. S, Odhiambo, G. O., Mengistu, M. G. & Jarmain, C., 2004. Theory and practice of evaporation measurement, with special focus on SLS as an operational tool for the estimation of spatially-averaged evaporation. Water Research Commission, WRC Report No. 1335/1/04.

Sawunyama, T., Senzanje, A. & Mhizha, A., 2006. Estimation of small reservoir storage capacities in Limpopo River Basin using geographical information systems and remotely sensed surface areas: case of Mzingwane catchment, *Physics and Chemistry of Earth*, 31: 935-943.

Schulze, R. E., 2007. *South African Atlas of Climatology and Agrohydrology*. Water Research Commission, Pretoria, RSA, WRC Report 1489/1/06.

Schulze, R. E., Angus, G. R., Lynch, S. D. & Smithers, J. C., 1995. ACRU: Concepts and Structure. In: Schulze, R. E. *Hydrology and Agrohydrology: A Text to Accompany the ACRU 3.00 Agrohydrological Modelling System*. Water Research Commission, Pretoria, RSA, Report TT69/95. AT2-1 to AT2-26.

Schulze, R. E. & Maharaj, M., 2007. A-Pan Equivalent Reference Potential Evaporation. *In:* Schulze, R.E. (Ed). 2007. *South African Atlas of Climatology and Agrohydrology*. Water Research Commission, Pretoria, RSA, WRC Report 1489/1/06, Section 13.2.

SCWG, 1991. *Soil Classification – Taxonomic System for South Africa.* Department of Agricultural Development, Pretoria, RSA, SIRI Soil Classification Working Group. pp. 257.

Sloto, R. A. & Crouse, M. Y., 1996. HYSEP: A computer program for streamflow hydrograph separation and analysis. Tech. Rep. Water-Resources Investigations report 96-4040, U.S. Geological Survey. [online]. Available at http://water.usgs.gov/software/HYSEP/

Smith, J. H, Wickham, J. D, Stehman, S. V. & Yang, L., 2002. Impacts of Patch Size and Land-Cover Heterogenity on Thematic Image Classification Accuracy. *Photogrammetric Engineering & Remote Sensing.* 68: 65-70.

Steiner, M., Sieck, L. C. & Burges, S. J., 2005. Revisiting "ground truth" – assessment of wind and out-of-level collector funnel effects on rain gauge catch. 32nd Conference on Radar Meteorology and 11th Conference on Mesoscale Processes. Albuquerque, New Mexico. American Meteorological Society. [online]. Available at URL: http://ams.confex.com/ams/32Rad11Meso/techprogram/paper_97019.htm [Accessed March 2009].

Su, Z., 2002. The surface energy balance system (SEBS) for estimation of turbulent heat fluxes. *Hydrology and Earth System Sciences*, 6: 85-99.

Su, Z., Wen, J. & Wan, L., 2003. A Methodology for the Retrieval of Land Physical Parameters and Actual Evaporation using NOAA/AVHRR data. *Journal of Jilin University (Earth Science Edition)*, 33(sup.): 106-118.

Su, Z. & Roerink, G. J. (editors), 2004. *Drought Risk Reduction.* Wageningen, Alterra, Alterra-rapport 1135. 87 pp., 18 figs.; tables.; 37 refs.

Su, H., McCabe, M. F., Wood, E. F., Su, Z. & Prueger, J. H., 2005. Modeling Evapotranspiration during SMACEX: Comparing Two Approaches for Local- and Regional-Scale Prediction. *Journal of Hydrometeorology – Special Section*, 6: 910-922.

Su, Z., 2006a. Surface radiation budget: measurements and parameterisation. PowerPoint presentation. Presented at ESA TIGER Capacity Building Facility 1st Training Course on "Advanced optical remote sensing". 22-25 November 2006. Cape Town.

Su, Z., 2006b. An introduction to the surface energy balance system (SEBS). Lecture notes. Presented at ESA TIGER Capacity Building Facility 1st Training Course on "Advanced optical remote sensing". 22-25 November 2006. Cape Town.

Su, Z., 2009a. Personal communication with Lesley Gibson. E-mail dated 25 March 2009.

Su, Z., 2009b. Personal communication with Lesley Gibson. E-mail dated 12 March 2009.

Svoray, T. & Shoshany, M., 2004. Multi-scale analysis of intrinsic soil factors from SAR-based mapping of drying rates. *Remote Sensing of Environment*, 92: 233-246.

Townshend, J. R. G., Huang, C., Kalluri, S. N. V., Defries, R. S. & Liang, S., 2000. Beware of per-pixel characterization of land cover. *International Journal of Remote Sensing*, 21: 839-843.

Turesson, A., 2006. Water content and porosity estimated from ground-penetrating radar and resistivity. *Journal of Applied Geophysics,* 58: 99-111.

USDA, 1951. Soil survey manual. Tech. Rep. Handbook no. 18, U.S. Dept. Agriculture Soil Survey Staff.

Van de Giesen, N., Liebe, J., Andreini, M. & Steenhuis, T. 2004. Use of small reservoirs in West Africa as remotely-sensed cumulative runoff gauges, in *Proceedings of the 2nd international CAHMDA workshop on: The Terrestrial Water Cycle: Modelling and Data Assimilation Across Catchment Scales*, edited by A.J. Teuling, H. Leijnse, P.A. Troch, J. Sheffield and E.F. Wood, pp. 32-35, Princeton, NJ, October 25-27

Van Mook, F. J. R., 2002. Diameter of a Raindrop. Published as issue 69 in the Bouwstenen series of the Faculty of Architecture, Planning and Building of the Eindhoven University of Technology. [online]. Available at URL: http://sts.bwk.tue.nl/drivingrain/ fjrvanmook2002/node8.htm [Accessed March 2009]

Van Wyk, E., 2009. Personal communication. Email dated 2009/02/25.

Voogt, M. P., 2006. Meteolook, a physically based regional distribution model for measured meteorological variables. MSc Thesis TU Delft. [Abstract available online]. Available at URL: www.citg.tudelft.nl/live/pagina.jsp?id=50e40a94-07c2-4ccc-a3e9-849c85ecbfd0&lang=en&binary=/doc/Voogt2006.pdf [Accessed 31 March 2009]

Wagner, W. & Pathe, C., 2005. Has SAR failed in soil moisture retrieval? Proceedings of the 2004 Envisat & ERS Symposium, Salzburg, Austria 6-10 September 2004.

Wang, L., 2008. Processing MODIS level_1B data for SEBS in ILWIS Instructions. Unpublished report.

Ward, R. C., 1975. *Principles of hydrology*, 2nd Edition. McGraw-Hill, UK. p. 4, Fig. 1.1.

WaterWatch, 2008. Water use efficiency of table and wine grapes in Western Cape, South Africa: The spatial and temporal variation of water use efficiency in grape cultivation using remote sensing technology. [online]. Available at http://www.waterwatch.nl/download/projects/0169_WUEgrapes_finalreport.pdf [Accessed 30 March 2009].

Western, A. W., Grayson, R. B., Sadek, T. & Turral, H., 2004. On the ability of AirSAR to measure patterns of dielectric constant at hillslope scale. *Journal of Hydrology*, 289: 9-22.

WRC, 2006. Remote sensing as a tool for Resource Assessment and determination of the legal compliance of surface and groundwater use. Deliverable 1b: Literature Review. WRC Project K5/1690. Water Research Commission, Pretoria.

WRC, 2007a. Remote sensing as a tool for Resource Assessment and determination of the legal compliance of surface and groundwater use. Deliverable 2: Progress Report. WRC Project K5/1690. Water Research Commission, Pretoria.

WRC, 2007b. Remote sensing as a tool for Resource Assessment and determination of the legal compliance of surface and groundwater use. Deliverable 3b: Methodology Development. WRC Project K5/1690. Water Research Commission, Pretoria.

WRC, 2008a. Remote sensing as a tool for Resource Assessment and determination of the legal compliance of surface and groundwater use. Deliverable 4: Progress Report. WRC Project K5/1690. Water Research Commission, Pretoria.

WRC, 2008b. Remote sensing as a tool for Resource Assessment and determination of the legal compliance of surface and groundwater use. Deliverable 5: Progress Report. WRC Project K5/1690. Water Research Commission, Pretoria.

Xin, S., 2007. Regional evapotranspiration over the arid inland Heihe River Basin in Northwest China. M.Sc thesis: International Institute for Geo-information Science and Earth Observation, The Netherlands. 98 pp.

Xu, Y. & Van Tonder, G. J., 2001. Estimation of recharge using a revised CRD method. *Water SA*., 27 (3): 341-344.

Zietsman, H. L., Vlok, A. C. & Nel, I., 1996. The Identification of Irrigated Land in an Intensively Cultivated Agricultural Area in the South-Western Cape by means of Remote Sensing, Water Research Commission: Pretoria.

Zribi, M., Baghdadi, N., Holah, N. & Fafin, O., 2005a. New methodology for soil surface moisture estimation and its application to ENVISAT-ASAR multi-incidence data inversion. *Remote Sensing of Environment*, 96: 485-496.

Zribi, M., Baghdadi, N., Holah, N., Fafin, O. & Guérin, C., 2005b. Evaluation of a rough soil surface description with ASAR-ENVISAT radar data. *Remote Sensing of Environment,* 95: 67-76.